USGS
science for a changing world

Prepared in cooperation with the City of Aberdeen

Revised Groundwater-Flow Model of the Glacial Aquifer System North of Aberdeen, South Dakota, Through Water Year 2015

Scientific Investigations Report 2018–5137

U.S. Department of the Interior
U.S. Geological Survey

Cover. View looking downstream from the Elm River, north of Aberdeen, South Dakota. Photograph by Larry Putnam, U.S. Geological Survey.

Revised Groundwater-Flow Model of the Glacial Aquifer System North of Aberdeen, South Dakota, Through Water Year 2015

By Joshua F. Valder, William G. Eldridge, Kyle W. Davis, Colton J. Medler, and Karl R. Koth

Prepared in cooperation with the City of Aberdeen

Scientific Investigations Report 2018–5137

U.S. Department of the Interior
U.S. Geological Survey

U.S. Department of the Interior
RYAN K. ZINKE, Secretary

U.S. Geological Survey
James F. Reilly II, Director

U.S. Geological Survey, Reston, Virginia: 2018

For more information on the USGS—the Federal source for science about the Earth, its natural and living resources, natural hazards, and the environment—visit https://www.usgs.gov or call 1–888–ASK–USGS.

For an overview of USGS information products, including maps, imagery, and publications, visit https://store.usgs.gov.

Suggested citation:
Valder, J.F., Eldridge, W.G., Davis, K.W., Medler, C.J., and Koth, K.R., 2018, Revised groundwater-flow model of the glacial aquifer system north of Aberdeen, South Dakota, through water year 2015: U.S. Geological Survey Scientific Investigations Report 2018–5137, 56 p., https://doi.org/10.3133/sir20185137.

ISSN 2328-0328 (online)

Contents

Figures

Appendix Figures

Tables

Supplemental Tables

Conversion Factors

U.S. customary units to International System of Units

Multiply	By	To obtain
	Length	
inch (in.)	2.54	centimeter (cm)
foot (ft)	0.3048	meter (m)
mile (mi)	1.609	kilometer (km)
	Area	
square mile (mi^2)	2.590	square kilometer (km^2)
	Flow rate	
foot per day (ft/d)	0.3048	meter per day (m/d)
foot per year (ft/yr)	0.3048	meter per year (m/yr)
cubic foot per second (ft^3/s)	0.02832	cubic meter per second (m^3/s)
inch per year (in/yr)	25.4	millimeter per year (mm/yr)
	Transmissivity	
foot squared per day (ft^2/d)	0.09290	meter squared per day (m^2/d)
	Volume	
gallon (gal)	3.785	liter (L)
gallon (gal)	0.003785	cubic meter (m^3)

Temperature in degrees Fahrenheit (°F) may be converted to degrees Celsius (°C) as follows:

$$°F = (1.8 \times °C) + 32.$$

Datum

Vertical coordinate information is referenced to the North American Vertical Datum of 1988 (NAVD 88).

Horizontal coordinate information is referenced to the North American Datum of 1983 (NAD 83).

Elevation, as used in this report, refers to distance above the vertical datum.

Supplemental Information

The standard unit for transmissivity is cubic foot per day per square foot times foot of aquifer thickness [$(ft^2/d)/ft^2$]ft. In this report, the mathematically reduced form, foot squared per day (ft^2/d), is used for convenience.

Water year is the 12-month period from October 1 through September 30 and is designated by the calendar year in which it ends.

Abbreviations

CHD	Time-Variant Specified-Head (Package)
DRN	Drains (Package)
ElmR	Elm River outflow
EVT	Evapotranspiration (Package)
GPS	global positioning system
H/V	horizontal to vertical
MocC	Moccasin Creek
PEST	Parameter ESTimation (software)
R^2	coefficient of determination
RCH	Recharge (Package)
RIV	River (Package)
RTK	real-time kinematic
SFR2	Stream Flow Routing (Package)
SWB	Soil-Water-Balance (model)
USGS	U.S. Geological Survey
WEL	Wells (Package)
WY	water year

Acknowledgments

The authors thank the City of Aberdeen for their support of past and ongoing studies that provided valuable information for this study.

Several personnel at the U.S. Geological Survey (USGS) assisted with the collection, processing, and analysis of geophysical data. Janet Carter, Brian Clark, Greg Delzer, Mike Fienen, Galen Hoogestraat, Randy Hunt, and Joseph Jones (USGS) provided insightful edits and comments for this report. Andrew Leaf (USGS) calculated and formatted streamflow routing for the groundwater-flow model, and Jennifer Bednar (USGS) contributed estimations of stream base flow.

Revised Groundwater-Flow Model of the Glacial Aquifer System North of Aberdeen, South Dakota, Through Water Year 2015

By Joshua F. Valder, William G. Eldridge, Kyle W. Davis, Colton J. Medler, and Karl R. Koth

Abstract

The city of Aberdeen, in northeastern South Dakota, requires an expanded and sustainable supply of water to meet current and future demands. Conceptual and numerical models of the glacial aquifer system in the area north of Aberdeen were developed by the U.S. Geological Survey in cooperation with the City of Aberdeen in 2012. The U.S. Geological Survey, in cooperation with the City of Aberdeen, completed a study to revise the original numerical groundwater-flow model using data through water year (WY) 2015 to aid the City of Aberdeen in their development of plans and strategies for a sustainable water supply and to increase understanding of the glacial aquifer system and groundwater-flow system near Aberdeen. The original model was revised to improve the fit between model-simulated values and observed (measured or estimated) data, provide greater insight into surface-water interactions, and improve the usefulness of the model for water-supply planning. The revised groundwater-flow model (hereafter referred to as the "revised model") presented in this report supersedes the original model.

The purpose of this report is to describe a revised groundwater-flow model including data collection, model calibration, and model results for the glacial aquifer system including the Elm, Middle James, and Deep James aquifers north of Aberdeen, South Dakota, using updated hydrologic data through WY 2015. The original numerical model was revised in several ways. The model was modified by adding four new layers, which included a surficial layer, two intervening confining layers, and a shale bedrock layer. The revised model provides an improved understanding of the groundwater-flow system in comparison to the original model.

The principal aquifers of the model area include portions of the Elm, Middle James, and Deep James aquifers. The lithologic information used to define and describe the aquifers in the model area was unaltered; however, aquifer properties and boundary conditions were reviewed and updated using geological information reported by the South Dakota Department of Environmental and Natural Resources and information obtained from geophysical investigations for this study. The horizontal extent of the Elm, Middle James, and Deep James aquifers was unaltered from the original model. The thickness of the Deep James aquifer was modified based on interpretations from the geophysical investigations. In general, groundwater in the Elm aquifer flowed from northwest to southeast and locally towards rivers and streams. Similarly, in the Middle James and Deep James aquifers, groundwater also typically flowed southeast.

The revisions made to the original model include use of the following MODFLOW stress packages: Recharge, Evapotranspiration, Time-Variant Specified Head, Wells, Drains, and Stream Flow Routing, all of which were updated from the original model except for the Stream Flow Routing Package, which replaced the River Package used in the original model. Model calibration is the process of estimating model parameters to minimize the differences, or residuals, between observed data and simulated values; therefore, Parameter ESTimation (PEST) software was used to optimize model input parameters by matching model-simulated values to observed data. Calibration parameters included horizontal hydraulic conductivity, vertical hydraulic conductivity, specific yield, specific storage, and vertical streambed conductance for stream and drain cells. Multipliers were used to calibrate the recharge and evapotranspiration stresses. Evapotranspiration extinction depth also was adjusted during model calibration.

Comparisons to the original model are described to highlight the changes made in the revised model. In general, the revised model adequately simulates the natural system and compares favorably with observed hydrologic data. Simulated water levels were evaluated by comparing them to single water-level observations at selected well locations. The selected wells were the same wells used in the original model. The coefficient of determination value between simulated and observed water levels for the revised model was 0.89 and included simulated and observed values from October 1, 1974 (WY 1975), through September 30, 2015 (WY 2015). The coefficient of determination value for the original model was 0.94 and included simulated and observed values from October 1, 1974, through September 30, 2009. The difference may indicate that the original model could

have been overfit to hydraulic head observations because base flow was not simulated. The additional data used in the revised model included some climatically wetter, more extreme periods, such as 2011, in which annual precipitation was 30.9 inches. Average annual precipitation for the original model timeframe, which included data from WYs 1975–2009, was 20.26 inches. Additional precipitation data for WYs 2010–15, included in the revised model timeframe, resulted in an average annual precipitation for WYs 1975–2015 in the model area of 20.6 inches. The larger variability in climate data coupled with the additional water-level data could explain the lower coefficient of determination for water levels in the revised model.

The revised model was used to calculate various groundwater-budget components for steady-state and transient conditions for WYs 1975–2015. The time-variant specified-head cells in the revised model had the largest change when compared to the original steady-state model for inflows and outflows. Comparing the transient budget components between the original and the revised models indicated that inflow from recharge and time-variant specified-head cells had the greatest effect on groundwater inflows, and outflow from storage had the greatest effect on groundwater outflows. The simulated potentiometric contours from the revised model were compared with (1) the observed (interpreted) potentiometric surface (layer 2) and the hydraulic head values (layers 4 and 6) and (2) the simulated contours from the original model. The simulated hydraulic gradients and general direction of groundwater flow in the Elm aquifer in the revised model generally matched the observed potentiometric contours, the simulated potentiometric contours from the original model, and general flow directions interpreted to be perpendicular to the contours. Minor discrepancies between simulated potentiometric contours from the revised model and the observed potentiometric contours may be due to the lack of observed data in the model area.

The revised model was designed to reduce the limitations of the original model. The revisions were validated by comparing the results of the original model with the revised model. A primary benefit of the revised model is the inclusion of the surficial deposits and the confining units as explicit layers in the model. The addition of the surficial layer was beneficial for three primary reasons: (1) more accurate representation of recharge from precipitation, (2) more accurate representation of groundwater evapotranspiration, and (3) more accurate representation of groundwater and surface-water interactions. The groundwater model is a numeric approximation of a complex physical hydrologic system, and the revised model data were interpolated in regions with sparse data. Additionally, model discretization included averaged and interpolated values for water use, withdrawal rates, and hydraulic conductivity. The revised model provides a useful estimate for hydraulic gradients, groundwater-flow directions, and aquifer response to groundwater withdrawals.

Introduction

The city of Aberdeen, in northeastern South Dakota (fig. 1), requires an expanded and sustainable supply of water to meet current and future demands. The city of Aberdeen obtains most of its potable water from the Elm River (Marini and others, 2012); however, during times of low streamflow in the Elm River, groundwater is withdrawn from wells completed in the Elm aquifer, a shallow glacial outwash aquifer about 7 miles (mi) north of Aberdeen. Economic development, increasing population, and a goal to transition the water supply from stream water to groundwater require the city of Aberdeen to reassess its water-supply sources. Conceptual and numerical models of the glacial aquifer system in the area north of Aberdeen were developed by the U.S. Geological Survey (USGS) in cooperation with the City of Aberdeen in 2012 and are described by Marini and others (2012). The USGS, in cooperation with the City of Aberdeen, completed a study to revise the original numerical model by Marini and others (2012; hereafter referred to as the "original model") using data through water year (WY) 2015 (a WY is the 12-month period from October 1 through September 30 and is designated by the calendar year in which it ends). The study's purpose was to aid the City of Aberdeen in their development of plans and strategies for a sustainable water supply and to increase understanding of the glacial aquifer system and groundwater-flow system near Aberdeen. The original model was revised to improve the fit between model-simulated and observed (measured and estimated) data, provide greater insight into surface-water interactions, and improve the usefulness of the model for water-supply planning. The revised groundwater-flow model (hereafter referred to as the "revised model") presented in this report supersedes the original model.

The original model (Marini and others, 2012) used the USGS finite-difference groundwater model MODFLOW-2005 (Harbaugh, 2005) to simulate groundwater flow in the glacial aquifer system. The revised model used the USGS finite-difference groundwater-flow model MODFLOW-NWT, developed by Niswonger and others (2011). In addition to updating the finite-difference model version, the original model was revised in several other ways. The original model was modified by adding four new layers, which included a surficial layer, two intervening confining layers, and a shale bedrock layer. Additionally, the structural hydrogeology, specifically the thickness of the Deep James aquifer, was modified with data collected in 2014 from noninvasive subsurface geophysical mapping of the bedrock topology (see supplemental table 1.1). Recharge and evapotranspiration estimates also were updated, and the simulation period was increased from 35 years to 41 years, ending in September 2015. Finally, the revised model simulated routed stream base flow in the study area (hereafter referred to as "model area"); the original model used nonrouted streams. The revised model provides an improved understanding of the groundwater-flow system in comparison to the original model.

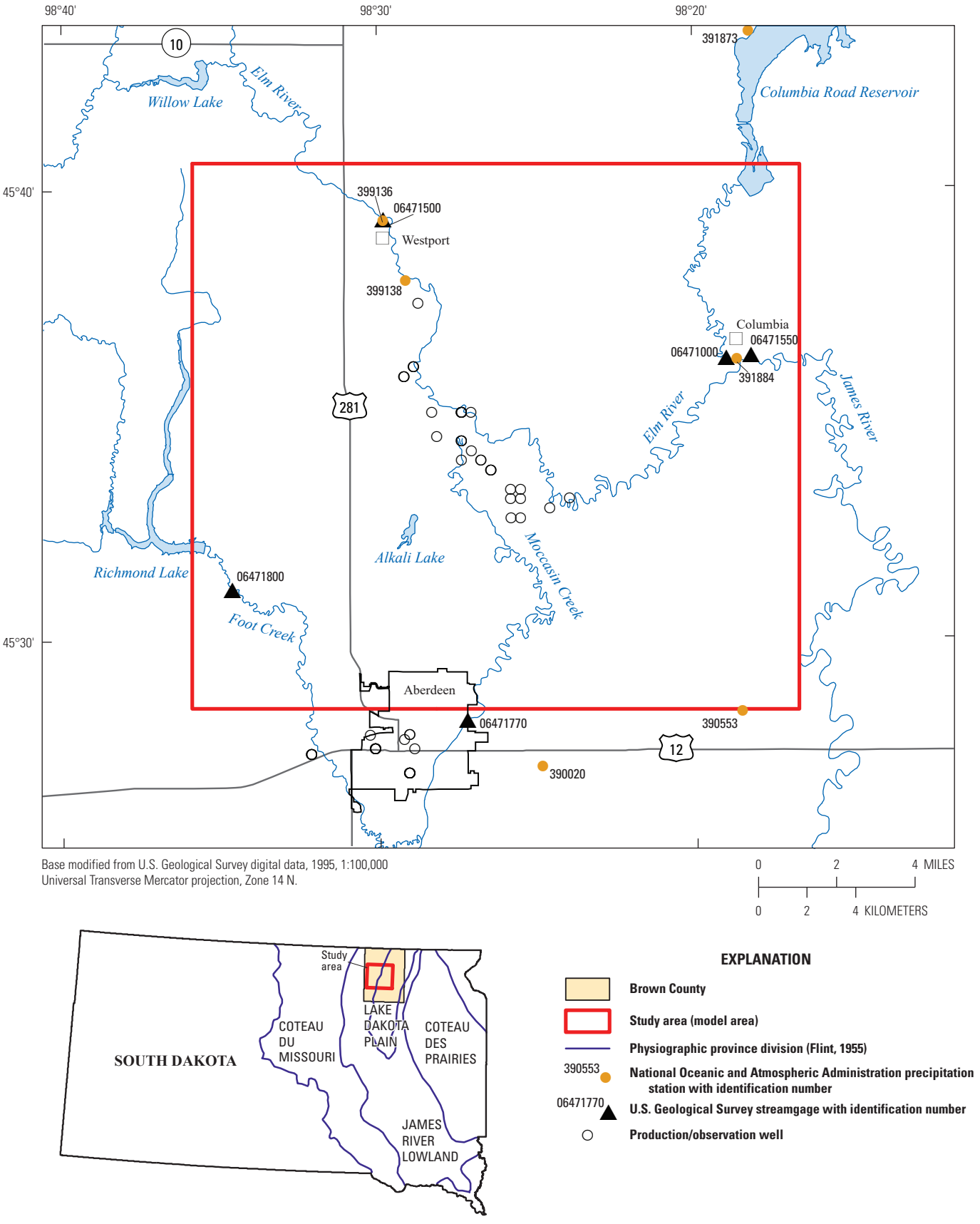

Figure 1. Locations of study area (model area), streamgages, precipitation stations, and production/observation wells. Inset shows model area location in Brown County and physiographic provinces in eastern South Dakota (Flint, 1955).

Purpose and Scope

The purpose of this report is to describe a revised groundwater-flow model including data collection, model calibration, and model results for the glacial aquifer system including the Elm, Middle James, and Deep James aquifers north of Aberdeen, South Dakota, using updated hydrologic data through WY 2015. To document the model revision process, this report describes (1) revisions to the original model described by Marini and others (2012), (2) boundary conditions and model input parameters, (3) calibration approach, (4) water-budget calculations, and (5) sensitivity analysis. The geophysical investigations used to characterize the subsurface using noninvasive subsurface methods as part of this study are described in the appendix of this report. The revised model is available as a USGS data release (Eldridge and others, 2018).

Location and Description of Model Area

The city of Aberdeen is in Brown County in northeastern South Dakota. The model area encompasses 490 square miles (mi^2) north of Aberdeen in the James River Lowland and Lake Dakota Plain physiographic provinces (fig. 1). The study area, which is the same area used for the groundwater-flow model (model area), includes the glacial aquifer system north of Aberdeen between Foot Creek and the James River, where assessment of the groundwater resources is needed. A total of 4 USGS streamgages and 6 National Oceanic and Atmospheric Association precipitation stations are in or near the model area. Data from streamgages and precipitation stations were used for model input and calibration. The model boundary, grid location, and grid resolution for the revised model were unchanged from the original model.

Previous Investigations

Marini and others (2012) constructed the original model and described the conceptual model of the glacial aquifer system north of Aberdeen. In addition to Marini and others (2012), several authors, including Rothrock (1955), Tipton (1977), Emmons (1987, 1990), and Schaap (2000), have characterized the water resources of the model area. Geologic and hydrogeologic characterizations of the glacial aquifers of the region were completed by Koch and Bradford (1976) and Leap (1986).

Hydrogeologic Setting

The principal aquifers of the model area include parts of the Elm, Middle James, and Deep James aquifers. Koch and Bradford (1976) and Marini and others (2012) published descriptions, extents, and depths of the three aquifers. In general, the aquifers consist primarily of interbedded layers of gravel, sands, and silts. Interbedded tills and clays exist between the Elm and Middle James aquifers and between the Middle James and Deep James aquifers. These interbedded tills and clays form confining layers between the aquifers. The confining layers typically are present across the model area; however, as described in Marini and others (2012), confining layers may be absent in some areas.

Depths below land surface range from 15 to 100 feet (ft) for the Elm aquifer, from 40 to 250 ft for the Middle James aquifer, and from 125 to 390 ft for the Deep James aquifer. The Cretaceous-age Pierre Shale, composed of shale and claystone, underlies the Deep James aquifer. The Pierre Shale has a thickness of as much as 1,000 ft (Crandell, 1958) with low permeability in the model area.

The three aquifers in the model area receive recharge by various mechanisms. The Elm aquifer is recharged primarily from precipitation infiltration (Koch and Bradford, 1976); however, the Middle James and Deep James aquifers receive recharge from a hydrologic connection with overlying aquifers (Koch and Bradford, 1976; Emmons, 1990). Discharge from the Elm aquifer is attributed to evapotranspiration and discharge into rivers, including the Elm River and Foot Creek. Discharge from the Middle and Deep James aquifers is attributed primarily to losses to other adjoining aquifer units (Marini and others, 2012).

Geophysical Investigations

Two noninvasive subsurface geophysical techniques were used to map subsurface materials in the model area. First, microgravity measurements were collected with a Scintrex CG–5 relative gravimeter to better characterize the volume of unconsolidated material above the Pierre Shale using field methods similar to those described in Koth and Long (2012). Second, passive seismic methods were used to supplement lithologic information and to improve depth to bedrock mapping using methods described by Lane and others (2008). Both techniques were used to refine the geometry of the Deep James aquifer and to identify potential locations that may provide sustainable groundwater supplies. The geophysical survey points were selected to include areas overlying the Elm, Middle James, and Deep James aquifers. Additional geophysical measurements were collected in areas that were potential locations for additional production wells. In general, the surveys followed section lines and roadways to ensure land access. The locations of sites measured during the microgravity and passive seismic surveys are shown in figure 2. The appendix provides additional details regarding the techniques and methods used to analyze the geophysical surveys and survey results (supplemental table 1.1 and table 1.2).

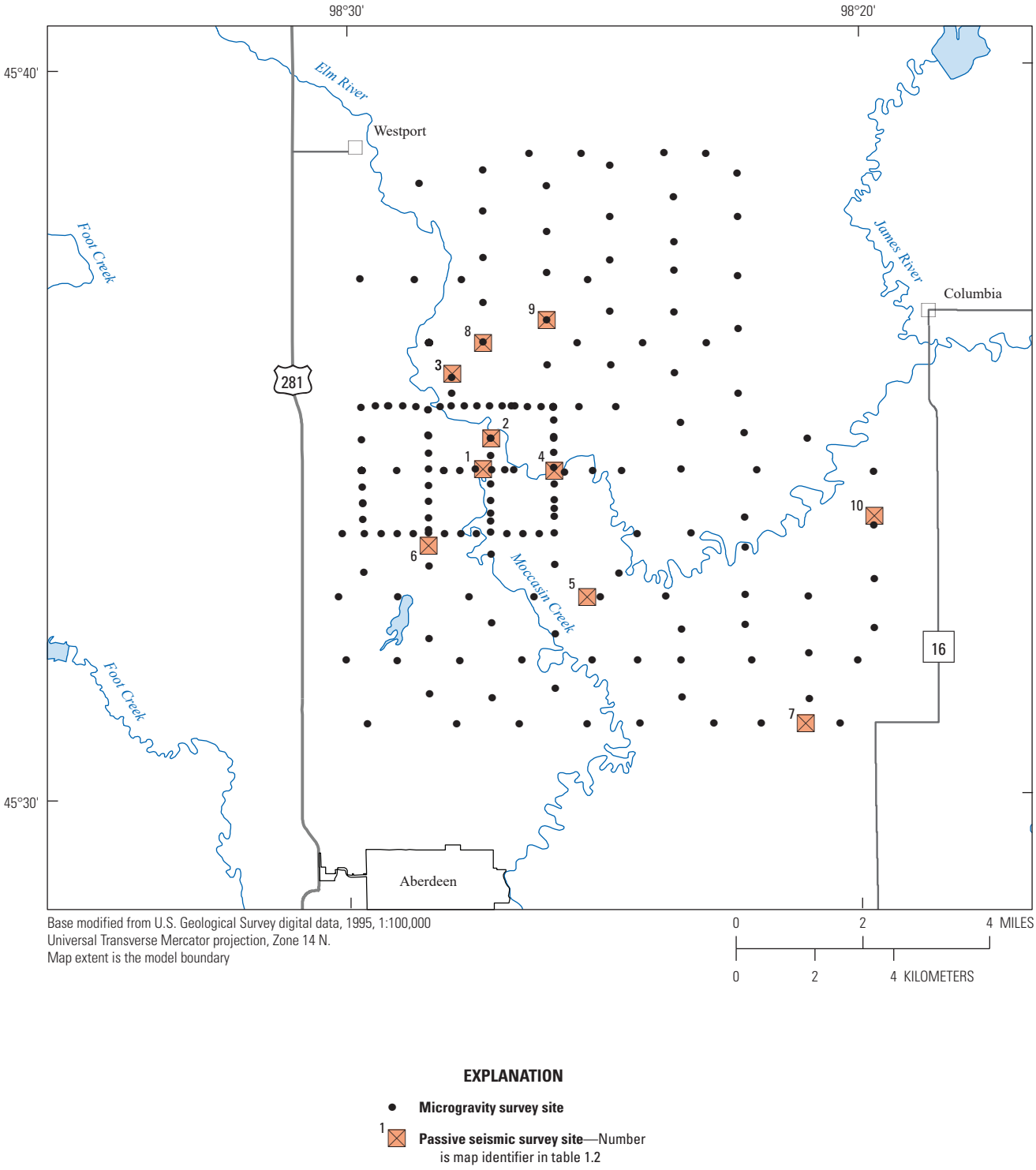

Figure 2. Microgravity and passive seismic survey sites in the model area north of Aberdeen, South Dakota.

Representation of Conceptual Model in Revised Groundwater-Flow Model

Marini and others (2012) described the conceptual model, hydrogeologic framework, groundwater flow, hydrologic properties, and water budget of the original model. In general, Marini and others (2012) described the conceptual model of the glacial aquifer system as having sand and gravel units within the glacial deposits for the Elm, Middle James, and Deep James aquifers. Each aquifer is separated and overlain by confining layers of glacial till with some interaction between aquifers where the confining glacial till is missing (Marini and others, 2012). The general direction of groundwater flow is towards the southeast, and the aquifers are generally transmissive (Marini and others, 2012). Data collected or compiled after 2009 were used to adjust the hydrogeologic framework, groundwater flow, and Soil-Water-Balance (SWB) model (Westenbroek and others, 2010) used in the revised model. The SWB model calculates recharge based on a modified Thornthwaite-Mather SWB approach (Thornthwaite, 1948; Thornthwaite and Mather, 1957) as further described in the "Precipitation Recharge and Groundwater Evapotranspiration" section.

The conceptual model described by Marini and others (2012) was not changed for this study; however, the aquifers and intervening confining units were represented differently, as described in the following "Hydrogeologic Framework" section. For example, in the original model, the surficial deposits overlying the Elm aquifer and the confining layers between the aquifers were not explicitly simulated; however, the surficial deposits and confining layers were included in the revised model. The revised model includes 7 model layers representing the following: surficial deposits, 3 aquifer units, 2 confining units, and the underlying low-permeability bedrock (fig. 3). The conceptual model also describes the primary groundwater stresses including evapotranspiration, well withdrawal, losses and gains to rivers and streams, and groundwater flux at the model boundaries (fig. 3).

Hydrogeologic Framework

The lithologic information used by Marini and others (2012) to define and describe the aquifers in the model area was unaltered; however, aquifer properties and boundary conditions were reviewed and updated using geological information reported by the South Dakota Department of Environmental and Natural Resources (South Dakota Geological Survey, 2017) and information obtained from the geophysical investigations. The horizontal extent of the Elm, Middle James, and Deep James aquifers was unaltered from the original model. The thickness of the Deep James aquifer was modified based on interpretations from the geophysical investigations.

The surficial deposits overlying the Elm aquifer were not explicitly simulated in the original model but were included as a separate layer in the revised model. The original model numerically accounted for the surficial deposits by adjusting input parameters (namely, recharge). The thickness of the surficial deposits in the revised model was calculated as the difference between the land-surface elevation from Landsat 10-meter (m) digital elevation models (https://nationalmap.gov/) and the elevation of the top of the Elm aquifer from Marini and others (2012).

Confining layers exist between the Elm and Middle James aquifers and between the Middle James and Deep James aquifers. These confining layers were not explicitly simulated by the original model. In the original model, the confining layers were numerically accounted for using quasi-three-dimensional confining layers between aquifers. In the revised model, the confining layers were represented numerically as individual model layers. The horizontal extent and thickness of the confining layers were determined using overlying and underlying aquifer extents and elevations from the original model. The Pierre Shale, which underlies the Deep James aquifer, was added as a model layer. The bottom elevation of the Pierre Shale was assigned an arbitrary value of 900 ft below the North American Vertical Datum of 1988 (NAVD 88) with a bottom layer approximately 100 ft thick. In general, the Pierre Shale represents the underlying low-permeability layer in the model area; however, it was added to the revised model to allow minimal interaction of groundwater at the base of the Deep James aquifer and to provide stability to the numerical solution.

Groundwater Flow

Marini and others (2012) determined groundwater-flow directions from potentiometric maps and hydraulic head values of each aquifer. Water levels in 91 wells were used to map potentiometric contours for the Elm aquifer. In general, groundwater in the Elm aquifer flowed from northwest to southeast, and locally towards rivers and streams, which matched results from Koch and Bradford (1976) and Emmons (1990). Groundwater in the Middle James and Deep James aquifers also typically flowed southeast; however, groundwater flow in the Deep James aquifer was relatively slow, as represented by the shallow gradient of its mapped potentiometric contours (Emmons, 1990; Marini and others, 2012).

Marini and others (2012) mapped the average potentiometric surface of the Elm aquifer using water-level data from WYs 1975–2009 using 91 wells completed in the Elm aquifer. Observation wells with multiple records and single water-level measurements were used to construct the potentiometric surface. Few data were available to construct average potentiometric surface maps for the Middle James and Deep James aquifers (Marini and others, 2012); however, maps modified by Emmons (1990) were used for comparisons by Marini and others (2012). Wells completed in the Elm, Middle James, and Deep James aquifers that had single water-level measurements before WY 1975 were included to supplement

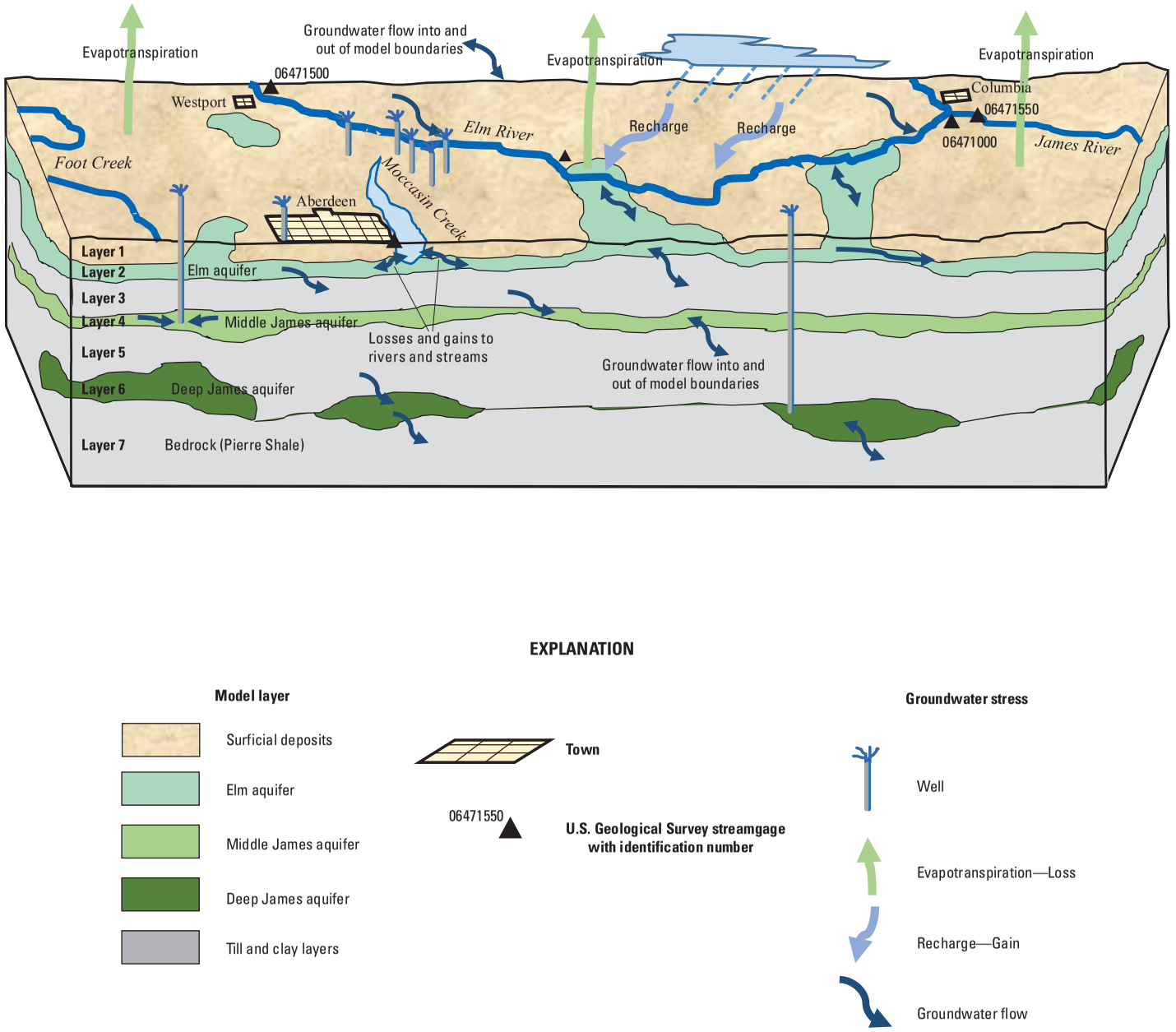

Figure 3. Representation of the conceptual model for seven model layers in the model area north of Aberdeen, South Dakota (not drawn to scale). Layer 1 includes surficial deposits; layers 2, 4, and 6 represent the Elm, Middle James, and Deep James aquifers, respectively; and layers 3, 5, and 7 are confining units. Groundwater stresses for the system include evapotranspiration, well withdrawals, losses and gains to rivers and streams, and flow into and out of the model boundaries.

data in areas where long-term water-level data did not exist. The revised model included groundwater-level measurements for WYs 2010–15 for five wells (BN–77L, BN–82E, BN–77M, BN–82F, and BN–82K) and WYs 2010–14 for one well (BN–77V) completed in the Elm aquifer in the model area. These additional data supplemented the water-level data used by Marini and others (2012) and are listed in supplemental table 1.3. All water-level data used to map the potentiometric surfaces for this study are available in the USGS National Water Information System database (U.S. Geological Survey, 2017).

The water-level data from the 91 wells (including data through 2015) completed in the Elm aquifer were used to interpolate an updated generalized average potentiometric surface in the model area for WYs 1975–2015 (fig. 4). The average hydraulic head and well identifier are shown for each well (fig. 4) and summarized in supplemental table 1.3. Sufficient information was not available to produce potentiometric maps for the Middle James and Deep James aquifers. The hydraulic head values are shown for wells completed in the Middle James and Deep James aquifers in figure 4. Hydraulic head measurements from 10 wells completed in the Middle James aquifer were available from 1949 to 1984, and hydraulic head measurements from 5 wells completed in the Deep James aquifer were available from 1926 to 1984.

Precipitation Recharge and Groundwater Evapotranspiration

Recharge to the aquifers in the model area is from infiltration of precipitation below the root zone in the surficial deposits. Groundwater evapotranspiration, which is discharge from the aquifer that is from direct evaporation from the aquifer and plant transpiration, typically is where the water table is at or near the land surface (Marini and others, 2012). The spatial and temporal distribution of recharge and potential evapotranspiration in the model area was estimated using the SWB model (Westenbroek and others, 2010), which calculates recharge based on a modified Thornthwaite-Mather SWB approach (Thornthwaite, 1948; Thornthwaite and Mather, 1957). The SWB model estimated precipitation recharge and potential evapotranspiration for calendar years 1970–2015 (Eldridge and others, 2018), and results for WYs 1975–2015 are presented in this report. An initial SWB model start-up period, January 1, 1970–September 30, 1974, was completed to provide the model estimated antecedent conditions for soil moisture and snow cover for WYs 1975–2015. Potential evapotranspiration is the amount of water that can be removed from the system if there never was a deficiency of water in the soil for use by vegetation (Wilson and Moore, 1998); therefore, actual groundwater evapotranspiration is calculated by the numerical model (described in the "Revised Groundwater-Flow Model" and "Numerical Model Results" sections), and actual groundwater evapotranspiration is equivalent to potential evapotranspiration when the water table is at the land surface and decreases linearly to 0 below the root zone (extinction depth; Harbaugh, 2005).

The SWB model calculates recharge on a daily time step as the difference between the sources and sinks of water in a model cell and the change in soil moisture. Primary inputs for the SWB model are precipitation and temperature data, land-use characteristics, and available soil-water capacity. Marini and others (2012) provided a full description of SWB model inputs. The SWB input files used in the revised model were updated to include additional climate data from October 1, 2009, through September 30, 2015. Climate data compiled for this study (January 1, 1970, through December 31, 2015) are available as a USGS data release (Eldridge and others, 2018).

Precipitation data through WY 2009 were compiled by Marini and others (2012) from six National Oceanic and Atmospheric Administration climate stations; for the revised model, additional precipitation data through WY 2015 were compiled from these same precipitation stations (fig. 1; National Climatic Data Center, 2017). Two stations had long-term precipitation data and four stations had shorter periods of data. The Columbia climate station (391884) had the longest period of precipitation recorded followed by the Aberdeen Regional Airport (390020). The average precipitation and temperature for the model area were calculated using the average of the available daily data from each climate station. Average annual precipitation for the original model timeframe, which included data from WYs 1975–2009, was 20.26 inches (in.). Additional precipitation data for WYs 2010–15, included in the revised model timeframe, resulted in an average annual precipitation for WYs 1975–2015 in the model area of 20.6 in. (National Climatic Data Center, 2017).

Temperature data also were collected from three National Oceanic and Atmospheric Association climate stations located in the model area for the revised model (fig. 1). Marini and others (2012) reported temperature data from two of the three climate stations in the model area; the average monthly temperature from 1971 through 2000 for January was 9.6 degrees Fahrenheit (°F), and the average monthly temperature for July was 71.7 °F. Using data for all three climate stations for the period 1971 through 2015 indicated that the average monthly temperature for January was 10.9 °F, and the average monthly temperature for July was 72.1 °F (National Climatic Data Center, 2017), which are higher than those compiled for the original model.

The SWB-calculated recharge and potential evapotranspiration were used as initial values in the revised model. These initial estimates of recharge and potential evapotranspiration were adjusted during model calibration (described in the "Groundwater Model Calibration" section). The SWB-calculated average annual recharge rate for the model area for WYs 1975–2015 was 0.59 in., and the annual average recharge rate ranged from 0 to about 19.7 inches per year (in/yr) spatially (fig. 5). Recharge rates typically were higher near rivers, along gravel roads, and in areas where the surficial deposits are thin; for example, where the surficial deposit thicknesses are between 0 and 10 ft (fig. 9 in Marini and others, 2012).

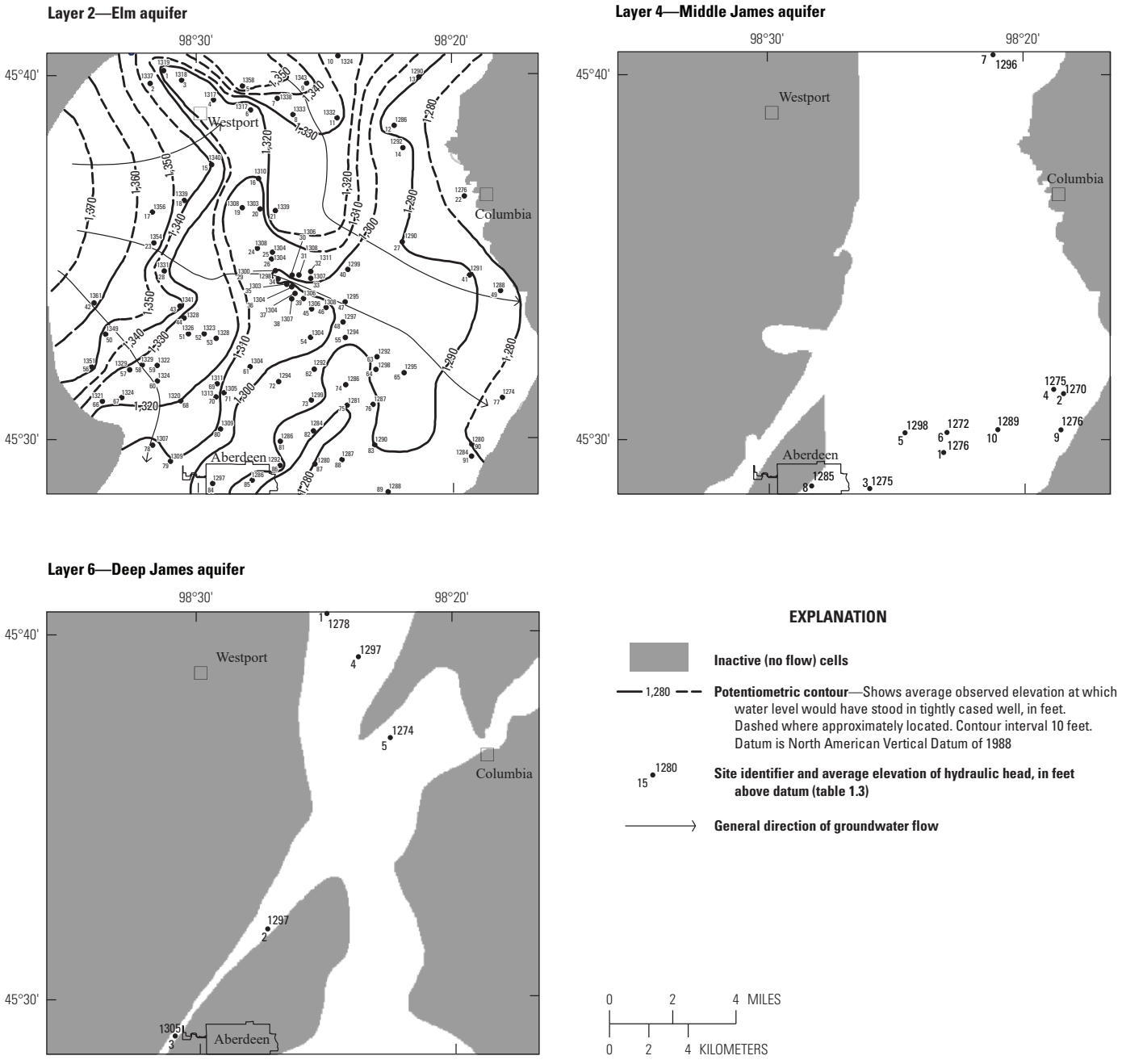

Figure 4. Generalized contours of the average potentiometric surface and groundwater flow direction (water years 1975–2015) for the Elm aquifer, and hydraulic head values for the Middle James and Deep James aquifers in the model area.

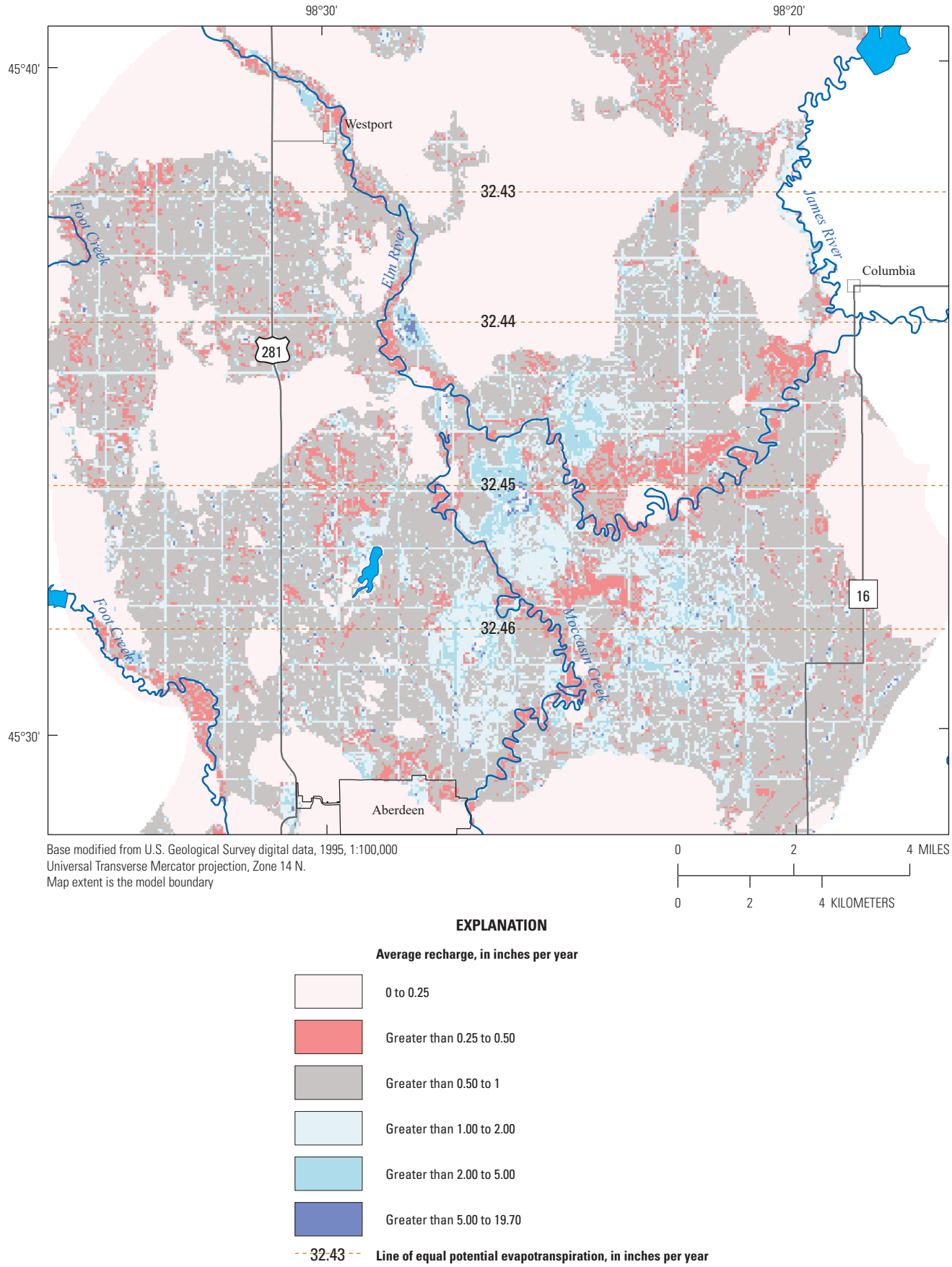

Figure 5. Average annual recharge rate and potential evapotranspiration rate in the model area north of Aberdeen, South Dakota, calculated using the Soil-Water-Balance model for water years 1975–2015.

The SWB-calculated average annual potential evapotranspiration rate in the model area for calendar year 1975–2015 was 32.4 in/yr. Annual average potential evapotranspiration rates ranged from 28.6 in/yr (calendar year 1996) to 38.4 in/yr (calendar year 1976). In the original model, potential evapotranspiration rates were adjusted spatially by till thickness using the method described by Marini and others (2012). The greater the till thickness, the smaller the multiplier value. The revised model no longer needed the till thickness multiplier described in Marini and others (2012) because the revised model numerically simulates the upper surficial deposits as a layer. The average annual SWB-calculated potential evapotranspiration rates varied spatially along lines of latitude because the rate was calculated using the Hargreaves method (Hargreaves and Samani, 1985), which requires inputs of average, minimum, and maximum air temperatures as well as latitude boundaries (Westenbroek and others, 2010). In the model area, the SWB-calculated average annual potential evapotranspiration rate ranged from 32.43 in/yr to 32.46 in/yr (fig. 5).

Groundwater and Surface-Water Interactions

The shallow glacial outwash deposits of the Elm aquifer are highly connected to surface-water features in the model area (Marini and others, 2012). Base flow is the portion of streamflow that is not attributed to direct runoff from precipitation or snowmelt (Wilson and Moore, 1998), and it generally represents the groundwater contribution to streamflow. Base flow is an important proxy to estimate the amount of groundwater from aquifers discharging to streams, and it is critical for sustaining surface-water flows (Miller and others, 2016). To better understand the interaction of groundwater and surface water, estimates of base flow were calculated at the Elm River at Westport, S. Dak., and Foot Creek near Aberdeen, S. Dak. (USGS streamgages 06471500 and 06471800, respectively), using the hydrograph separation method, PART (Rutledge, 1998) with streamflow measurements available from the U.S. Geological Survey (2017). Estimates of base flow at Moccasin Creek at Aberdeen, S. Dak. (USGS streamgage 06471770), and at the confluence of the Elm and James Rivers near Columbia, S. Dak. (fig. 1), were based on Marini and others (2012) because no new data were available at these locations.

Revised Groundwater-Flow Model

Changes to the original model were made to improve the comparison of model-simulated results to observed (measured or estimated) data, provide greater insight into groundwater and surface-water interactions, and improve the usefulness of the model for water-supply planning. This section describes revisions made to the original model design and documents the updates within the revised model MODFLOW packages. The revised model for this study and associated data are available in Eldridge and others (2018).

Model Design

The original model (Marini and others, 2012) used the USGS finite-difference groundwater model MODFLOW-2005 (Harbaugh, 2005) to simulate groundwater flow in the glacial aquifer system for WYs 1975–2009. The revised model uses the USGS finite-difference groundwater-flow model MODFLOW-NWT, developed by Niswonger and others (2011), and was used to simulate WYs 1975–2015. The revisions made to the original model include use of the following MODFLOW stress packages: Recharge (RCH; Harbaugh and others, 2000), Evapotranspiration (EVT; McDonald and Harbaugh, 1988), Time-Variant Specified Head (CHD; Harbaugh and others, 2000), Wells (WEL; Harbaugh and others, 2000), Drains (DRN; Harbaugh, 2005), and Stream Flow Routing (SFR2; Niswonger and Prudic, 2005), all of which were updated from the original model except for the SFR2 Package. In the revised model, the SFR2 Package replaced the River (RIV) Package, which was used in the original model, to better simulate the interaction of groundwater and surface water and to provide estimates of routed stream base flow. The updates to the temporal, spatial, and vertical discretization, hydraulic properties, and stress packages (boundary conditions) are described in the following subsections.

Temporal Discretization

The revised model was used to simulate aquifer conditions for the period beginning on October 1, 1974 (WY 1975) and ending September 30, 2015 (WY 2015). The revised model period was discretized into 99 stress periods and included an initial steady-state stress period representing long-term average conditions followed by 98 stress periods of differing lengths (table 1). The original model included a pseudo-steady-state stress period to approximate steady-state conditions, and aquifer storage was simulated with a value close to zero; however, the revised model included a steady-state stress period without an aquifer storage value. The revised model used the original model initial conditions and data for the first 75 stress periods (through September 30, 2009). The initial hydraulic head condition was based on the average of hydrologic data from WYs 1975–2015 (420 months). Additional hydrologic data from October 1, 2009, through September 30, 2015, were included in the revised model and combined into 24 additional seasonal stress periods (stress periods 76 through 99 in table 1). The additional seasonal stress periods for the revised model followed the monthly combinations used in the original model and resulted in four seasonal stress periods per year. The four seasonal stress periods represented the combination of aquifer stress for October through February (5 months), March through April (2 months), May through June (2 months), and July through September (3 months) for each WY.

Table 1. Simulated stress periods, water years 1975–2015, for the revised groundwater-flow model.

[--, not representative of a specific time frame but represents long-term average conditions]

Stress period (SP)	Beginning date	Ending date	Stress length, in months
SP1	--	--	--
SP2	10/01/1974	09/30/1975	12
SP3	10/01/1975	09/30/1976	12
SP4	10/01/1976	09/30/1977	12
SP5	10/01/1977	09/30/1978	12
SP6	10/01/1978	09/30/1979	12
SP7	10/01/1979	02/29/1980	5
SP8	03/01/1980	04/30/1980	2
SP9	05/01/1980	06/30/1980	2
SP10	07/01/1980	09/30/1980	3
SP11	10/01/1980	02/28/1981	5
SP12	03/01/1981	04/30/1981	2
SP13	05/01/1981	06/30/1981	2
SP14	07/01/1981	09/30/1981	3
SP15	10/01/1981	02/28/1982	5
SP16	03/01/1982	04/30/1982	2
SP17	05/01/1982	06/30/1982	2
SP18	07/01/1982	09/30/1982	3
SP19	10/01/1982	09/30/1983	12
SP20	10/01/1983	09/30/1984	12
SP21	10/01/1984	09/30/1985	12
SP22	10/01/1985	09/30/1986	12
SP23	10/01/1986	09/30/1987	12
SP24	10/01/1987	09/30/1988	12
SP25	10/01/1988	09/30/1989	12
SP26	10/01/1989	09/30/1990	12
SP27	10/01/1990	09/30/1991	12
SP28	10/01/1991	09/30/1992	12
SP29	10/01/1992	09/30/1993	12
SP30	10/01/1993	09/30/1994	12
SP31	10/01/1994	09/30/1995	12
SP32	10/01/1995	09/30/1996	12
SP33	10/01/1996	09/30/1997	12
SP34	10/01/1997	09/30/1998	12
SP35	10/01/1998	09/30/1999	12
SP36	10/01/1999	02/29/2000	5
SP37	03/01/2000	04/30/2000	2
SP38	05/01/2000	06/30/2000	2
SP39	07/01/2000	09/30/2000	3
SP40	10/01/2000	02/28/2001	5
SP41	03/01/2001	04/30/2001	2
SP42	05/01/2001	06/30/2001	2
SP43	07/01/2001	09/30/2001	3
SP44	10/01/2001	02/28/2002	5
SP45	03/01/2002	04/30/2002	2
SP46	05/01/2002	06/30/2002	2
SP47	07/01/2002	09/30/2002	3
SP48	10/01/2002	02/28/2003	5
SP49	03/01/2003	04/30/2003	2
SP50	05/01/2003	06/30/2003	2
SP51	07/01/2003	09/30/2003	3
SP52	10/01/2003	02/29/2004	5
SP53	03/01/2004	04/30/2004	2
SP54	05/01/2004	06/30/2004	2
SP55	07/01/2004	09/30/2004	3
SP56	10/01/2004	02/28/2005	5
SP57	03/01/2005	04/30/2005	2
SP58	05/01/2005	06/30/2005	2
SP59	07/01/2005	09/30/2005	3
SP60	10/01/2005	02/28/2006	5
SP61	03/01/2006	04/30/2006	2
SP62	05/01/2006	06/30/2006	2
SP63	07/01/2006	09/30/2006	3
SP64	10/01/2006	02/28/2007	5
SP65	03/01/2007	04/30/2007	2
SP66	05/01/2007	06/30/2007	2
SP67	07/01/2007	09/30/2007	3
SP68	10/01/2007	02/29/2008	5
SP69	03/01/2008	04/30/2008	2
SP70	05/01/2008	06/30/2008	2
SP71	07/01/2008	09/30/2008	3
SP72	10/01/2008	02/28/2009	5
SP73	03/01/2009	04/30/2009	2
SP74	05/01/2009	06/30/2009	2
SP75	07/01/2009	09/30/2009	3
SP76	10/1/2009	2/28/2010	5
SP77	3/1/2010	4/30/2010	2
SP78	5/1/2010	6/30/2010	2
SP79	7/1/2010	9/30/2010	3
SP80	10/1/2010	2/28/2011	5
SP81	3/1/2011	4/30/2011	2
SP82	5/1/2011	6/30/2011	2
SP93	7/1/2011	9/30/2011	3
SP84	10/1/2011	2/28/2012	5
SP85	3/1/2012	4/30/2012	2
SP86	5/1/2012	6/30/2012	2
SP87	7/1/2012	9/30/2012	3
SP88	10/1/2012	2/28/2013	5
SP89	3/1/2013	4/30/2013	2
SP90	5/1/2013	6/30/2013	2
SP91	7/1/2013	9/30/2013	3
SP92	10/1/2013	2/28/2014	5
SP93	3/1/2014	4/30/2014	2
SP94	5/1/2014	6/30/2014	2
SP95	7/1/2014	9/30/2014	3
SP96	10/1/2014	2/28/2015	5
SP97	3/1/2015	4/30/2015	2
SP98	5/1/2015	6/30/2015	2
SP99	7/1/2015	9/30/2015	3

Spatial Discretization

In the revised model, the spatial discretization, cell size, and number of rows and columns were unchanged from the original model (Marini and others, 2012). Each layer of the finite-difference grid consists of 368 rows and 410 columns with a cell size of 200 by 200 ft. The grid orientation is north-south with no rotation and an upper left corner coordinate of latitude 16,595,275.20 ft N and longitude 1,743,237.98 ft W, in Universal Transverse Mercator, Zone 14 North (Eldridge and others, 2018).

Vertical Discretization

The revised model was used to simulate seven stratigraphic layers (fig. 3): surficial deposits (layer 1), the Elm aquifer (layer 2), the intervening confining layer of till and silt between the Elm and Middle James aquifers (layer 3), the Middle James aquifer (layer 4), the intervening confining layer between the Middle James and Deep James aquifers (layer 5), the Deep James aquifer (layer 6), and a layer to represent the lower confining unit of the Pierre Shale bedrock below the Deep James aquifer (layer 7). The surficial deposit layer (layer 1) was included to provide a more accurate representation of groundwater and surface-water interactions. The three confining layers were added to represent the conceptual model more accurately and to allow for a more complete water-budget analysis.

The layer elevations were determined using the aquifer tops and bottoms for the Elm and Middle James aquifers from the original model. For layer 1 (surficial deposits), a Landsat 10-m digital elevation model was used to determine the top (land surface) elevation (https://nationalmap.gov/), and the bottom elevation was defined using the elevation of the top of the Elm aquifer from the original model. The bottom elevation of the Elm aquifer defined the top of the confining unit (layer 3). The bottom elevation of layer 3 was the same as the top elevation of the Middle James aquifer from the original model. The aquifer top and bottom elevations in the original model were derived from lithologic logs available from the South Dakota Geological Survey (2017), and the same elevations were used in the revised model, except for the bottom of the Deep James aquifer. The top and bottom elevations from the original model were used to define the Middle James aquifer (layer 4), and the bottom elevations were used to define the top of layer 5. The top elevation of the Deep James aquifer (layer 6) from the original model was used to define the bottom elevation of layer 5; however, the bottom elevation of the Deep James aquifer was revised from the original model based on results of the geophysical investigations.

The thickness of layer 6, representing the Deep James aquifer, was determined using interpretations from the geophysical investigations. Marini and others (2012) determined the extent and thickness of the Deep James aquifer using the interpretation by Leap (1986) and modifying the bedrock map using lithological logs from driller's reports and test holes. In the original model, the thickness of the Deep James aquifer ranged from less than 10 to 165 ft in the central and northern parts of the model area. For the revised model, microgravity and passive seismic surveys were used to interpret the elevation of top of bedrock (Pierre Shale) in the model area (see appendix for additional details and Eldridge and others [2018] for the revised top of Pierre Shale [top of model layer 7]). Using the revised interpreted elevation of the top of the Pierre Shale along with the elevation of the top of Deep James aquifer from the original model, a revised thickness map of the Deep James aquifer was constructed (fig. 6*B*). The horizontal extents of the Deep James aquifer were unchanged from the original model (fig. 6*A*); however, the aquifer's thickness decreased in some areas and increased in others based on the geophysical interpretations. The revised thickness of the Deep James aquifer ranged from about 5 to 99 ft (fig. 6*B*), and the average revised thickness was about 9 ft (fig. 7*B*), compared to Marini and others (2012) thickness of the Deep James aquifer, which ranged from less than 1 to 165 ft, with an average thickness of 23 ft.

The bottom of layer 7 was set to an arbitrary elevation of 900 ft below NAVD 88. For model stability, a minimum of thickness of 5 ft was assigned to the active portions of each layer. Layer thickness varied within each of the model layers, and the range of thickness is shown in figure 7.

The horizontal extents of the aquifers were not changed from the original model. The boundaries for the additional layers in the revised model were clipped to the appropriate adjoining aquifer because the effect of the extents of the additional layers beyond each aquifer's boundaries was not considered substantial. For example, the active model extent for layer 1 was clipped to match the active area for layer 2 (the Elm aquifer). Similarly, the active extent of layer 3 was clipped to match layer 4 (the Middle James aquifer). Confining layers 5 and 7 were clipped to match the extents of layer 6 (the Deep James aquifer). The horizontal extents and thicknesses (minimum, maximum, and average) of the model layers used in the revised model are shown in figure 7.

Hydraulic Properties

Simulated hydraulic properties for each model layer included specific yield (unitless), specific storage (per foot), horizontal hydraulic conductivity (feet per day), vertical hydraulic conductivity (feet per day), and vertical bed conductance (feet squared per day) for stream cells and drain cells. Precalibration hydraulic property values for the Elm, Middle James, and Deep James aquifers in the revised model were modified from the calibrated values from the original model (table 13 in Marini and others, 2012) by including additional values for the added model layers. Initial hydraulic property values and calibration ranges for the surficial deposits in layer 1 were assigned values and allowed calibration constraints based on the deposit type (Freeze and Cherry, 1979). Confining layers 3, 5, and 7 also were assigned initial hydrologic property values and constraints based on the general

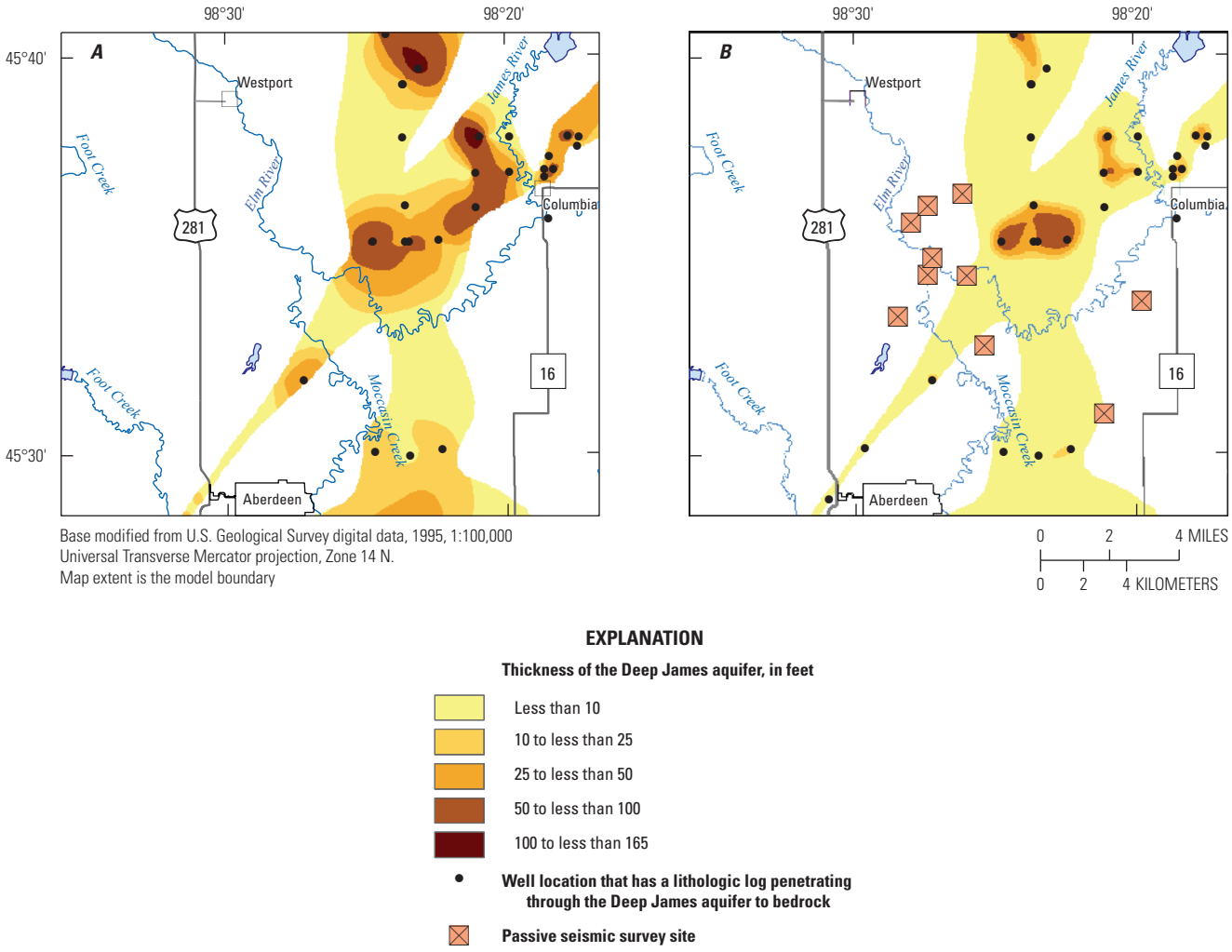

Figure 6. Interpreted thickness of the Deep James aquifer, locations of wells with lithologic logs fully penetrating the Deep James aquifer, and passive seismic survey sites. *A*, original model (Marini and others, 2012); and *B*, revised model.

values for silts and clays from Freeze and Cherry (1979). The spatial distribution of hydraulic properties in the model area was determined during model calibration.

Boundary Conditions

The revised model simulated aquifer stresses using several boundary conditions (MODFLOW stress packages) and include the CHD, RCH, EVT, WEL, DRN, and SFR2 Packages (Harbaugh and others, 2000; Harbaugh, 2005; Niswonger and Prudic, 2005). The RIV Package used in the original model was replaced with the SFR2 Package to simulate routed stream base flow. Additional information on the various aquifer stresses is provided in this section, and complete descriptions of various MODFLOW stress packages are available through USGS online resources (Winston, 2017).

Lateral and Lower Boundaries

The outer extent of the model was simulated using no-flow and time-variant specified-head boundaries (figs. 28, 29, and 30, in Marini and others, 2012). A no-flow boundary was assumed to exist at the base of model layer 7, which artificially represents the base of the Pierre Shale. No-flow boundaries at the outer extent of the model were assigned to the model in areas where it was assumed that no groundwater flux was at the boundary. In areas where groundwater flux was assumed to be at the model boundary, groundwater flux in and out of the model was simulated using the CHD Package.

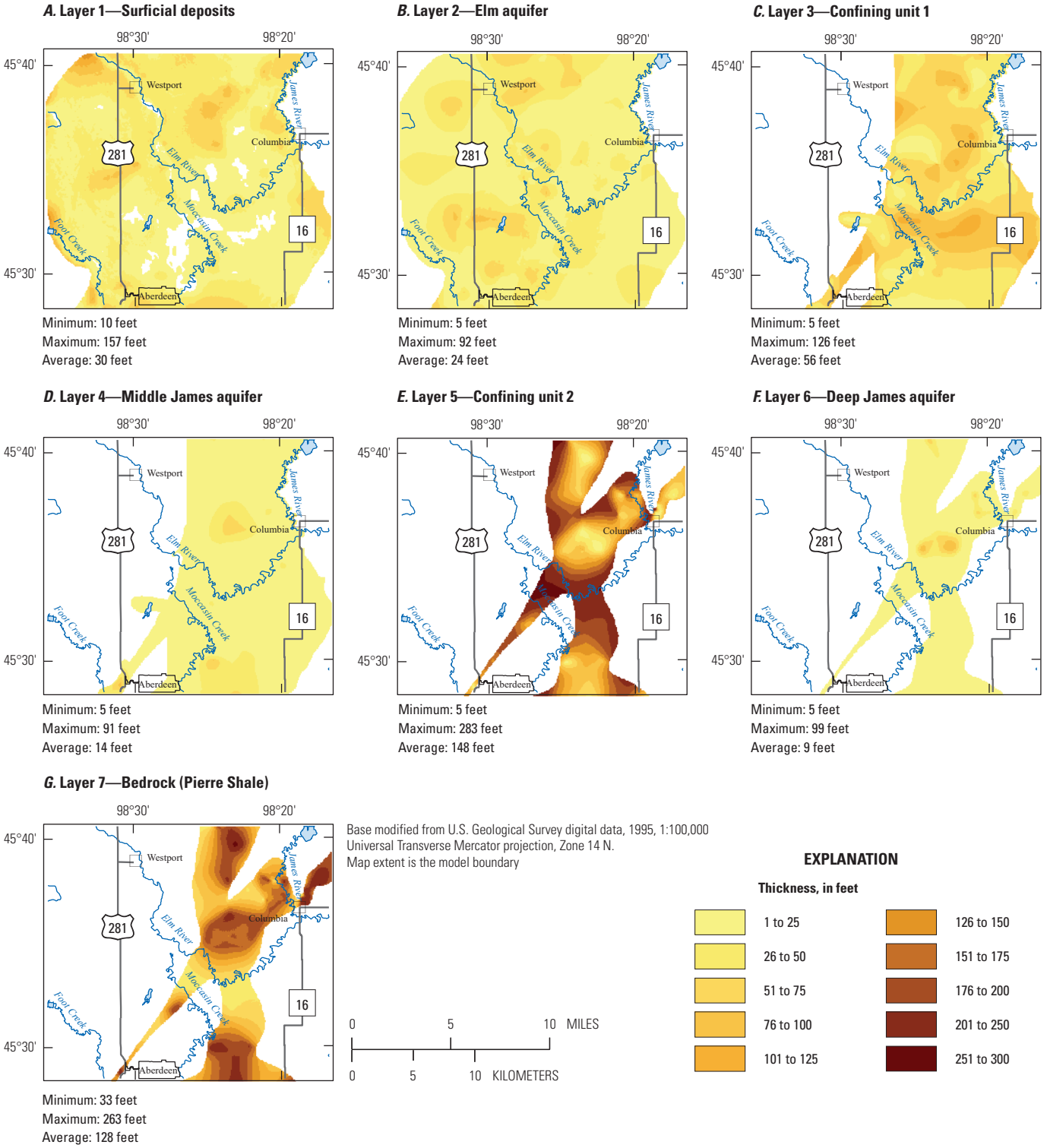

Figure 7. Aquifer horizontal extents and thickness (minimum, maximum, and average) for seven layers included in the revised groundwater-flow model for the area north of Aberdeen, South Dakota. *A*, surficial deposits; *B*, Elm aquifer; *C*, confining unit 1; *D*, Middle James aquifer; *E*, confining unit 2; *F*, Deep James aquifer; and *G*, bedrock (Pierre Shale) layer.

The time-variant specified-head cells used in the revised model, applied to the first 75 stress periods (table 1; simulated using the CHD Package), were assigned to the Elm, Middle James, and Deep James aquifers and were modified slightly from the original model (figs. 28, 29, and 30, respectively, in Marini and others, 2012). The starting and ending specified-heads used by Marini and others (2012) were averaged for the first stress period in the revised model to ensure a constant value during that stress period, which simulated steady-state conditions. The hydraulic head values for time-variant specified-head cells from stress period 75 were applied to all remaining stress periods (76–99) in the revised model. The revised model layers representing confining units (layers 3, 5, and 7) were not assigned hydraulic head values at the extent boundaries because these layers were assumed to have low vertical and horizontal transmissivity and, therefore, little to no groundwater flux across the extent boundary. The upper layer (layer 1) also was not assigned hydraulic head values at the extent boundary based on the assumption that any groundwater flow in this layer would be contributing directly to the Elm aquifer either through precipitation recharge or stream losses. No other modifications to the CHD Package were made in the revised model.

Precipitation Recharge

Recharge to the aquifer from deep percolation of precipitation was simulated using the RCH Package. The RCH Package is applied to the upper layer (layer 1) to simulate the flux exchange distributed over the surface for a specified length and time (Harbaugh and others, 2000). The average annual recharge rate for WYs 1975–2015 (fig. 5) was applied to stress period 1, and the temporally differing recharge estimates that were applied in the original model were used for stress periods 2–75. Spatially variable estimates of recharge for stress periods 76–99 (WYs 2010–15) were calculated using the SWB model (Westenbroek and others, 2010) and were included in the revised model (Eldridge and others, 2018). No other modifications to the RCH Package were made for use in the revised model. The spatial estimates of recharge were adjusted during model calibration using a parameter multiplier.

Groundwater Evapotranspiration

Groundwater evapotranspiration was simulated using the EVT Package. The EVT Package simulates a head-dependent flux out of the model where water is removed from the groundwater system for a specified length and time (McDonald and Harbaugh, 1988). Groundwater evapotranspiration, simulated by the model, is highest when the water table is at the land surface and decreases linearly to 0 at the evapotranspiration extinction depth. An initial uniform extinction depth of 9 ft was used throughout the model area but was varied during model calibration. The average annual potential evapotranspiration rate, determined using the SWB model (Eldridge and others, 2018), for WYs 1975–2015 (fig. 5) was applied to stress period 1. Potential evapotranspiration rates for stress periods 2–99 also were calculated using the SWB model (Eldridge and others, 2018), and the rate was varied during model calibration using a parameter multiplier.

Groundwater Withdrawal

Groundwater withdrawals for the numerical model were simulated using the WEL Package. The withdrawal rates for stress periods 1–75 used in the revised model were unaltered from the original model. Except for the withdrawal rates at 11 production wells in the model area, the withdrawal rates for nonproduction wells for the additional 24 stress periods were repeated in the revised model based on the last four stress periods (72, 73, 74, and 75) in the original model to be consistent with the seasonal stress periods (table 1). For the 11 production wells, monthly withdrawal rates were calculated from 2009 to 2015 based on daily withdrawal records provided by the City of Aberdeen (J. Ellingson, City of Aberdeen, written commun., 2016). Withdrawal rates for each well in the model were calculated as a time-weighted average based on each stress period length (table 1) and are available in Eldridge and others (2018). Withdrawal rates for wells were assigned to an individual aquifer based on either (1) the well owner's knowledge; (2) drilling reports; or (3) the well depth, the well screen interval, or both.

Surface-Water Features

Streams in the revised model area were represented using the DRN and SFR2 Packages. The DRN Package was used to simulate discharge to nonrouted streams at the lateral boundary of the revised model. The SFR2 Package was used to simulate recharge and discharge from all routed streams in the revised model (fig. 8), replacing the RIV Package that was used in the original model. River cells in the RIV Package use a fixed minimum water level, which commonly provides an acceptable simulation; however, if the model must account for dry periods where river stage could drop below the fixed minimum value, then the model could overpredict groundwater inflows because the river cells will continue to provide a source of water. In such periods, the SFR2 Package may reduce the stage and route less water downstream.

Nonrouted Streams

The DRN Package simulates groundwater discharge from an aquifer at a rate proportional to the water level in the aquifer, the vertical conductance of the drain bed, and a drain elevation that is designated at each of the drain cell locations (Harbaugh, 2005). Water removed at a drain cell is not routed to other drain cells and does not return to the model. In the original model, the DRN Package was used to simulate groundwater losses to Moccasin Creek. Generally, Moccasin Creek flows less than 1 cubic foot per second (ft^3/s) during the late summer and fall (Marini and others, 2012). The drain cells representing Moccasin Creek in the original model were

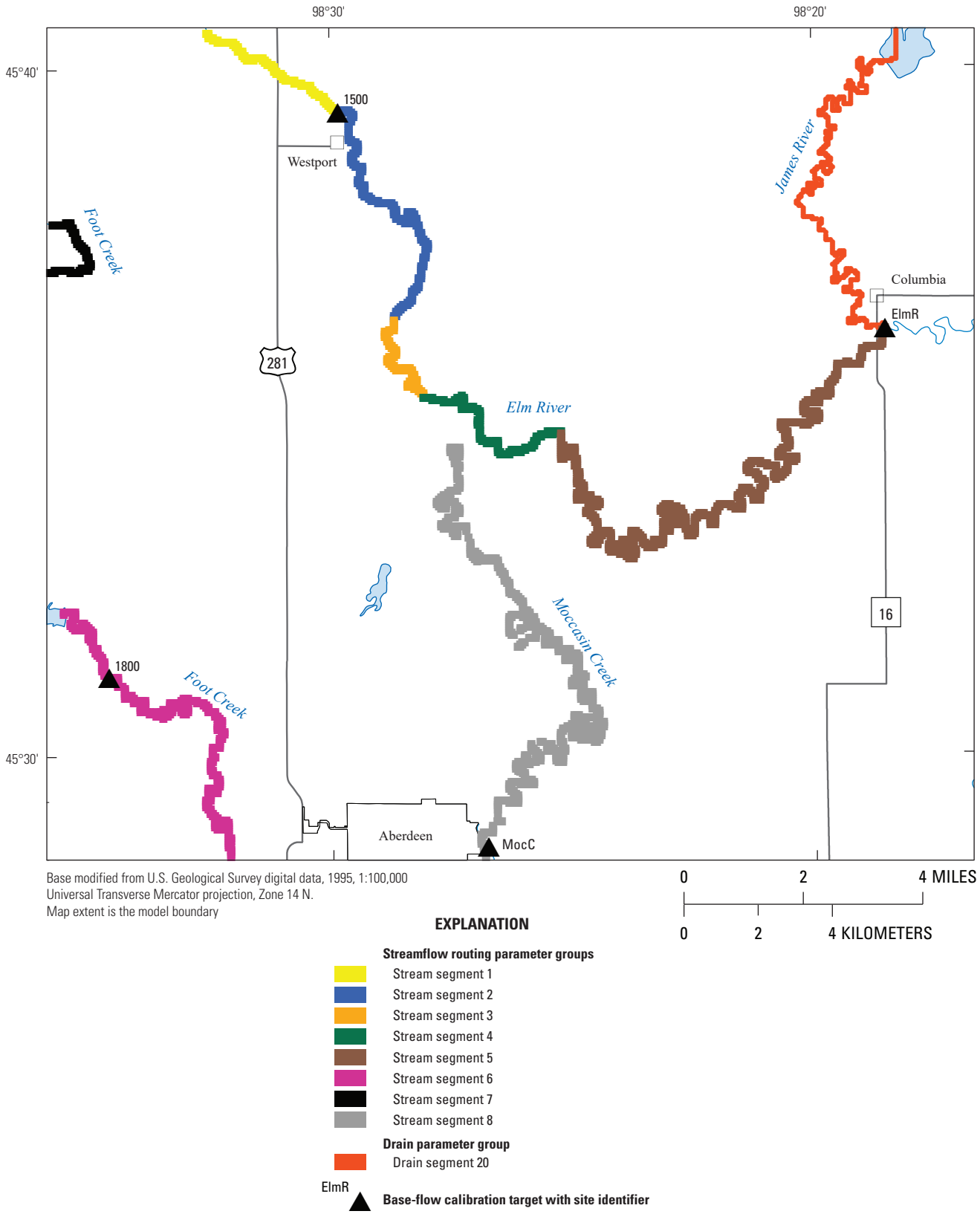

Figure 8. Locations of base-flow calibration targets on the Elm River, Moccasin Creek, and Foot Creek; locations of stream segments represented by the MODFLOW Stream Flow Routing Package; and drain cells representing the James River along the model boundary for the revised model of the area north of Aberdeen, South Dakota.

replaced with routed stream cells using the SFR2 Package in the revised model (described in the following "Routed Streams" section). In the revised model, drain cells were used to represent groundwater flow out of the model and into the James River along the eastern model boundary. The James River was not simulated in the original model because it likely does not contribute substantial volumes of water to the Elm aquifer. This assumption is based on the observation that the general direction of groundwater flow in the Elm aquifer (fig. 4) is from the northwest to the southeast, with eventual discharge into the James River; therefore, in the revised model, drain cells were added along the James River boundary to allow discharge from the Elm aquifer at the boundary. Initial estimates of drain bed vertical conductance were from Marini and others (2012). The final drain bed vertical conductance was determined during model calibration.

Routed Streams

The SFR2 Package was used to simulate routed stream base flow and to simulate streamflow gains and losses for the Elm River, Moccasin Creek, and Foot Creek. The SFR2 Package calculates the interaction between groundwater and surface water for stream reaches that are hydraulically connected to an underlying aquifer (Niswonger and Prudic, 2005). The SFR2 Package simulates groundwater recharge to and discharge from an aquifer at a rate proportional to the water level in the aquifer, the value of vertical conductance of the stream bed, the stream bed elevation that is designated at each of the stream cell locations, and the stage in the stream cell. Additionally, the SFR Package routes streamflow (or base flow) to and from adjacent model stream cells, which permits calculation of simulated streamflow or base flow at any stream cell in the model.

The streams were divided into eight segments (fig. 8) to match the divisions used in the original model for the RIV Package; these eight segments were based on changes in field measured streambed conductance (Marini and others, 2012). Initial values for streambed hydraulic conductivity for each segment were the same as those used in the original model for the RIV Package, and the final values of streambed hydraulic conductivity were optimized during model calibration.

Streamflow simulated by the SFR2 package was assumed to represent stream base flow and not total streamflow because, conceptually, base flow better represents groundwater's contribution to streamflow compared to total streamflow and is not affected substantially by runoff from precipitation and snowmelt. Estimated monthly base flows at USGS streamgages 06471500 and 06471800 were used to determine inflows into the Elm River and Foot Creek, respectively (fig. 1). The estimated base flow was scaled by the ratio of the drainage area outside the model to the drainage area contributing to each streamgage because streamgages on the Elm River and Foot Creek were not exactly at the inlet of the streams at the model boundaries. The base flow into the Elm River was scaled by 99.6 percent of that estimated at USGS streamgage 06471500. The inflow into the southern segment of Foot Creek was scaled by 96.6 percent of the streamflow measured at USGS streamgage 06471800. An inflow of 0 was specified at Moccasin Creek because the headwaters for this creek originate in the model area. An inflow of 0 also was used at the northern segment of Foot Creek because no data were available for the segment, and the creek's contribution to groundwater flow was assumed to be negligible at this location.

Groundwater Model Calibration

Model calibration is the process of estimating model parameters to minimize the differences, or residuals, between observed (measured or estimated) data and simulated values; therefore, Parameter ESTimation software (PEST++, version 3.7.0; Welter and others, 2015) was used to optimize model input parameters by matching model-simulated values to estimated or measured observations. Model calibration using PEST identifies an optimum set of model input parameters that minimizes the sum of the squared and weighted residuals where constraints can be placed on the ranges of parameter values and the relations among parameters (Doherty, 2004). Calibration parameters included horizontal hydraulic conductivity, vertical hydraulic conductivity, specific yield, specific storage, and vertical streambed conductance for stream and drain cells. Additionally, recharge and evapotranspiration arrays for each stress periods were calibrated using multipliers applied to each array. Evapotranspiration extinction depth also was adjusted during model calibration. During calibration, observation weights, such as those for multiple water-level measurements, were defined in the PEST instruction files and were unaltered from what was documented in the original model by Marini and others (2012). Minimum and maximum parameter values were determined based on acceptable ranges in literature including those listed by Marini and others (2012).

Calibration Targets

Calibration targets are observed values (measured or estimated) to which model-simulated values are compared and generally consist of measured groundwater levels and estimated base flow at streamgage locations. Calibration targets for the revised model included hydraulic head measurements at wells (groundwater levels) and estimated stream base flow at streamgage locations for WYs 1975–2015.

Groundwater Levels

The revised model included transient calibration targets that represented single and multiple water-level measurements at observations wells (fig. 39 in Marini and others, 2012). The calibration targets from the original model for WYs 1975–2009 were unaltered, although a new layer assignment was necessary given the revised representation of the hydrogeologic framework. Water-level measurements for

WYs 2010–15 were included in the revised model. Calibration targets that represented water-level measurements during the steady-state stress period of the revised model were calculated as the average of all measurements in the simulation period. Calibration targets that represented water-level measurements during the transient part of the simulation represented the change in water level from the previous measurement (previous water-level measurement minus existing water-level measurement) and were assigned on the date of the measurement.

Stream Base Flow

The revised model included calibration targets that represented transient stream base flow at four USGS streamgage locations in the model area (fig. 8). Two base-flow calibration targets were assigned at USGS streamgage locations: calibration target 1500 represented base flow at USGS streamgage 06471500, and calibration target 1800 represented base flow at USGS streamgage 06471800 (fig. 1). Two base-flow calibration targets were assigned at locations in the model where routed base flow exits the model at a boundary: the calibration target for the Elm River outflow (ElmR) represented base flow at the confluence of the Elm River into the James River, and the calibration target for Moccasin Creek (MocC) represented base flow at the model boundary at the outlet of Moccasin Creek. The calibration targets that represented stream base flow for USGS streamgages 06471500 and 06471800 represented the average estimated base flow for each stress period. Calibration targets of ElmR (Elm River outflow, fig. 8) were calculated by subtracting base flow at USGS streamgage 06471550 from base flow at USGS streamgage 06471000 (fig. 1). The calibration target at MocC (Moccasin Creek, fig. 8) was assigned a constant value of 2 ft^3/s for all stress periods.

Calibration Parameters

Horizontal and vertical hydraulic conductivities were calibrated using a combination of pilot points (Doherty, 2004) and zones. Pilot points are discrete locations in the model that represent surrogate parameters from which hydraulic property values are interpolated to the model grid (Doherty and Hunt, 2010). If more than one pilot point was placed in a zone, semivariograms were used to define the method of interpolation of the calibration results between pilot points. The semivariogram definitions were unaltered from the original model. The model area was divided into 20 hydraulic conductivity zones (fig. 9). Layer 1, representing the surficial deposits, included 6 zones based on descriptions of the surficial deposits defined by Marini and others (2012). Layer 2, representing the Elm aquifer, was partitioned into 9 zones, which were the same zones used in the original model. The remaining five layers were each assigned their own unique zone.

Pilot points were distributed sparsely in layer 1 because of the lack of calibration targets available in that layer. Layer 2 used a denser grid of pilot points and included an additional point at an aquifer-test location (Schaap, 2000). Pilot point placement in layer 2 was identical to that used in the original model. Layers 3, 5, and 7 (representing the three confining layers) had only one pilot point each, representing a single uniform value, for calibrating horizontal hydraulic conductivity and one point for calibrating vertical hydraulic conductivity. Layers 4 and 6, representing the Middle James and the Deep James aquifers, respectively, included several pilot points to calibrate horizontal hydraulic conductivity because of additional calibration targets available in the layer. The zones and horizontal and vertical pilot point locations used for calibrating hydraulic conductivity are depicted in figure 9. During calibration, parameters were constrained using the same upper and lower limits as the original model.

The average values for horizontal and vertical hydraulic conductivity in each zone were calculated for layers with spatially variable hydraulic conductivity distributions. This was done to compare parameter calibration results with those reported in table 13 by Marini and others (2012). The minimum, average, and maximum parameter values in each layer for each parameter zone are presented in table 2. Generally, horizontal hydraulic conductivity was higher in the revised model than in corresponding layers and zones in the original model. Specific yield and specific storage were lower in the revised model. Streambed conductance and recharge could not be compared because the simulation methods and stress packages differed between the original and revised models. The average annual evapotranspiration rate was lower in the revised model.

Postcalibration horizontal hydraulic conductivity for each layer and zone is shown in figure 10 and in table 2. Horizontal hydraulic conductivity values in layer 1 ranged from 0.1 foot per day (ft/d) (zone 5) to 500 ft/d (zone 4). In layer 2, horizontal hydraulic conductivity ranged from 3 ft/d (zone 8) to 1,000 ft/d (zones 7, 9, and 12). Horizontal hydraulic conductivity values for confining layers 3, 5, and 7 ranged from 0.002 ft/d (single value in layer 5, zone 18) to 0.2 ft/d (layers 3 and 7, zones 16 and 20, respectively). Layer 4, representing the Middle James aquifer, had horizontal hydraulic conductivity values ranging from 30 to 500 ft/d, and values for layer 6, representing the Deep James aquifer, ranged from 50 to 500 ft/d.

Vertical hydraulic conductivities were simulated using a ratio of horizontal hydraulic conductivity to vertical hydraulic conductivity for each zone (table 2). The average postcalibration vertical hydraulic conductivity divisor (that is, the number that the horizontal hydraulic conductivity was divided by) ranged from a minimum of 1.0 in zone 16 (layer 3) to a maximum of 1,000 in zone 18 (layer 5) as presented in table 2. Specific yield was 0.01 and 0.06 in layers 1 and 2, respectively. Specific storage ranged from 0.00001 per foot in layers 5 and 7 to 0.00013 per foot in layer 3. Vertical hydraulic conductivity of sediments separating streams and aquifer ranged from 0.00010 ft/d in stream segment 5 to 2.17 ft/d in stream segment 8. The vertical hydraulic conductivity in

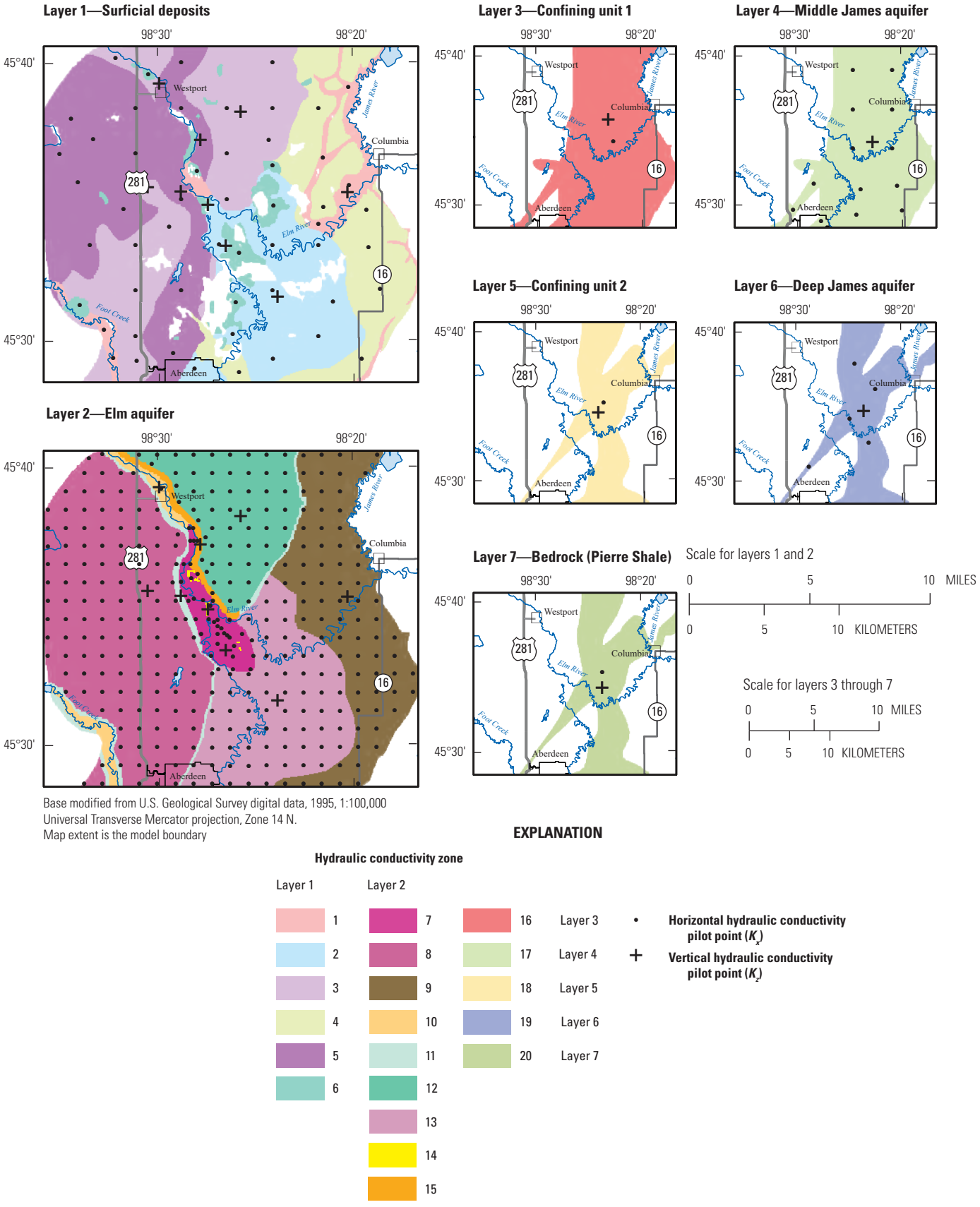

Figure 9. Hydrologic zones and horizontal and vertical pilot points used for calibrating horizontal and vertical hydraulic conductivity for the seven model layers in the revised model for the area north of Aberdeen, South Dakota.

Table 2. Summary statistics of estimated hydraulic parameters by zone and layer using the revised model after calibration.

[--, not applicable]

Parameter	Minimum parameter value	Average or single parameter value	Maximum parameter value	Layer
Horizontal hydraulic conductivity, in feet per day (see fig. 9 for zones)				
kx1	0.2	10	26	Layer 1
kx2	3	154	350	
kx3	0.3	45	100	
kx4	50	436	500	
kx5	0.1	20	100	
kx6	7	69	191	
kx7	5	205	1,000	Layer 2
kx8	3	76	990	
kx9	5	397	1,000	
kx10*	--	7	--	
kx11*	--	5	--	
kx12	3	521	1,000	
kx13	5	159	500	
kx14*	--	200	--	
kx15*	--	392	--	
kx16*	--	0.2	--	Layer 3
kx17	30	290	500	Layer 4
kx18*	--	0.002	--	Layer 5
kx19	50	363	500	Layer 6
kx20*	--	0.2	--	Layer 7
Vertical hydraulic conductivity divisor (see fig. 9 for zones)				
kz1	--	18.0	--	Layer 1
kz2	--	3.0	--	
kz3	--	7.2	--	
kz4	--	31.7	--	
kz5	--	7.6	--	
kz6	--	6.4	--	
kz7	--	1.7	--	Layer 2
kz8	--	25.0	--	
kz9	--	7.6	--	
kz10	--	1.2	--	
kz11	--	1.4	--	
kz12	--	4.3	--	
kz13	--	10.6	--	
kz14	--	16.5	--	
kz15	--	3.1	--	
kz16	--	1.0	--	Layer 3
kz17	--	31.4	--	Layer 4
kz18	--	1,000	--	Layer 5
kz19	--	4.5	--	Layer 6
kz20	--	5.7	--	Layer 7
Specific yield				
sy1	--	0.01	--	Layer 1
sy2	--	0.06	--	Layer 2
Specific storage, in feet				
ss1	--	0.00002	--	Layer 1
ss2	--	0.00012	--	Layer 2
ss3	--	0.00013	--	Layer 3
ss4	--	0.00010	--	Layer 4
ss5	--	0.00001	--	Layer 5
ss6	--	0.00010	--	Layer 6
ss7	--	0.00001	--	Layer 7
Vertical hydraulic conductivity of sediments separating streams and aquifer, in feet per day (see fig. 8 for stream segments)				
st1	--	0.4064	--	--
st2	--	0.0010	--	--
st3	--	0.0010	--	--
st4	--	0.0010	--	--
st5	--	0.0001	--	--
st6	--	0.0010	--	--
st7	--	0.0037	--	--
st8	--	2.1732	--	--
dr20	--	0.0010	--	--

*Only one pilot point used in this zone.

US. Geological Survey streamgage, Elm River at Westport, South Dakota (06471500), North of Aberdeen. Photograph by Karl Koth, U.S. Geological Survey.

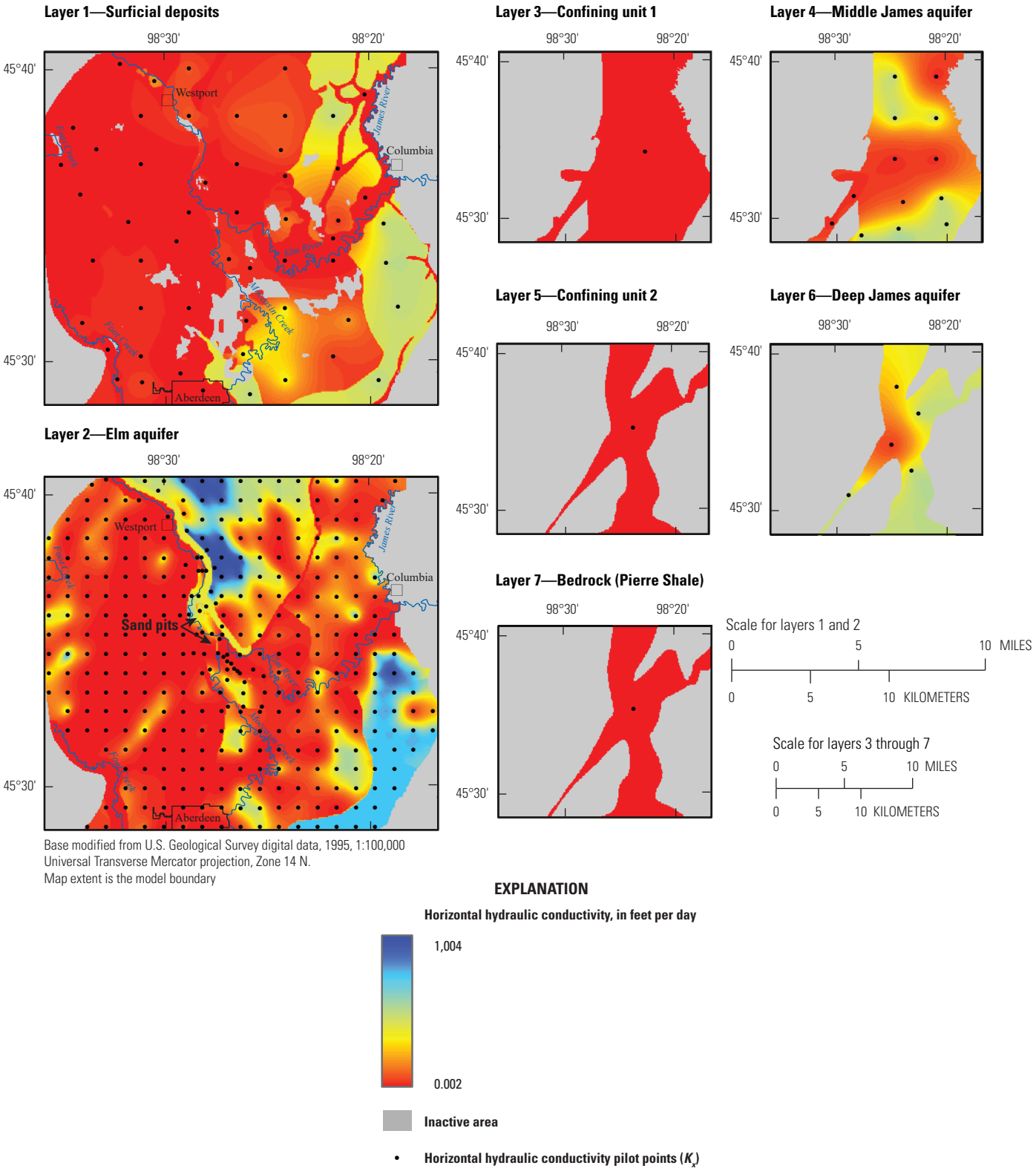

Figure 10. Horizontal hydraulic conductivities for each model layer after model calibration and locations of horizontal pilot points (K_x) used for calibration of the revised model for the area north of Aberdeen, South Dakota.

the drain cells representing the James River (zone parameter group dr20 in table 2) was 0.0010 ft/d. The calibrated recharge multiplier of 0.76 resulted in an average annual recharge of 0.45 in/yr, and the calibrated evapotranspiration multiplier of 0.1 resulted in an average annual potential evapotranspiration rate of 3.2 in/yr. The calibrated evapotranspiration extinction depth was 9.0 ft.

Numerical Model Results

The revised model is an improvement over the original model because the revised model includes a more detailed hydrogeologic layering scheme including four new layers, a more robust representation of streams, and a longer simulation period (WYs 1975–2015 compared to WYs 1975–2009 in the original model) that simulates a broader range of climatic conditions. Comparisons to the original model are described to highlight the changes made in the revised model. In general, the revised model adequately simulates the natural system and compares favorably with observed and estimated hydrologic data. This section presents comparisons of simulated and observed water levels, simulated water budgets, simulated and observed stream base flow, simulated and observed potentiometric contours, and groundwater flow for the Elm, Middle James, and Deep James aquifers. Model sensitivity for selected parameters and model benefits and limitations also are presented.

Water Levels

Model performance was evaluated by comparing average simulated water levels and average observed water-levels at well locations. The observation wells from the revised model used for comparison were the same wells used in the original model; water-level data for the observation wells are available in a USGS data release (Eldridge and others, 2018). Observed water levels were plotted with the model-simulated water levels by aquifer (fig. 11). A best-fit line was determined using linear regression (Helsel and Hirsch, 2002), and a coefficient of determination (R^2; fraction of the variance explained by regression and based on the simulated and observed data) was calculated. An R^2 value of 1 is considered the best possible fit with no difference between the observed and simulated water levels. The R^2 value for the revised model was 0.89 and included simulated and observed values from October 1, 1974 (WY 1975), through September 30, 2015 (WY 2015), available in a USGS data release (Eldridge and others, 2018). The R^2 value for the original model was 0.94 and included simulated and observed values from October 1, 1974, through September 30, 2009. The difference between R^2 values for the original and revised models may indicate that the original model could have been overfit to head observations because base flow was not simulated. Another reason for the difference in R^2 values between the original and revised models could be due to the addition of the stress period observation data from September 30, 2009, through September 30, 2015. The additional data included some climatically wetter, more extreme periods such as 2011, in which annual precipitation was 30.9 in. In the original model, the largest annual precipitation was 29.06 in. and occurred in 1998. As described previously in the "Precipitation Recharge and Groundwater Evapotranspiration" section, average annual precipitation for the original model timeframe, which included data from WYs 1975–2009, was 20.26 in. (National Climatic Data Center, 2017). Additional precipitation data for WYs 2010–15, included in the revised model timeframe, resulted in an average annual precipitation for WYs 1975–2015 in the model area of 20.6 in. The larger variability in climate data coupled with the additional water-level data could explain the lower R^2 value for water levels in the revised model. The 1:1 best fit line indicates that the model typically overestimated hydraulic head for observations less than about 1,300 ft above NAVD 88 and underestimated hydraulic head for observations greater than about 1,300 ft above NAVD 88. Positive and negative hydraulic head residuals were distributed randomly within the model area.

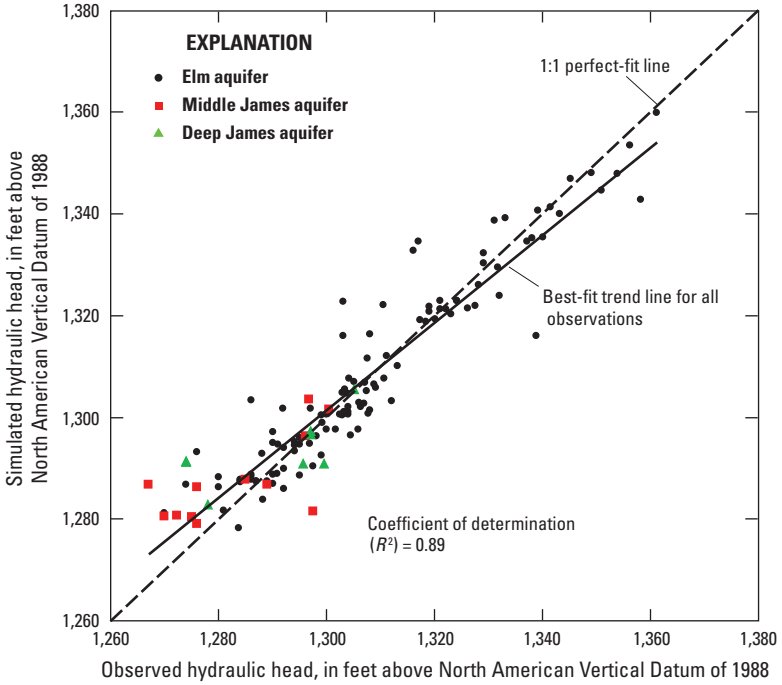

Figure 11. Plot of simulated and observed average water levels from water years 1975–2015 by aquifer including a best-fit line from linear regression. The 1:1 perfect fit-line also is shown for reference to visualize bias, and data are available in a USGS data release (Eldridge and others, 2018).

In addition to comparing average simulated and observed water-level measurements to determine the best-fit linear regression, wells with multiple water-level observations were used to compute transient water-level changes for WYs 1975–2015. Selected observation wells established and maintained by the South Dakota Department of Environmental and Natural Resources Water Rights Program (South Dakota Department of Environmental and Natural Resources, 2018) or South Dakota Geological Survey (South Dakota Geological Survey, 2017) were used as transient water-level-change calibration targets during model calibration (fig. 12). The six South Dakota Department of Environmental and Natural Resources Water Rights Program (2018) wells shown in figure 13 had water-level measurements that spanned most of the model period, and the same six wells were used to generate hydrographs for comparison of simulated and observed water levels because these six wells were those used in the original model (fig. 42 in Marini and others, 2012). The observed hydrographs of the six wells are compared with the simulated hydrographs in figure 13.

A visual comparison of the hydrographs for wells BN–82F, BN–77V, and BN–82K indicated that the model adequately simulated water-level elevations and water-level changes for those wells (fig. 13); however, the average simulated water level for well BN–77L was about 20 ft less than observed water levels. In comparison, the original model also underpredicted the water level at well BN–77L by about 13 ft. In general, the simulated observation water levels were lower than the observed water levels for all the wells. Simulated water levels generally were higher in later model stress periods (WYs 2010–15) than earlier stress periods (WYs 1975–2009), which was expected because of the wetter climatic conditions in WYs 2010–15 as described in the "Precipitation Recharge and Groundwater Evapotranspiration" section.

Water Budget

The revised model was used to calculate various groundwater-budget components for steady-state and transient conditions for WYs 1975–2015. The groundwater budget consists of several components including (1) inflow from specified-head boundaries, (2) groundwater inflow from routed stream leakage, (3) recharge from precipitation, (4) outflow to specified-head boundaries, (5) groundwater withdrawal at wells, (6) groundwater discharge to drain cells (nonrouted streams), (7) groundwater discharge to streams, and (8) groundwater discharge because of evapotranspiration (table 3). The simulated steady-state groundwater budget is shown in figure 14, and simulated transient groundwater-budget components for WYs 1975–2015 are shown in figures 15 and 16.

Steady-State Conditions

The revised model steady-state stress period represented long-term average conditions using the inputs from the pseudo-steady-state stress period from the original model. The original model used a pseudo-steady-state stress period to approximate steady-state conditions where aquifer storage was close to zero (table 3); however, aquifer storage was not considered in the steady-state stress period for the revised model. The steady-state budget for the revised model was compared to the pseudo-steady-state budget for the original model to characterize the differences between the revised and original model (table 3). It was assumed that the pseudo-steady-state conditions from the original model were comparable to steady-state conditions simulated by the revised model.

The revised model calculated a total steady-state inflow of about 48 ft^3/s compared to about 25 ft^3/s in the original model (table 3). The greatest contributor to inflows in the original model was precipitation recharge, which accounted for about 84 percent of total inflows. Groundwater flux from time-variant specified-head cells and routed streams were the remaining sources of inflow, contributing about 13 and 2 percent, respectively, in the original model. The greatest inflow in the revised model was from time-variant specified-head cells, which accounted for about 87 percent of total inflows. Precipitation recharge accounted for about 13 percent of total inflow, whereas routed streams contributed about 0.4 percent. Using the SFR2 Package in the revised model resulted in less surface water infiltration (from routed streams) compared to the original model that used river cells.

The revised model calculated a total steady-state outflow of about 48 ft^3/s compared to about 25 ft^3/s in the original model (table 3). Results from the original model indicate that evapotranspiration was the greatest model outflow, accounting for about 63 percent total outflows. Groundwater flux from time-variant specified-head cells, routed streams, groundwater withdrawal, then nonrouted streams were the next largest outflows of original model. Groundwater flux time-variant specified-head cells accounted for about 18 percent, routed streams accounted for about 14 percent, groundwater withdrawals accounted for about 5 percent, and the nonrouted streams and storage combined accounted for less than 1 percent of the groundwater discharge. The greatest source of simulated outflow in the revised model was time-variant specified-head cells, which accounted for about 75 percent of total outflow. Evapotranspiration, routed streams, and groundwater withdrawal were the next three largest sources of groundwater discharge. Evapotranspiration was the second largest source of outflow, accounting for about 13 percent of total outflow. Routed streams and groundwater withdrawal were the third and fourth largest sources of outflow, accounting for about 8 percent and 3 percent, respectively, of total outflow. The nonrouted stream cells representing groundwater discharged to the James River accounted for about 1 percent of total outflow.

The time-variant specified-head cells in the revised model had the largest change when compared to the original steady-state model for inflows and outflows (table 3). One possible reason for the increase in simulated groundwater inflow through time-variant specified-head cells in the revised model is the increase in the simulated aquifer volume

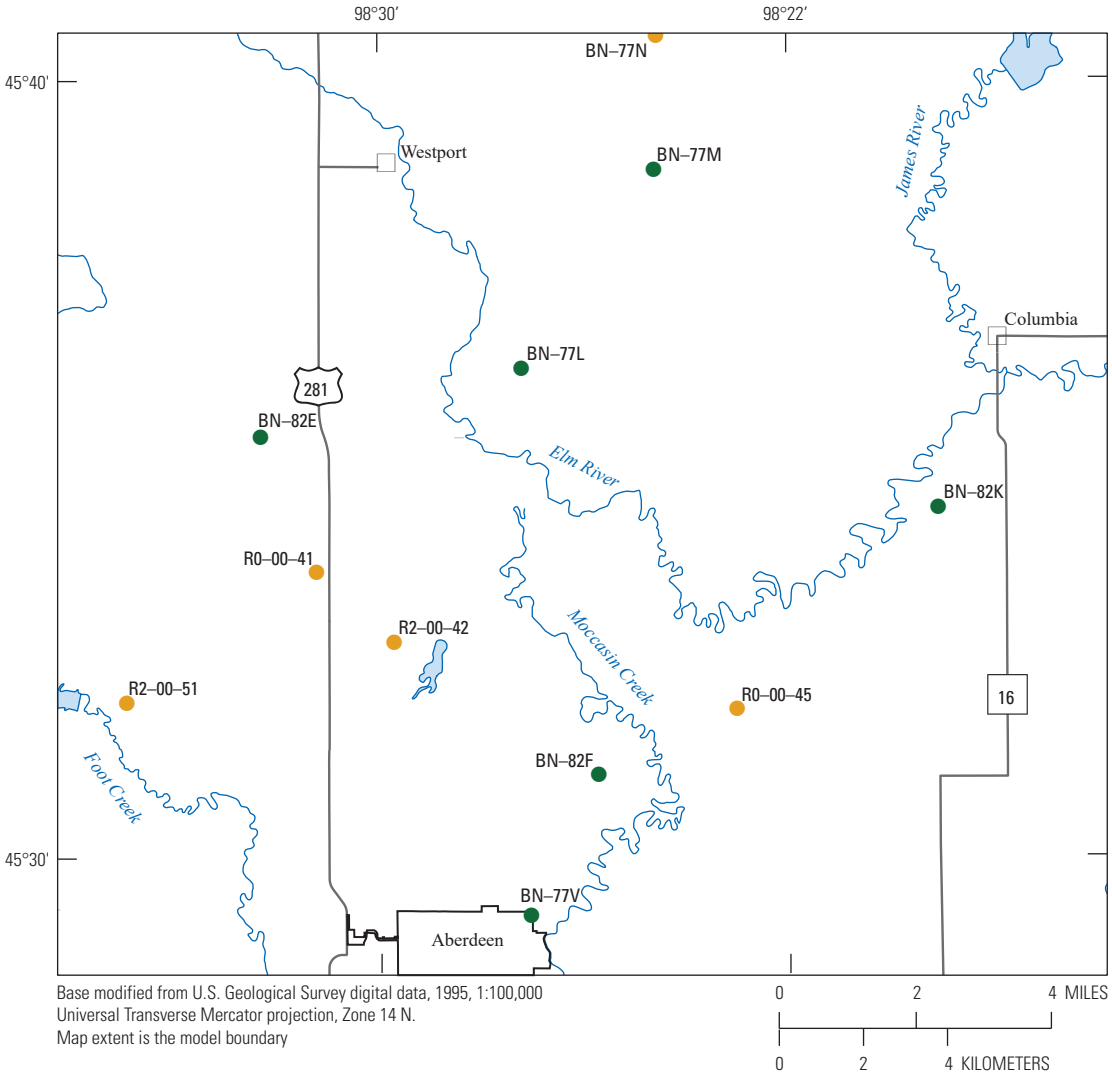

EXPLANATION

R0–00–45 **Observation well and identifier (South Dakota Department of Environmental and Natural Resources, 2018)**

BN–82F **Observation well and identifier (South Dakota Department of Environmental and Natural Resources, 2018) used to show the simulated and observed hydraulic heads for model layer 2 (fig. 13)**

Figure 12. Location of observation wells from the South Dakota Department of Environmental and Natural Resources Water Rights Program in model area.

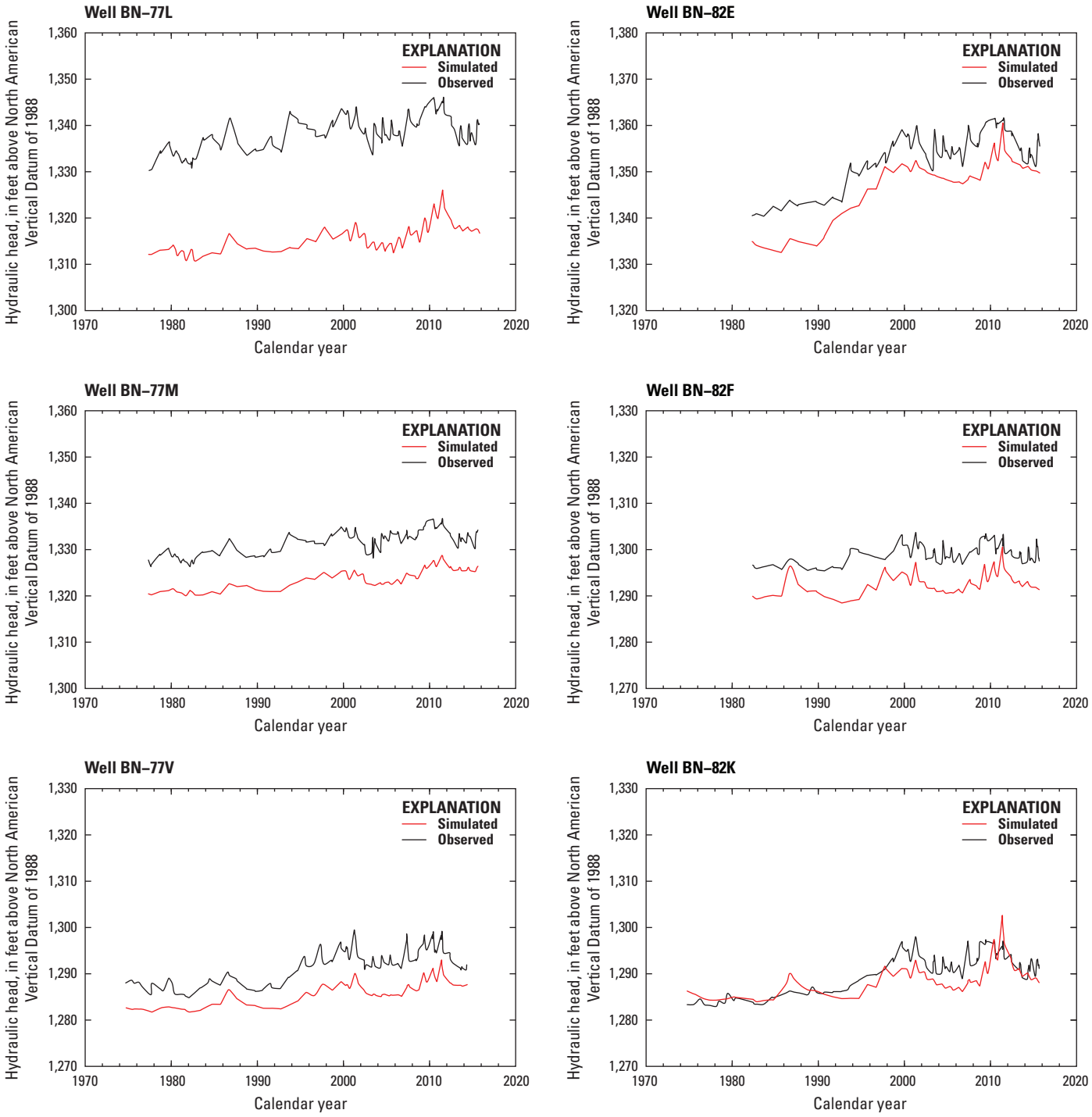

Figure 13. Hydrographs of simulated and observed water levels in the Elm aquifer (layer 2) at six observation wells maintained by the South Dakota Department of Environmental and Natural Resources Water Rights Program.

Table 3. Model budgets for the original pseudo-steady-state model (water years 1975–2009) and revised steady-state model (water years 1975–2015).

[Values may not sum to total due to rounding. --, no data]

Original model pseudo-steady-state budget, in cubic feet per second (approximates steady state)			Revised model steady-state budget, in cubic feet per second			Percentage of original model	Percentage of revised model
In			**In**			**Total in**	**Total in**
Storage	=	0.0089	Storage	=	0	0.04	0
Time-variant specified head	=	3.34	Time-variant specified head	=	42.08	13.12	86.87
Groundwater withdrawal	=	0	Groundwater withdrawal	=	0	0	0
Nonrouted streams	=	0	Nonrouted streams	=	0	0	0
Routed streams	=	0.62	Routed streams	=	0.19	2.44	0.39
Evapotranspiration	=	0	Evapotranspiration	=	0	0	0
Precipitation recharge	=	21.48	Precipitation recharge	=	6.17	84.40	12.74
Total in	=	25.45	Total in	=	48.44	--	--
Out			**Out**			**Total out**	**Total out**
Storage	=	0.0071	Storage	=	0	0.03	0
Time-variant specified head	=	4.48	Time-variant specified head	=	36.53	17.63	75.40
Groundwater withdrawal	=	1.28	Groundwater withdrawal	=	1.26	5.04	2.60
Nonrouted streams	=	0.19	Nonrouted streams	=	0.57	0.75	1.18
Routed streams	=	3.49	Routed streams	=	3.90	13.74	8.05
Evapotranspiration	=	15.96	Evapotranspiration	=	6.19	62.82	12.78
Precipitation recharge	=	0	Precipitation recharge	=	0	0	0
Total out	=	25.41	Total out	=	48.45	--	--

from the addition of four model layers in the revised model. Accounting for this additional aquifer volume, coupled with the interactions between layers shown in figure 14, demonstrates the complexity added to the model because more horizontal and vertical groundwater movement is possible among the layers. The revised model had much higher vertical interaction between adjacent layers, specifically between layers 1 (surficial deposit layer) and 2 (Elm aquifer) (fig. 14). Additionally, the simulated outflow from the Middle James aquifer was highest in specified-head cells when compared to the other layers in the revised and original models. This may be due to the large amount of vertical flow from the upper layers (fig. 14).

In the original pseudo-steady-state model, about 2 percent of the budget was from stream losses into the aquifers (groundwater inflow from routed streams), compared to only about 0.4 percent of the budget in the revised model; however, budget differences were not substantial (less than 0.4 ft^3/s) between the two models for groundwater losses from the aquifer to the streams (groundwater outflow to routed streams) (table 3). Comparing both models, about 14 percent from the original model and 8 percent from the revised model of the water-budget outflows from the aquifers contributed to stream waters. Because the revised model used the SFR2 Package, and not the RIV Package used in the original model, comparing the stream and river budgets may not be appropriate.

Transient Conditions

Water budgets for the transient simulation for the revised model were computed and compared to that of the original model for each of the inflow water-budget components including storage, time-variant specified head, routed and nonrouted streams, and precipitation recharge (table 4). Comparison of the transient inflow budget components between the original and the revised models indicated that inflow from recharge and time-variant specified-head cells had the greatest effect on groundwater inflows (fig. 15; table 4). The storage values ranged from 0 to about 79 ft^3/s for the original model and from 0 to about 51 ft^3/s for the revised model. The time-variant specified-head values ranged from about 2 to 6 ft^3/s for the original model and from about 36 to 64 ft^3/s for the revised model. The routed stream values ranged from 0.01 to about 3 ft^3/s for the original model and from 0.01 to about 2 ft^3/s for the revised model. The precipitation recharge values ranged from 0 to 201 ft^3/s for the original model and from 0 to 208 ft^3/s for the revised model. The difference between the original and revised model for each budget component in each stress period is shown in figure 15. Although the range of inflows from routed streams was small for the original and revised models, the values deviated more than for any other component when comparing by stress periods (fig. 15).

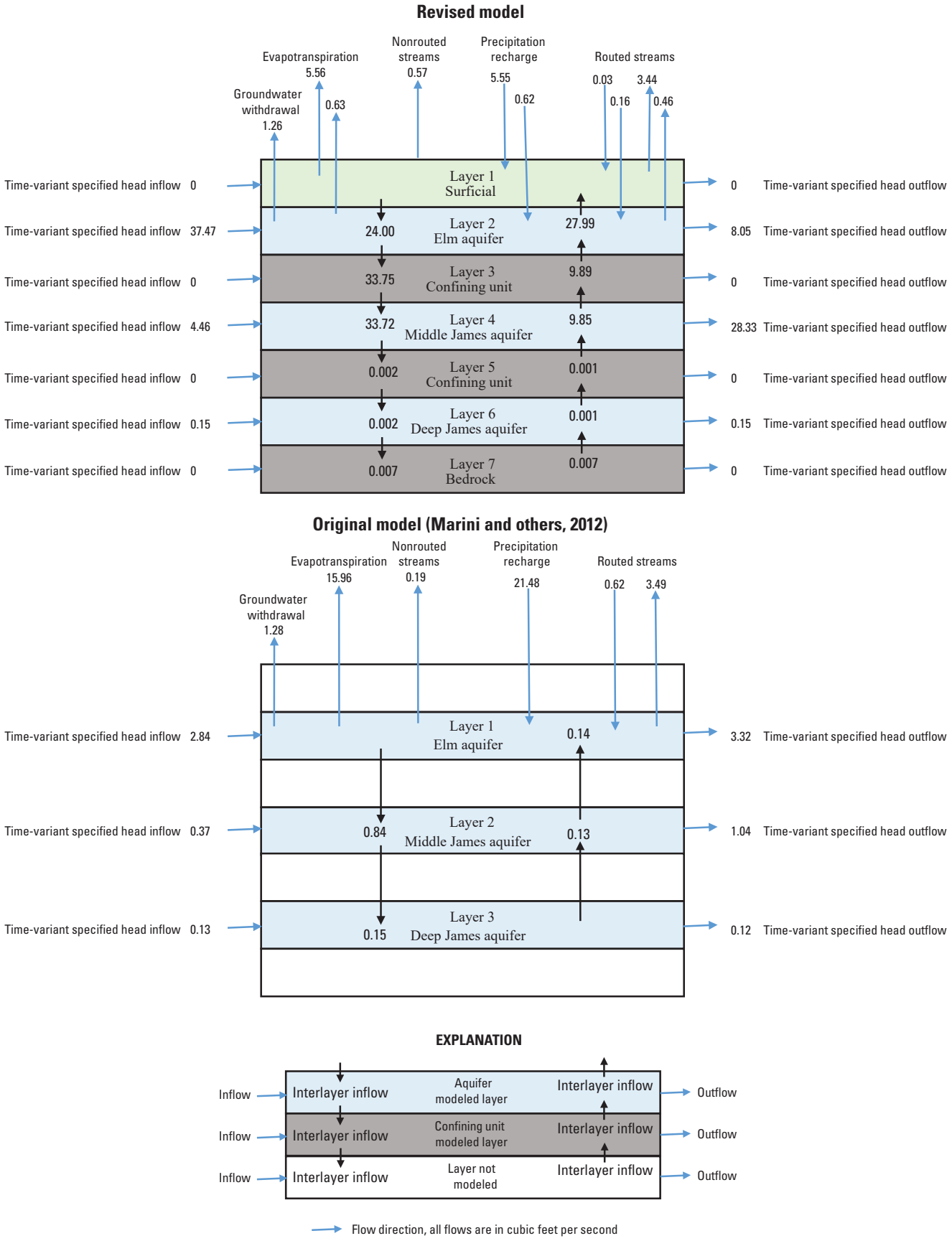

Figure 14. Simulated groundwater-flow budget for steady-state conditions for revised model (water years 1975–2015) and pseudo-steady-state conditions for original model (water years 1975–2009).

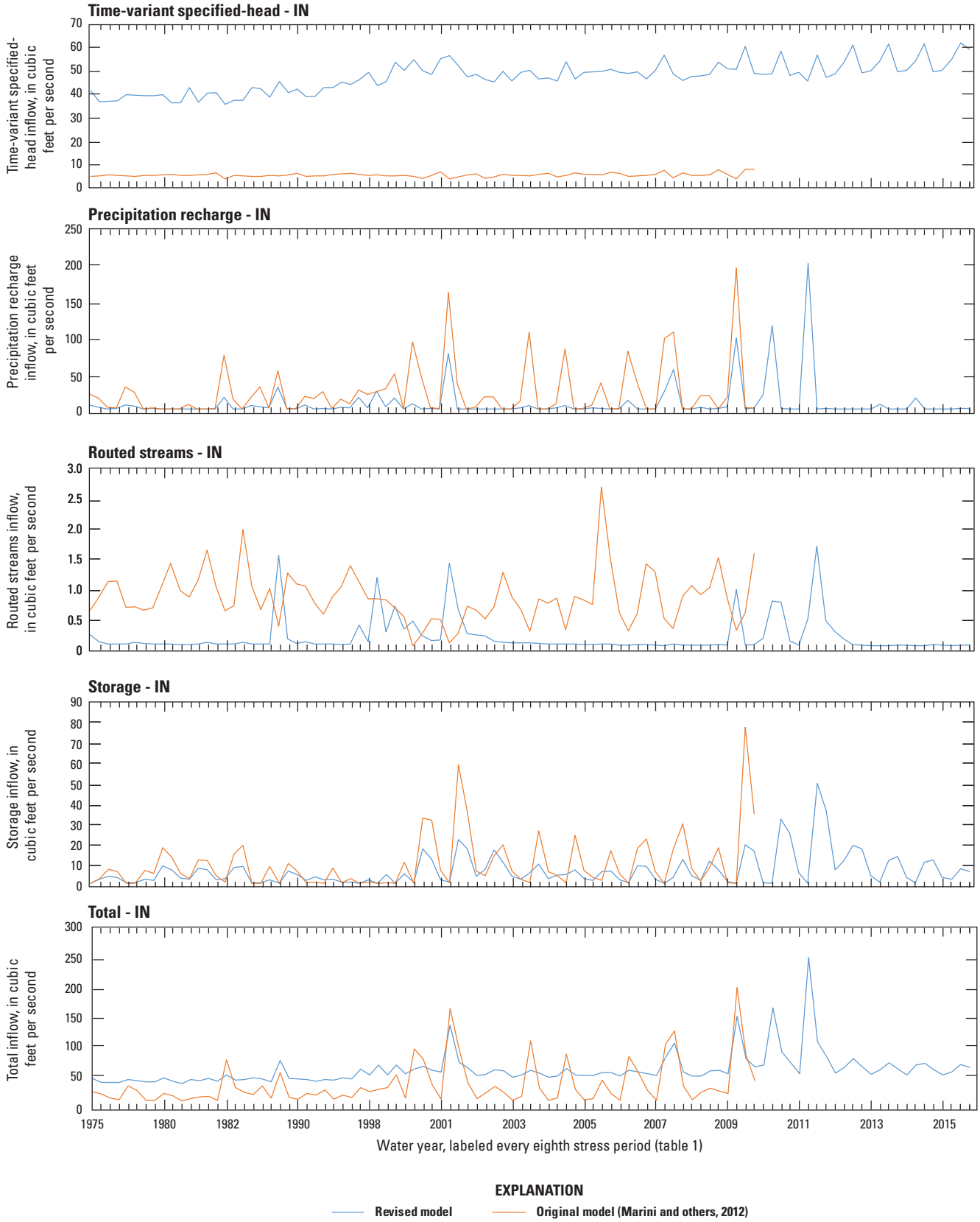

Figure 15. Groundwater-inflow budget comparisons between the original and revised models by groundwater-budget component by stress period for water years 1975–2015.

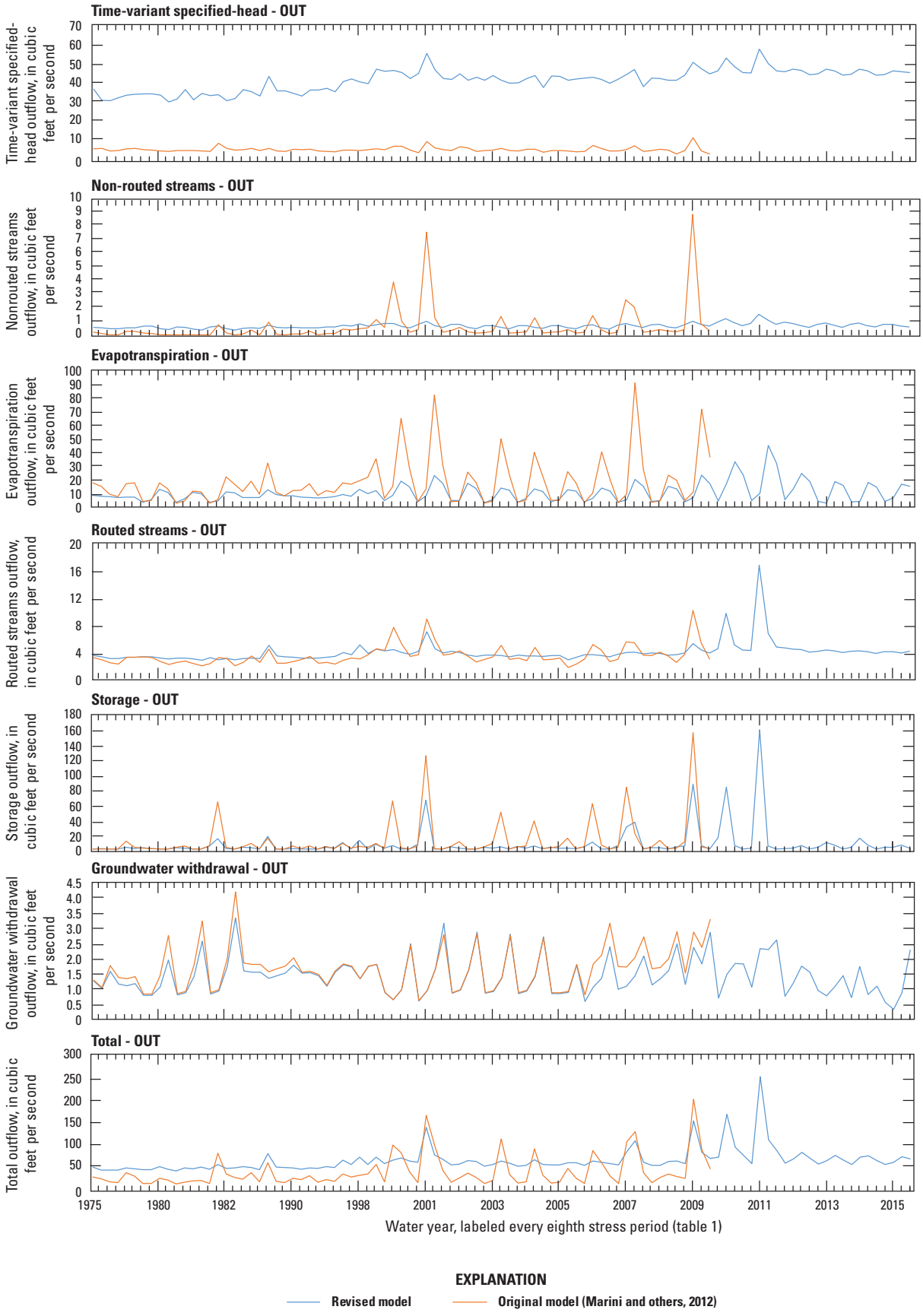

Figure 16. Groundwater-outflow budget comparisons between the original and revised models by groundwater-budget component by stress period for water years 1975–2015.

Table 4. Range of transient model budget values from the original model (water years 1975–2009) and revised model (water years 1975–2015).

[--, no data]

Water budget component	Original model inflow		Revised model inflow	
	Minimum value, in cubic feet per second	Maximum value, in cubic feet per second	Minimum value, in cubic feet per second	Maximum value, in cubic feet per second
Storage	0	79.1	0	50.6
Time-variant specified head	2.03	6.39	35.8	63.9
Groundwater withdrawal	--	--	--	--
Nonrouted streams	--	--	--	--
Routed streams	0.01	2.74	0.01	1.73
Evapotranspiration	--	--	--	--
Precipitation recharge	0	201	0	208

Water budget component	Original model outflow		Revised model outflow	
	Minimum value, in cubic feet per second	Maximum value, in cubic feet per second	Minimum value, in cubic feet per second	Maximum value, in cubic feet per second
Storage	0.004	160	0	163
Time-variant specified head	1.59	10.4	29.7	58.3
Groundwater withdrawal	0.6	4.28	0.29	3.39
Nonrouted streams	0	9.08	0.36	1.54
Routed streams	1.6	12.6	3	21.3
Evapotranspiration	0.33	92.2	0.26	44.3
Precipitation recharge	--	--	--	--

Water budgets for the revised model transient simulation were computed and compared to the original model for each of the outflow water-budget components including time-variant specified head, nonrouted streams, evapotranspiration, routed streams, storage, and groundwater withdrawals (table 4). Comparing the transient budget components for the original and revised models indicated that outflow from storage had the greatest effect on groundwater outflows (fig. 16; table 4). The storage values ranged from 0.004 to 160 ft^3/s for the original model and from 0 to 163 ft^3/s for the revised model. The time-variant specified-head values ranged from about 2 to 10 ft^3/s for the original model and from about 30 to 58 ft^3/s for the revised model. The groundwater withdrawal values ranged from about 0.6 to 4 ft^3/s for the original model and from about 0.3 to 3 ft^3/s for the revised model. The nonrouted stream values ranged from 0 to about 9 ft^3/s for the original model and from about 0.4 to 1.5 ft^3/s for the revised model. The routed stream values ranged from about 2 to 13 ft^3/s for the original model and from about 3 to 21 ft^3/s for the revised model. The evapotranspiration values ranged from about 0.3 to 92 ft^3/s for the original model and from about 0.3 to 44 ft^3/s for the revised model. Although the range of values differed for all budget components, the range of values for nonrouted streams had more deviation among stress periods than any of the other outflow components (fig. 16).

Stream Base Flow

Simulated base flow from the revised model was compared to observed (estimated) base flow at calibration targets, and in general, simulated base flow compared well with observed values. A comparison of base flow with the original model could not be made because the original model did not simulate routed base flow in streams. In the revised model, the simulated steady-state base flows at calibration targets 1500 (Elm River) and 1800 (Foot Creek) were reasonable approximations of the average base flow when compared to average base flow (fig. 17); however, at the ElmR and MocC calibration targets, the differences were large. The simulated base flow at ElmR was about 20 percent of the observed base flow, and the simulated steady state base flow at MocC was zero compared to a target of 2 ft^3/s. The simulated base flow in Moccasin Creek was difficult to calibrate because of historical low flows (Marini and others, 2012).

In addition to steady-state base flow, the observed and simulated base flows during the transient period of the model also were compared (fig. 18). Observed-simulated pairs that plot below the one-to-one line in figure 18 indicate that the model underpredicted base flow. Observed-simulated pairs above the one-to-one line indicate that the model overpredicted the observed value. Transient simulated base

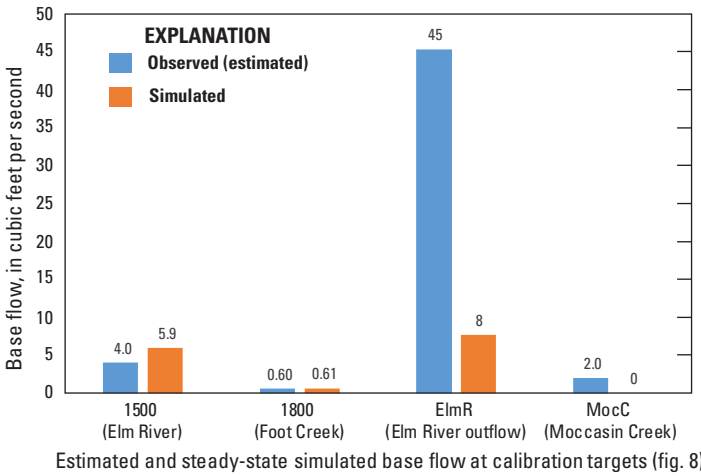

Figure 17. Plot of observed (estimated) and simulated steady-state base flow at calibration targets for Elm River, Foot Creek, Elm River outflow, and Moccasin Creek.

flow at calibration targets 1500, 1800, and ElmR reasonably matched observed base flow except at higher base-flow rates at 1800 and ElmR for which the model slightly underpredicted base flow. Most simulated base flows at MocC were underpredicted when compared to the estimated base flow of 2 ft^3/s documented by Marini and others (2012). Base flow at MocC likely is variable in time, and comparison to a constant value of 2 ft^3/s for this location may not be appropriate. As a result, the 2 ft^3/s calibration target value generally was higher than the simulated transient base flow at MocC.

Potentiometric Contours and Groundwater Flow

The simulated potentiometric contours from the revised model were compared with (1) the observed potentiometric contours (layer 2) and the observed hydraulic head values (layers 4 and 6) (fig. 4) and (2) the simulated potentiometric contours determined from the original model. The potentiometric contours for layer 1 in the revised model were not evaluated with observed data because layer 1 is not a defined aquifer used for water withdrawals and no estimated potentiometric contours were available for comparison. The simulated hydraulic gradients and general direction of groundwater flow (interpreted to be perpendicular to the contours) from the revised model for the Elm aquifer generally matched the observed potentiometric contours and the simulated potentiometric contours from the original model (fig. 19). Minor discrepancies between simulated potentiometric contours from the revised model and the observed potentiometric contours exist and may be due to the lack of water-level data in the model area. For example, in the western part of the model area, few wells with water levels were available for use as calibration targets, and as a result, there is a 10-ft difference between the potentiometric contours from the revised model and the observed hydraulic head values (fig. 4). The simulated potentiometric surface contours from the revised model compared well spatially to the hydraulic head values and the simulated potentiometric contours from the original model for the Middle James aquifer. The simulated potentiometric contours from the revised model differed from the observed hydraulic head values and the simulated potentiometric contours from the original model of the Deep James aquifer. The difference likely is due to the different thickness used for the Deep James aquifer in the revised model compared to the original model and the few observed hydraulic head values available to constrain the simulation (fig. 19).

An assessment of the simulated potentiometric contours in the Elm aquifer in the northern part of the model area near the Elm River indicated that the groundwater flows towards the river. Based on estimates of base flow in the Elm River, simulated base flow in the Elm River, and interpretation of potentiometric data, the Elm aquifer likely contributes groundwater discharge, as base flow, to the Elm River.

Synopsis of Comparisons Between the Original and Revised Models

The revised model represents an improved approximation of groundwater flow based on the available data from WYs 1975–2015. Several changes were applied to the revised model, including adding new layers to better represent the hydrogeologic system and revising and adding new parameters and data, where applicable, for additional stress periods (76–99; table 1) in each of the stress packages. The SFR2 Package, which includes estimates of base flow, was added to replace the RIV Package in the original model. Using geophysical investigations, the thickness of the Deep James aquifer was modified to better represent the aquifer thickness. Lastly, the calibration of the revised model was completed for a longer period, independent of what was defined in the original model.

Model Sensitivity

Parameter sensitivities were computed using PEST++ software (version 4.0.3; Welter and others, 2015). Composite parameter sensitivities were computed, which are numeric values assigned to each adjustable parameter based on their relative effect on the composite of all model observations, adjusted for their assigned weight (Doherty and Hunt, 2010). Composite sensitivity provides information on how changes in the value of a parameter affect changes in model output. The higher a parameter's value of composite sensitivity relative to the values of other parameters, the more effect a change in that parameter has on model results. The adjustable model parameters and their relative composite sensitivities are listed in table 5. Both horizontal (x) and vertical (z) pilot point sensitivities (hydraulic conductivity) were averaged by zone number, and the average composite sensitivity for each zone is listed in table 5. Nonpilot point parameters are listed by their parameter name. Generally, insensitive parameters

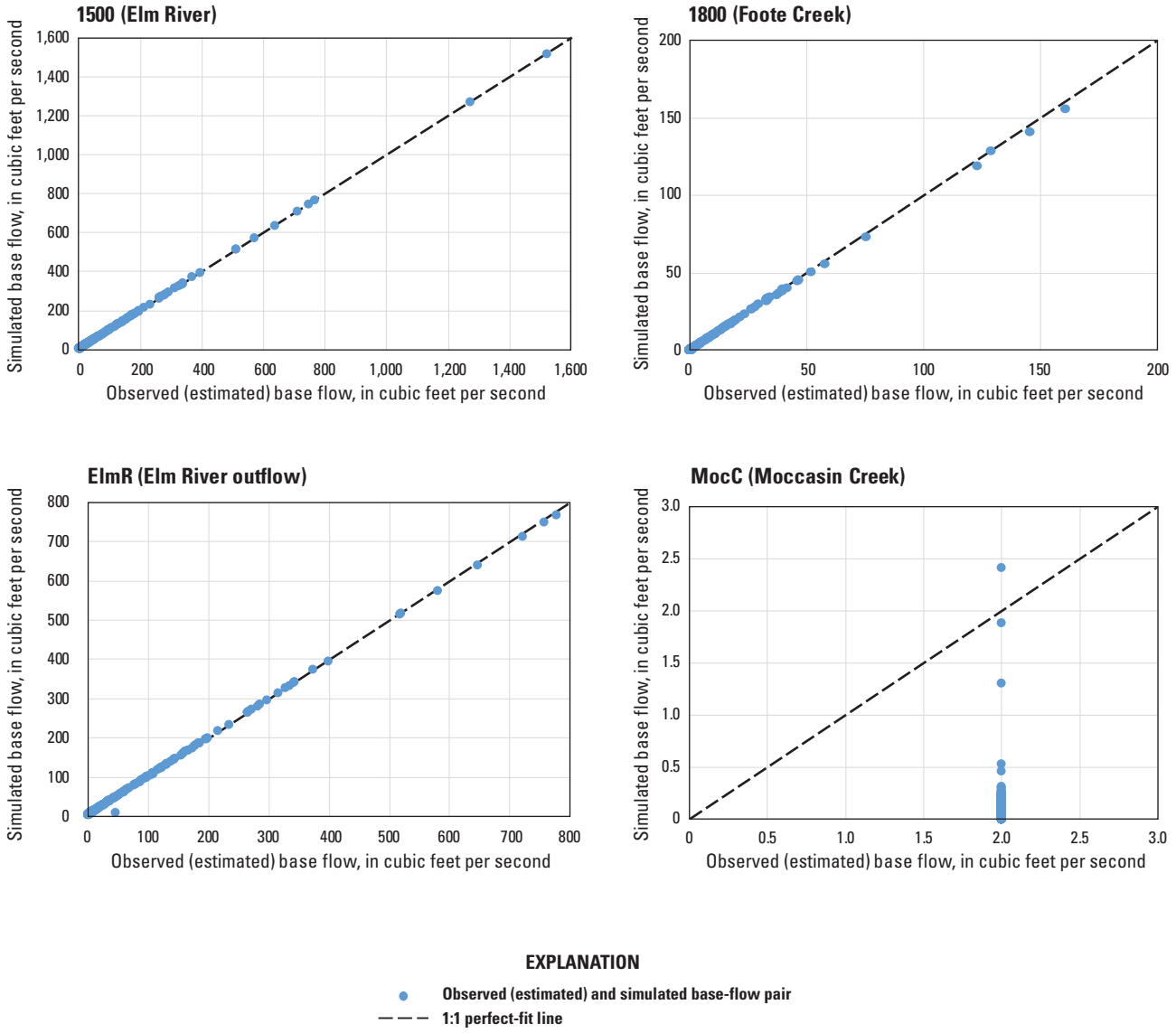

Figure 18. Plots of observed and simulated stream base flow at calibration targets. The 1:1 perfect fit line also is shown on each plot for reference to visualize bias.

are those with composite sensitivity values more than two orders of magnitude lower than the value of the most sensitive parameter (Anderson and others, 2015). The most sensitive parameters included the recharge multiplier, extinction depth, the evapotranspiration multiplier, specific yield in layers 1 and 2, and the specific storage in layers 2 and 3. Parameters with composite sensitivities less than 0.000834 were considered insensitive. The least sensitive parameters were the horizontal hydraulic conductivity pilot points in zone 20 and the vertical hydraulic conductivity pilot points in zone 19.

Model Benefits and Limitations

The revised model was designed to reduce the limitations of the original model. The revisions were validated by comparing the results of the original model with the revised model. The original model represented the hydrogeologic units using a simplified numerical model approach, using only three layers. This simplified approach limited the potential effect of explicitly simulating the surficial deposits and the confining units in the model area.

A primary benefit of the revised model is the inclusion of the surficial deposits and the confining units as explicit layers in the model. The addition of the surficial layer was beneficial for three primary reasons: (1) more accurate representation of recharge from precipitation, (2) more accurate representation of groundwater evapotranspiration, and (3) more accurate representation of groundwater and surface-water interactions.

The original model simulated recharge from precipitation recharge to the Elm aquifer using a multiplier that represents the thickness of the surficial deposit material overlying the Elm aquifer, effectively reducing the amount of recharge that

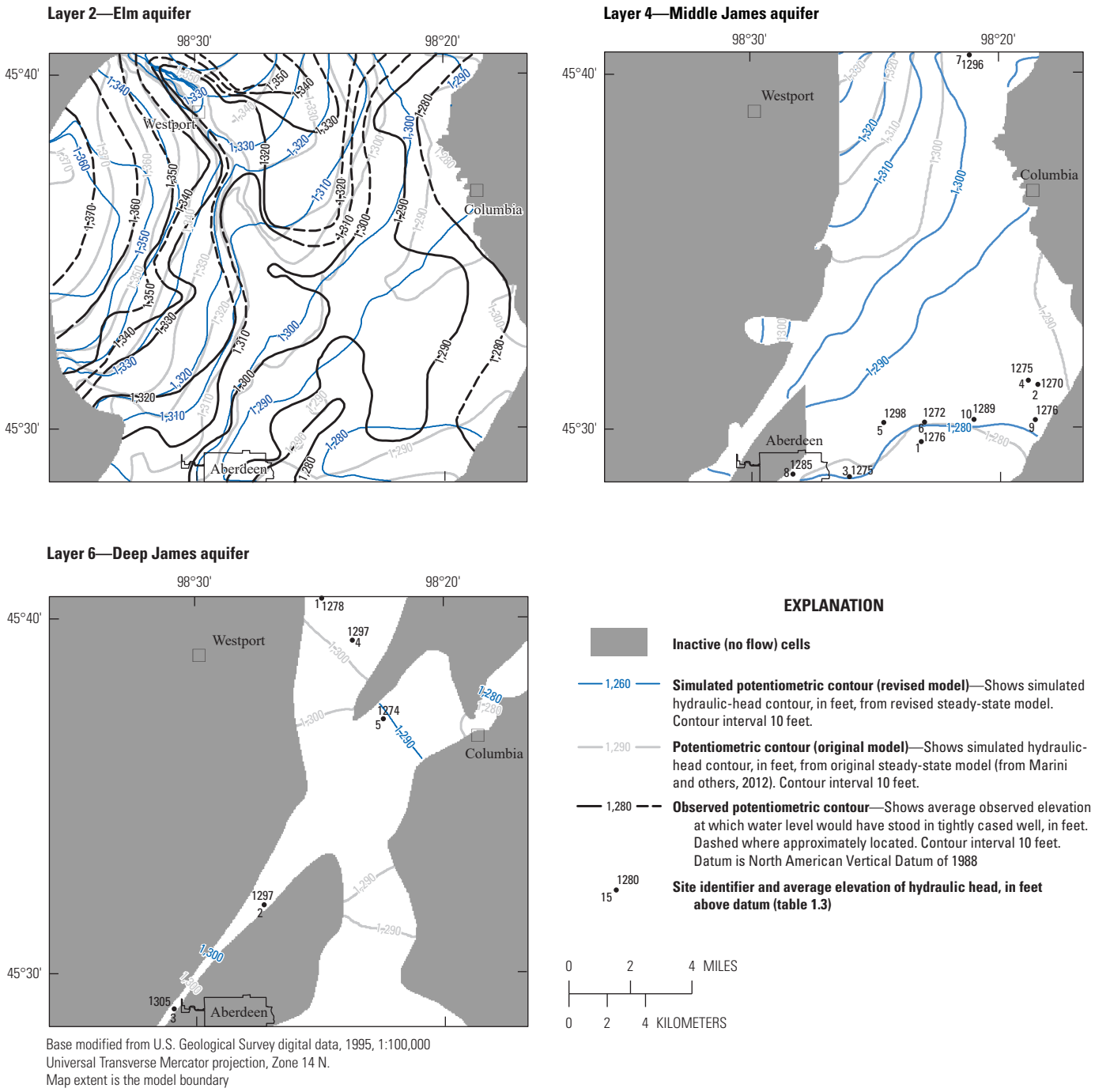

Base modified from U.S. Geological Survey digital data, 1995, 1:100,000
Universal Transverse Mercator projection, Zone 14 N.
Map extent is the model boundary

Figure 19. Simulated potentiometric contours for the revised and original model compared to observed potentiometric contours for layer 2 (Elm aquifer) and simulated potentiometric contours for the revised and original model compared to observed hydraulic head values for layers 4 (Middle James aquifer) and 6 (Deep James aquifer).

Table 5. Relative average parameter sensitivities with parameter name for the revised model.

[rm1, recharge; exdp, extinction depth; etm1, evapotranspiration; sy, specific yield; ss, specific storage; st, streambed conductance; kx, horizontal hydraulic conductivity; dr, drain conductance; kz, vertical hydraulic conductivity]

Parameter	Relative average sensitivity	Parameter	Relative average sensitivity
rm1	0.08340	kx5	0.00044
exdp	0.04348	kx3	0.00044
etm1	0.03809	kz5	0.00036
sy1	0.02137	kz8	0.00035
sy2	0.01476	kx13	0.00033
ss2	0.01456	kx1	0.00032
ss3	0.00991	kx9	0.00027
st2	0.00382	ss7	0.00027
st3	0.00334	kx6	0.00026
kx15	0.00296	kz18	0.00025
st4	0.00268	ss6	0.00022
kx17	0.00264	kz3	0.00016
ss4	0.00248	kz13	0.00016
kx11	0.00222	st7	0.00015
ss1	0.00178	ss5	0.00013
dr20	0.00156	kx18	0.00012
kx16	0.00152	kz6	0.00010
kz16	0.00145	kz10	0.00009
st6	0.00115	kz17	0.00008
kx4	0.00108	kz11	0.00008
st8	0.00098	kz2	0.00007
st5	0.00094	kz1	0.00006
kx8	0.00090	kz14	0.00006
kx19	0.00078	kz9	0.00006
kz4	0.00070	kz15	0.00005
kx10	0.00068	kz12	0.00005
kx12	0.00059	kz20	0.00005
st1	0.00056	kz7	0.00004
kx2	0.00051	kx20	0.00004
kx14	0.00046	kz19	0.00003
kx7	0.00045		

eventually makes it to the Elm aquifer (Marini and others, 2012). A limitation of this method is that the uppermost layer is not accounted for numerically; therefore, vertical groundwater flow resulting from the infiltration of precipitation could have been overestimated. Based on the analysis of the water budget in figure 14, the interaction between the surficial layer and the Elm aquifer is more complex than was previously simulated using the original model. The simulated steady-state inflow and outflow for the surficial deposit layer (layer 1) and the Elm aquifer (layer 2) for the revised model are important in both layers and may not have been adequately simulated using a multiplier to reduce recharge in the original model. The top layer that was added to the revised model represents the surficial deposits and more adequately simulates the infiltration of precipitation recharge and groundwater flux into and out of the Elm aquifer from the surficial deposits than did the original model.

The addition of the surficial deposit layer in the revised model also allows for a more accurate accounting of groundwater evapotranspiration. The original model included a multiplier to reduce the amount of water removed by evapotranspiration based on the thickness of the surficial deposits (Marini and others, 2012). The method used in the original model effectively simulates discharge from the Elm aquifer directly by evapotranspiration. In the model area, most groundwater evapotranspiration likely is in the surficial deposits and the Elm aquifer (fig. 14). The revised model more adequately simulates groundwater evapotranspiration from these sources.

The surficial layer in the revised model was added to provide a better representation of streams and to provide a more accurate interaction between groundwater and surface water. The original model used a nonrouted method for simulating streams (Marini and others, 2012). In the revised model, a routed streamflow method was incorporated and allowed direct interaction with the surficial deposit layer and the layer representing the Elm aquifer. The revised representation of streams not only allows for a better representation of groundwater and surface-water interactions, but also allows for the calculation of routed base flow in the model, which provided more appropriate information for model calibration targets.

In the revised model, the confining units that existed between the Elm and Middle James aquifers and between the Middle James and Deep James aquifers and the bedrock underlying the Deep James aquifer were simulated as explicit layers. This method allowed for a more appropriate representation of groundwater flow through the confining units and provided better estimates of groundwater flow among the three primary aquifers in the model area. Additionally, the underlying bedrock was included to improve model stability.

The additional layers in the revised model provided an opportunity for more complete estimates of hydraulic parameters in the model area, such as vertical and horizontal hydraulic conductivity. The addition of model layers, however, increases the need for spatial interpretation of hydraulic parameters for which model inputs had to be estimated based on literature. These new layers more adequately represent the hydrologic system, but simplifying assumptions are still inherent to adding these layers; for example, the thicknesses of the confining units were set based on the elevations of the top and bottom of the layers above and below each confining unit. An arbitrary thickness for the bedrock layer was set and was assumed constant for that layer. The horizontal extents for these new layers also were assumed to be the same as the overlying layers (fig. 7). The confining units could extend

beyond the model area, but the presence of the confining units outside the model area is beyond the scope of this study. Based on the assessment of the steady-state groundwater budget, the original model also may have overestimated the contribution of surface water to the aquifers because of the use of nonrouted streams.

Groundwater-flow models, by design, are intended to represent a simplification of complex natural systems and, as a result, contain differing degrees of uncertainty and limitations; for example, the interpretation of well logs and geophysical maps is subject to errors and uncertainty in interpolation, and those interpretations form the basis of the hydrogeologic framework used in the model. The hydraulic properties determined through model calibration minimized the difference between observations and model results, and these properties compared well with estimates from literature. In complex numeric groundwater systems, the inability to characterize processes, properties, and hydrologic outputs can result in a nonuniqueness of the calibration process (Leaf and others, 2013); therefore, different combinations of hydraulic properties that could result in an acceptable comparison of observations and model-simulated values could be applied to the model. Lastly, the final distribution of model parameters determined during model calibration, in addition to the resulting groundwater levels and flow directions, was based on the spatial and temporal availability of hydrologic data. In parts of the model area, hydrologic data were not available for use in model calibration; therefore, the results of the model as determined through the calibration process could be substantially different when new hydrologic data are available for regions with sparse data.

The groundwater model is a numeric approximation of a complex physical hydrologic system, and the revised model data were interpolated in regions with sparse data. Additionally, model discretization included averaged and interpolated values for water use, withdrawal rates, and hydraulic conductivity. The revised model provides a useful estimate for hydraulic gradients, groundwater-flow directions, and aquifer response to groundwater withdrawal.

Summary

The city of Aberdeen, in northeastern South Dakota, requires an expanded and sustainable supply of water to meet current and future demands. Conceptual and numerical models of the glacial aquifer system in the area north of Aberdeen were developed by the U.S. Geological Survey in cooperation with the City of Aberdeen in 2012. The U.S. Geological Survey, in cooperation with the City of Aberdeen, completed a study to revise the original numerical groundwater-flow model using data through water year (WY) 2015 to aid the City of Aberdeen in their development of plans and strategies for a sustainable water supply and to increase understanding of the glacial aquifer system and groundwater-flow system near Aberdeen. The original model was revised to improve the fit between model-simulated and observed (measured and estimated) data, provide greater insight into surface-water interactions, and improve the usefulness of the model for water-supply planning. The revised groundwater-flow model (hereafter referred to as the "revised model") presented in this report supersedes the original model.

For this study, the original numerical model was revised in several ways. The original model was modified by adding four new layers, which included a surficial layer, two intervening confining layers, and a shale bedrock layer. The revised model provides an improved understanding of the groundwater-flow system in comparison to the original model. The purpose of this report is to describe a revised groundwater-flow model including data collection, model calibration, and model results for the glacial aquifer system including the Elm, Middle James, and Deep James aquifers north of Aberdeen, South Dakota, using updated hydrologic data through WY 2015.

The principal aquifers of the model area include parts of the Elm, Middle James, and Deep James aquifers. The lithologic information used to define and describe the aquifers in the model area was unaltered from the original model; however, aquifer properties and boundary conditions were reviewed and updated using geological information reported by the South Dakota Department of Environmental and Natural Resources and information obtained from the geophysical investigations. The horizontal extent of the Elm, Middle James, and Deep James aquifers was unaltered from the original model. The thickness of the Deep James aquifer was modified based on interpretations from the geophysical investigations. In general, groundwater in the Elm aquifer flowed from northwest to southeast and locally towards rivers and streams. Similarly, in the Middle James and Deep James aquifers, groundwater also typically flowed southeast.

The revisions made to the original model include use of the following MODFLOW stress packages: Recharge, Evapotranspiration, Time-Variant Specified Head, Wells, Drains (DRN), and Stream Flow Routing (SFR2), all of which were updated from the original model except for the SFR2 Package. In the revised model, the SFR2 Package replaced the River (RIV) Package, which was used in the original model, to better simulate the interaction of groundwater and surface water and to provide estimates of routed stream base flow. Simulated hydraulic properties for each model layer included specific yield, specific storage, horizontal hydraulic conductivity, vertical hydraulic conductivity, and vertical bed conductance for stream cells and drain cells. Precalibration hydraulic property values for the Elm, Middle James, and Deep James aquifers in the revised model were assigned based on the calibrated values from the original model. Initial property values for the surficial deposits in layer 1 were assigned general values based on various deposit types. The confining layers 3, 5, and 7 also were assigned initial hydraulic property values based on the general values for silts and clays. The time-variant specified-head cells used in the revised model, applied to the first 75 stress periods (simulated using

the Time-Variant Specified-Head Package), were assigned to the Elm, Middle James, and Deep James aquifers and were unchanged from the original model. The average recharge was applied to stress period 1, and the temporally differing recharge estimates that were applied in the original model were used for stress periods 2–75 (WYs 1975–2009). Spatially variable estimates of recharge for stress periods 76–99 (WYs 2010–15) were calculated using the Soil-Water-Balance model and were included in the revised model. Streams in the revised model area were represented using the DRN and SFR2 Packages. The DRN Package was used to simulate discharge to nonrouted streams at the lateral boundary of the revised model. The SFR2 Package was used to simulate recharge and discharge from all routed streams in the revised model area, replacing the RIV Package.

Parameter ESTimation software was used to optimize model input parameters by matching model-simulated values to observed (estimated or measured) values. Calibration parameters included horizontal hydraulic conductivity, vertical hydraulic conductivity, specific yield, specific storage, and vertical streambed conductance for stream and drain cells. Additionally, multipliers were used to calibrate the recharge and evapotranspiration stresses. Evapotranspiration extinction depth also was adjusted during model calibration. During calibration, observation weights such as those for synoptic water-level measurements, were defined in the Parameter ESTimation instruction files and were unaltered from what was documented in the original model. Horizontal and vertical hydraulic conductivities were calibrated using a combination of pilot points. Pilot points were distributed sparsely in layer 1 because of the lack of calibration targets available in that layer. Layer 2 used a denser grid of pilot points and included an additional point at an aquifer-test location. During calibration, parameters were constrained using the upper and lower limits based on values found in literature.

The revised model is an improvement over the original model because the revised model includes a more detailed hydrogeologic layering scheme including four new layers, a more robust representation of streams, and a longer simulation period (WYs 1975–2015 compared to WYs 1975–2009 in the original model) that simulates a broader range of climatic conditions. In general, the revised model adequately simulates the natural system and compares favorably with observed hydrologic data. Simulated water levels were evaluated by comparing them to single water-level observations at selected well locations. The selected wells were the same wells used in the original model. The coefficient of determination value for the revised model was 0.89 and included simulated and observed values from October 1, 1974 (WY 1975), through September 30, 2015 (WY 2015). The coefficient of determination value for the original model was 0.94 and included simulated and observed values from October 1, 1974, through September 30, 2009. The difference may indicate that the original model could have been overfit to head observations because base flow was not simulated. The reason for the difference in coefficient of determination values between the original and revised models could be due to the addition of the stress period observation data from September 30, 2009, through September 30, 2015. The additional data included some climatically wetter, more extreme periods, such as 2011, in which annual precipitation was 30.9 inches. Average annual precipitation for the original model timeframe (WYs 1975–2009) was 20.26 inches. Additional precipitation data for WYs 2010–15, included in the revised model timeframe, resulted in an average annual precipitation for WYs 1975–2015 in the model area of 20.6 inches. The larger variability in climate data coupled with the additional water-level data could explain the lower coefficient of determination for water levels in the revised model.

The revised model was used to calculate various groundwater-budget components for steady-state and transient conditions for WYs 1975–2015. The greatest inflow in the revised model was from time-variant specified-head cells, which accounted for about 87 percent of total inflows. Precipitation recharge accounted for about 13 percent of total inflow, whereas routed streams contributed about 0.4 percent. Time-variant specified-head cells were the greatest source of simulated outflow, accounting for about 75 percent of total outflow. Evapotranspiration accounted for about 13 percent of total outflow. Routed streams and groundwater withdrawal accounted for about 8 percent and 3 percent, respectively, of total outflow. The time-variant specified-head cells in the revised model had the largest change when compared to the original steady-state model for inflows and outflows.

Water budgets for the revised model transient simulation were computed and compared to the transient simulation of the original model for each of the inflow water-budget components including storage, time-variant specified head, routed and nonrouted streams, and precipitation recharge. Comparison of the transient budget components between the original and revised models indicated that inflow from recharge and time-variant specified-head cells had the greatest effect on groundwater inflows.

The simulated potentiometric contours from the revised model were compared with (1) the observed potentiometric surface (layer 2) and the hydraulic head values (layers 4 and 6) and (2) the simulated potentiometric contours determined from the original model. The potentiometric contours for layer 1 in the revised model were not evaluated with observed data because layer 1 is not a defined aquifer used for water withdrawals, and no estimated potentiometric contours were available for comparison. The simulated hydraulic gradients and general direction of groundwater flow in the Elm aquifer in the revised model generally matched the observed potentiometric contours, the simulated potentiometric contours from the original model, and general flow directions interpreted to be perpendicular to the contours. Minor discrepancies between simulated potentiometric contours from the revised model and the observed (interpreted) potentiometric surface exist and may be due to the lack of observation data in the model area. An assessment of the simulated potentiometric contours in the Elm aquifer in the northern part of the model area near

the Elm River indicated that the groundwater flowed towards the river. Based on estimates of base flow in the Elm River, simulated base flow in the Elm River, and the interpretation of potentiometric contours, the Elm aquifer likely contributes groundwater discharge, as base flow, to the Elm River.

Composite parameter sensitivities were computed, which are numeric values assigned to each adjustable parameter based on their relative effect on the composite of all model observations, adjusted for their assigned weight. Generally, insensitive parameters are those with composite sensitivity values more than two orders of magnitude lower than the value of the most sensitive parameter. The most sensitive parameters included the recharge multiplier, extinction depth, the evapotranspiration multiplier, specific yield in layers 1 and 2, and the specific storage in layers 2 and 3. The least sensitive parameters were the horizontal hydraulic conductivity pilot points in zone 20 and the vertical hydraulic conductivity pilot points in zone 19.

The revised model was designed to reduce the limitations of the original model. The revisions were validated by comparing the results of the original model with the revised model. A primary benefit of the revised model is the inclusion of the surficial deposits and the confining units as explicit layers in the model. The addition of the surficial layer was beneficial for three primary reasons: (1) more accurate representation of recharge from precipitation, (2) more accurate representation of groundwater evapotranspiration, and (3) more accurate representation of groundwater and surface-water interactions. The groundwater model is a numeric approximation of a complex physical hydrologic system, and the revised model data were interpolated in regions with sparse data. Additionally, model discretization included averaged and interpolated values for water use, withdrawal rates, and hydraulic conductivity. The revised model provides a useful estimate for hydraulic gradients, groundwater-flow directions, and aquifer response to groundwater withdrawal.

References Cited

Anderson, M.P., Woessner, W.W., and Hunt, R.J., 2015, Applied groundwater modeling, 2d edition: London, U.K., Academic Press, 630 p.

Carmichael, R.S., and Henry, G., Jr., 1977, Gravity exploration for groundwater and bedrock topography in glaciated areas: Geophysics, v. 42, no. 4, p. 850–859, accessed September 14, 2017, at https://doi.org/10.1190/1.1440752.

Crandell, D.R., 1958, Geology of the Pierre area, South Dakota: U.S. Geological Survey Professional Paper 307, 88 p. [Also available at https://pubs.er.usgs.gov/publication/pp307.]

Doherty, J., 2004, PEST—Model-independent parameter estimation user manual (5th ed.): Watermark Numerical Computing, variously paged, accessed March 30, 2018, at http://www.pesthomepage.org/.

Doherty, J.E., and Hunt, R.J., 2010, Approaches to highly parameterized inversion—A guide to using PEST for groundwater-model calibration: U.S. Geological Survey Scientific Investigations Report 2010–5169, 59 p., accessed June 28, 2010, at https://pubs.usgs.gov/sir/2010/5169/.

Eldridge, W.E., Davis, K.W., and Valder, J.F., 2018, MODFLOW–NWT revised model of the glacial aquifer system north of Aberdeen, South Dakota: U.S. Geological Survey data release, https://doi.org/10.5066/P9JVNFLY.

Emmons, P.J., 1987, Preliminary assessment of potential well yields and the potential for artificial recharge of the Elm and Middle James aquifers in the Aberdeen area, South Dakota: U.S. Geological Survey Water-Resources Investigations Report 87–4017, 33 p. [Also available at https://pubs.er.usgs.gov/publication/wri874017.]

Emmons, P.J., 1990, A digital simulation of the glacial-aquifer system in the northern three-fourths of Brown County, South Dakota: U.S. Geological Survey Water-Resources Investigations Report 88–4198, 74 p. [Also available at https://pubs.er.usgs.gov/publication/wri884198.]

Flint, R.F., 1955, Pleistocene geology of eastern South Dakota: U.S. Geological Survey Professional Paper 262, 173 p. [Also available at https://pubs.er.usgs.gov/publication/pp262.]

Freeze, R.A., and Cherry, J.A., 1979, Groundwater: Englewood Cliffs, N.J., Prentice-Hall Inc., 604 p.

Harbaugh, A.W., 2005, MODFLOW–2005—The U.S. Geological Survey modular ground-water model —The ground-water flow process: U.S. Geological Survey Techniques and Methods, book 6, chap. A16, variously paged. [Also available at https://pubs.er.usgs.gov/publication/tm6A16.]

Harbaugh, A.W., Banta, E.R., Hill, M.C., and McDonald, M.G., 2000, MODFLOW–2000, the U.S. Geological Survey modular ground-water model—User guide to modularization concepts and the ground-water flow process: U.S. Geological Survey Open-File Report 2000–92, 121 p. [Also available at https://pubs.er.usgs.gov/publication/ofr200092.]

Hargreaves, G.H., and Samani, Z.A., 1985, Reference crop evapotranspiration from temperature: Applied Engineering in Agriculture, v. 1, no. 2, p. 96–99.

Helsel, D.R., and Hirsch, R.M., 2002, Statistical methods in water resources: U.S. Geological Survey Techniques of Water-Resources Investigations, book 4, chap. A3, 523 p. [Also available at https://pubs.er.usgs.gov/publication/twri04A3.]

Hutchinson, M.F., and Gallant, J.C., 2000, Digital elevation models and representation of terrain shape *in* J.P. Wilson and J.C. Gallant, eds., Terrain analysis—Principles and applications: New York, Wiley and Sons, p. 29–50.

Koch, N.C., and Bradford, W., 1976, Geology and water resources of Brown County, South Dakota, part II—Water resources: South Dakota Geological Survey Bulletin no. 25, 53 p., accessed September 14, 2017, at http://www.sdgs.usd.edu/pubs/pdf/B-25(2).pdf.

Koth, K.R., and Long, A.J., 2012, Microgravity methods for characterization of groundwater-storage changes and aquifer properties in the karstic Madison aquifer in the Black Hills of South Dakota, 2009–12: U.S. Geological Survey Scientific Investigations Report 2012–5158, 22 p. [Also available at https://pubs.er.usgs.gov/publication/sir20125158.]

Kucks, R.P., and Zawislak, R.L., 2001, Principal facts for gravity data collected in South Dakota—A web site for distribution of data: U.S. Geological Survey Open-File Report 2001–423, accessed September 14, 2017, at https://pubs.er.usgs.gov/publication/ofr01423.

Lane, J.W., Jr., White, E.A., Steele, G.V., and Cannia, J.C., 2008, Estimation of bedrock depth using the horizontal-to-vertical (H/V) ambient-noise seismic method, *in* Symposium on the Application of Geophysics to Engineering and Environmental Problems, April 6–10, 2008, Philadelphia, Pennsylvania, Proceedings: Denver, Colorado, Environmental and Engineering Geophysical Society, 13 p. [Also available at https://water.usgs.gov/ogw/bgas/publications/SAGEEP2008-Lane_HV/.]

Leaf, A.T., Hunt, R.J., and Fienen, M.N., 2013, Teaching concepts of non-uniqueness and uncertainty in groundwater: 125th Anniversary Annual Meeting and Expo, The Geological Society of America, session abstract no. 388, accessed February 21, 2018, at https://gsa.confex.com/gsa/2013AM/webprogram/Paper233847.html.

Leap, D.L., 1986, Geology and water resources of Brown County, South Dakota, part I—Geology: South Dakota Geological Survey Bulletin no. 25, 48 p., accessed September 14, 2017, at http://www.sdgs.usd.edu/pubs/pdf/B-25(1).pdf.

Marini, K.A., Hoogestraat, G.K., Aurand, K.R., and Putnam, L.D., 2012, Conceptual and numerical models of the glacial aquifer system north of Aberdeen, South Dakota: U.S. Geological Survey Scientific Investigations Report 2012–5183, 98 p. [Also available at https://pubs.er.usgs.gov/publication/sir20125183].

McDonald, M.G., and Harbaugh, A.W., 1988, A modular three-dimensional finite-difference ground-water flow model: U.S. Geological Survey Techniques of Water-Resources Investigations, book 6, chap. A1, 586 p. [Also available at https://pubs.er.usgs.gov/publication/twri06A1.]

Miller, M.P., Buto, S.G., Susong, D.D., and Rumsey, C.A., 2016, The importance of base flow in sustaining surface water flow in the Upper Colorado River Basin: Water Resources Research, v. 52, no. 5, p. 3547–3562. [Also available at https://doi.org/10.1002/2015WR017963.]

National Climatic Data Center, 2017, Record of climatological observations: National Climatic Data Center web page, accessed January 13, 2017, at https://www.ncdc.noaa.gov/oa/ncdc.html.

Niswonger, R.G., and Prudic, D.E., 2005, Documentation of the Streamflow-Routing (SFR2) Package to include unsaturated flow beneath streams—A modification to SFR1: U.S. Geological Survey Techniques and Methods, book 6, chap. A13, 50 p. [Also available at https://pubs.er.usgs.gov/publication/tm6A13.]

Niswonger, R.G., Panday, S., and Ibaraki, M., 2011, MODFLOW-NWT, a Newton formulation for MODFLOW-2005: U.S. Geological Survey Techniques and Methods, book 6, chap. A37, 44 p. [Also available at https://pubs.usgs.gov/tm/tm6a37/.]

Rothrock, E.P., 1955, Ground water reservoirs near Aberdeen, South Dakota: University of South Dakota Report of Investigations no. 78, 47 p., accessed September 14, 2017, at http://www.sdgs.usd.edu/pubs/pdf/RI-078.pdf.

Rutledge, A.T., 1998, Computer programs for describing the recession of ground-water discharge and for estimating mean ground-water recharge and discharge from streamflow records—Update: U.S. Geological Survey Water-Resources Investigations Report 98–4148, 52 p. [Also available at https://pubs.usgs.gov/wri/wri984148/.]

Schaap, B.D., 2000, Aquifer test to determine hydraulic properties of the Elm aquifer near Aberdeen, South Dakota: U.S. Geological Survey Water-Resources Investigations Report 2000–4264, 23 p. [Also available at https://pubs.usgs.gov/wri/wri004264/.]

South Dakota Department of Environmental and Natural Resources, 2018, Observation well search: South Dakota Department of Environmental and Natural Resources web page, accessed March 30, 2018, at https://apps.sd.gov/NR69obswell/default.aspx.

South Dakota Geological Survey, 2017, Lithologic logs database: South Dakota Geological Survey web page, accessed November 15, 2017, at http://usd.maps.arcgis.com/apps/webappviewer/index.html?id=9888ec2e3ee844998385265dfa22e449&center=-100.33,%2044.36.

Telford, W.M., Geldart, L.P., and Sheriff, R.E., 1990, Applied geophysics: Melbourne, Cambridge University Press, 770 p.

Thornthwaite, C.W., 1948, An approach toward a rational classification of climate: Geographical Review, v. 38, no. 1, p. 55–94.

Thornthwaite, C.W., and Mather, J.R., 1957, Instructions and tables for computing potential evapotranspiration and the water balance: Publications in Climatology, v. 10, no. 3, p. 183–311.

Tipton, M.J., 1977, Ground-water study for the City of Aberdeen: University of South Dakota Open-File Report no. 16–UR, 7 p., accessed September 14, 2017, at http://www.sdgs.usd.edu/pubs/pdf/UR-16.pdf.

Torge, W., 1989, Gravimetry: Berlin, Walter de Gruyter, 465 p.

U.S. Geological Survey, 2017, USGS water data for the Nation: U.S. Geological Survey National Water Information System database: accessed December 13, 2017, at https://doi.org/10.5066/F7P55KJN.

Welter, D.E., White, J.T., Hunt, R.J., and Doherty, J.E., 2015, Approaches in highly parameterized inversion—PEST++ Version 3, a Parameter ESTimation and uncertainty analysis software suite optimized for large environmental models: U.S. Geological Survey Techniques and Methods, book 7, chap. C12, 54 p., https://doi.org/10.3133/tm7C12.

Westenbroek, S.M., Kelson, V.A., Dripps, W.R., Hunt, R.J., and Bradbury, K.R., 2010, SWB—A modified Thornthwaite-Mather Soil-Water-Balance code for estimating groundwater recharge: U.S. Geological Survey Techniques and Methods, book 6, chap. A31, 60 p. [Also available at https://pubs.usgs.gov/tm/tm6-a31/.]

Wilson, W.E., and Moore, J.E., eds., 1998, Glossary of hydrology: Alexandria, Virginia, American Geological Institute, 248 p.

Winston, R.B., 2017, Online guide to MODFLOW-2005: U.S. Geological Survey web page, accessed October 6, 2017, at https://water.usgs.gov/ogw/modflow/MODFLOW-2005-Guide/.

Appendix. Geophysical Methods to Characterize the Subsurface Using Noninvasive Subsurface Methods

This appendix describes the geophysical methods used to characterize the subsurface using noninvasive subsurface methods of microgravity and passive seismic for the geophysical investigations for this study. Additionally, the design intention and considerations are described.

Microgravity Methods

The Earth's gravitational field varies across the land's surface. These variations are a result of changes in elevation, the density of the underlying rock, and changes, either increasing or decreasing, in the underground fluids; for example, changes in groundwater storage levels. The density differences of rock types measured by gravity can be used to estimate changes in bedrock topography, such as the thicknesses of surface sediments or the depth to bedrock. This phenomenon was used successfully to identify buried channels in glacial sediments similar to those detected in the model area (Carmichael and Henry, 1977). To obtain this information, microgravity surveys use sensitive instruments that require precise data acquisition procedures, stringent quality controls, careful data reduction, and data analysis and interpretation techniques. Microgravity measurements for this study were collected periodically from November 2013 to June 2014 with a Scintrex CG–5 relative gravimeter using field methods similar to those described in Koth and Long (2012).

Site selection for the microgravity survey was restricted to public lands and rights-of-way; therefore, gravity survey lines followed roadways with sites at 0.5- to 1-mile (mi) intervals where suitable ground conditions existed. The site spacing was reduced to about 0.25 mi to increase the resolution of the microgravity anomaly map in selected areas. A microgravity anomaly map is a spatial representation of changes in the gravity field after reducing the raw microgravity measurements (Torge, 1989). Each microgravity site (figs. 2 and 1.1) was leveled on well compacted ground, and a magnetic survey pin was secured temporarily into the ground to serve as a reference point for one leg of the gravimeter tripod and the real-time kinematic (RTK) global positioning system (GPS). One designated survey base station was identified for all microgravity surveys and was used to start and end all survey loops. Also, the base station was used to identify and correct any instrument drift during the surveys (Torge, 1989). A plywood enclosure was placed over the gravimeter during each measurement to reduce the effects of wind and sunlight exposure. At least three 2-minute measurements were obtained at each site. During postprocessing of the microgravity data, measurements with errors from vehicle traffic or other environmental effects were eliminated from the dataset. Measurements were repeated at the survey's base station near the gravel pit (fig. 22 in Marini and others, 2012) three to four times per day to monitor the short-term instrument drift of the gravimeter. The raw microgravity measurements, that is the data collected before any post-processing and corrections applied to the data, collected for this study are presented in table 1.1 and in a USGS data release (Eldridge and others, 2018).

The raw microgravity data were reduced through standard processes described by Telford and others (1990) and Torge (1989). Earth tides were removed during data acquisition by programing the GPS location and time into the gravimeter. Datasets were downloaded from the instrument, and a correction calculated from a linear regression of the repeat drift measurements for the base station was applied to the data. Corrections for elevation, latitude, Bouguer gravity, and regional trend also were applied to the measurements. The aforementioned corrections and final processed microgravity data are presented in Eldridge and others (2018).

After correcting the data, surveys with the same base station were compiled into four survey groups: AN, WF, Pit, and 130th Street (fig. 1.1). The surveys were used to interpolate a gravity anomaly map of the model area (fig. 1.2). All the datasets were tied to a common survey station. The drift station "ANbase2" was used as the common station because it was used in all the surveys (fig. 1.1). The combined data then were spatially interpolated using the ESRI Inc. Topo to Raster interpolation tool (Hutchinson and Gallant, 2000). Comparison of the microgravity anomaly map to the regional Bouguer anomaly map (Kucks and Zawislak, 2001) indicated the presence of a large-scale southeast to northwest gravity high that likely was due to the Precambrian-age basement rock.

The microgravity anomaly map (fig. 1.2) was used to locate areas of high and low relative microgravity. Identifying these areas highlights density changes in subsurface materials, which is important for locating aquifer material. In figure 1.2, low relative microgravity anomalies are interpreted to be areas of thick, low density aquifer material; conversely, high relative microgravity anomalies correspond to areas of greater material density or shallow bedrock. In general, low relative microgravity values are observed near the Elm River in the study area, which correlates well with areas of greater hydraulic conductivity and low-density aquifer material.

Passive Seismic Method

In addition to the relative microgravity survey, a passive seismic survey of seismic horizontal-to-vertical (H/V) spectral ratios was completed. Data from the H/V spectral ratio survey were used to determine the depth to bedrock. The method uses a single, broad-band, three-component seismometer to record ambient seismic noise. The ratio of the H/V frequency spectrum components can be interpreted to estimate sediment thickness overlying bedrock (Lane and others, 2008). This method was used in geologic settings where glacial sediments overlaid weathered sedimentary rock, similar to the geologic setting in eastern South Dakota. Older techniques used heavy equipment and oftentimes explosives to induce a seismic disturbance. The advantage of this technique is the use of passive ambient seismic noise induced by wind, ocean waves, and human or animal activity to determine the thickness of unconsolidated sediments.

A Guralp three-component seismometer was used to acquire passive seismic data at 10 sites in the model area (fig. 2) during the summer of 2015. Similar to the microgravity

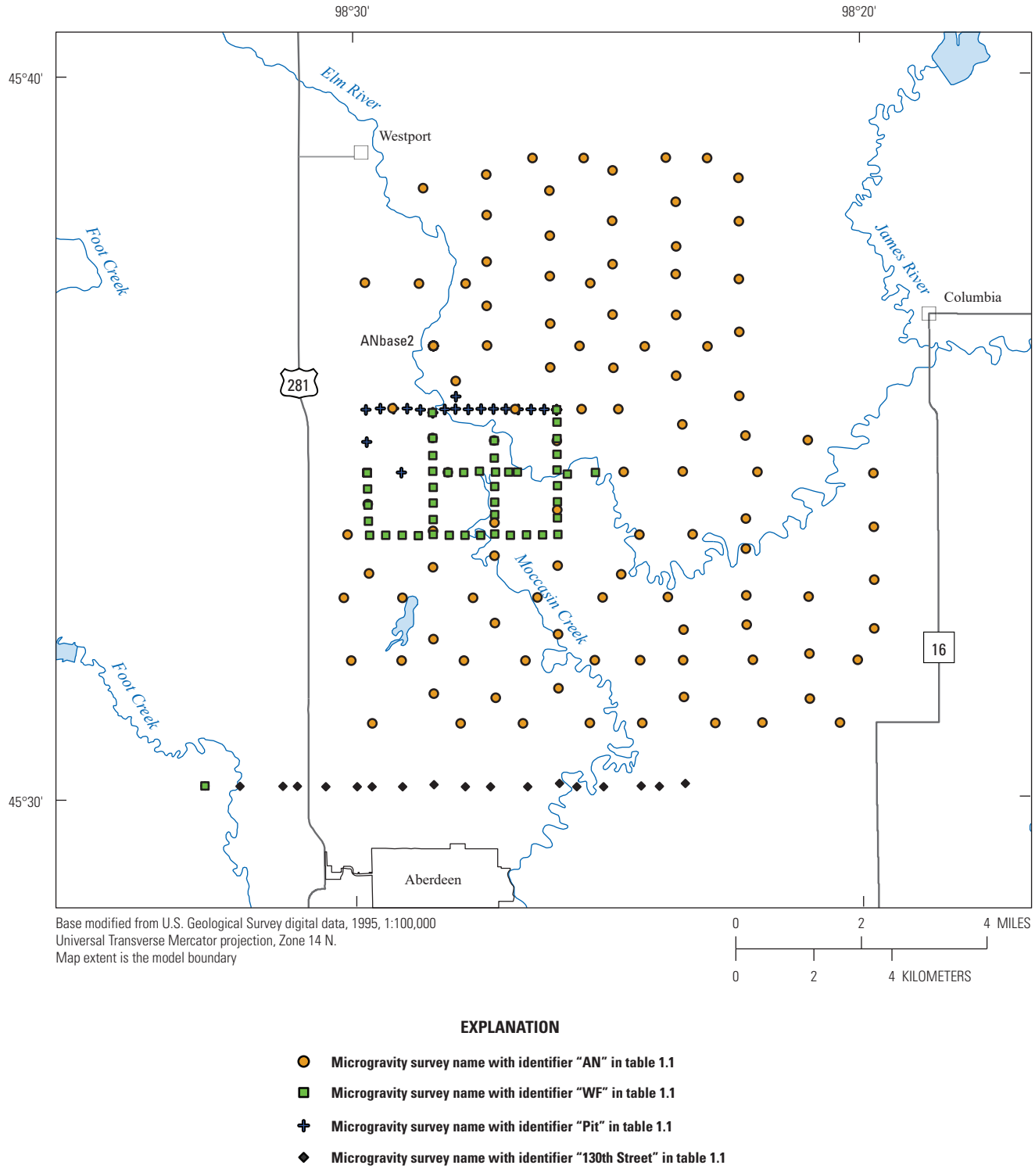

Figure 1.1. Microgravity survey sites by base station groups north of Aberdeen, South Dakota.

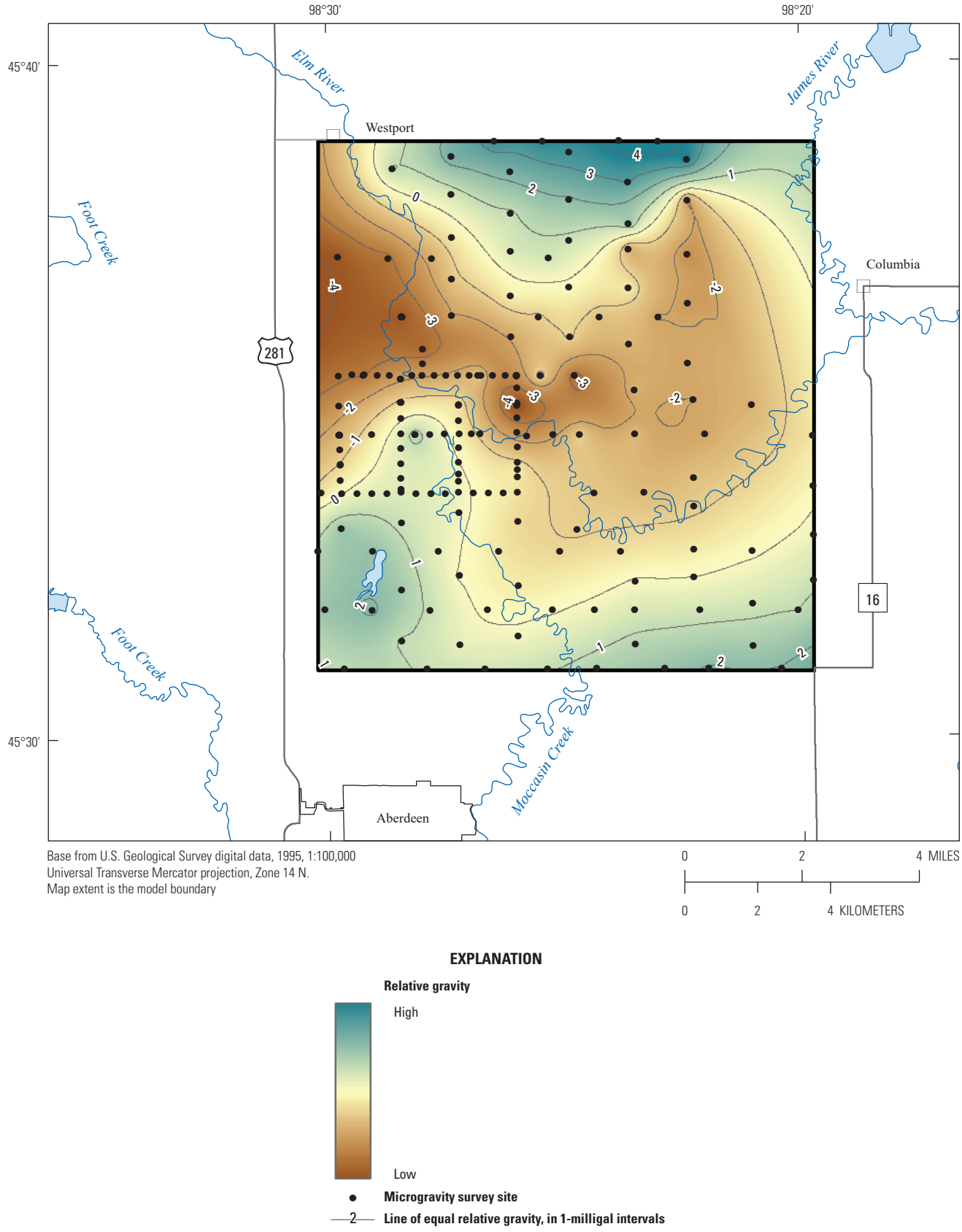

Figure 1.2. Microgravity anomaly map north of Aberdeen, South Dakota, using microgravity data from the AN survey.

surveys, H/V measurements were collected along roadways with 0.5- to 1-mi spacing between sites. At each H/V site, the seismometer was leveled and coupled to the ground using a leveling plate. An inverted 5-gallon bucket was used to protect the seismometer from wind gusts during measurements. One 30-minute measurement was made at each site based on the estimated depth to bedrock. Repeat measurements were made at two predetermined sites near wells with lithologic information available. The purpose of H/V measurements near wells was to extract an average shear wave velocity of a known thickness of sediment overlying bedrock. The H/V seismic data were analyzed using the Geopsy freeware software suite (http://geopsy.org/).

The passive seismic sites were colocated as near as possible to the microgravity sites along public access roads to enhance the interpretive power of the microgravity anomaly survey. Combining the H/V estimates of sediment thickness and existing well log information further enhances the characterization of the bedrock surface and, in turn, the thickness (and variations in density from the microgravity data) of glacial aquifer materials. The data collected were used to interpret the top of the Pierre Shale bedrock for the revised model (table 1.2). The passive seismic data generated during this study for the 10 sites with valid data are available as a USGS data release (Eldridge and others, 2018).

Supplemental Tables

Table 1.1. Microgravity survey sites with data collected north of Aberdeen, South Dakota.

[Data generated during this study are available as a U.S. Geological Survey data release (Eldridge and others, 2018)]

Survey name	Site	Date	Latitude	Longitude	Elevation, in meters	Raw gravity reading[1], in milligals
130th Street	1a	11/4/2013	45.50322	−98.5497	402.179	4,669.518
130th Street	2	11/4/2013	45.50306	−98.5383	402.419	4,668.088
130th Street	3	11/4/2013	45.50295	−98.5242	409.331	4,664.568
130th Street	4	11/4/2013	45.50293	−98.5195	405.381	4,664.945
130th Street	5	11/4/2013	45.50286	−98.5101	405.905	4,663.518
130th Street	6	11/4/2013	45.50281	−98.4999	404.449	4,662.337
130th Street	7	11/4/2013	45.50277	−98.4950	402.622	4,662.018
130th Street	8	11/4/2013	45.50269	−98.4849	401.223	4,662.353
130th Street	9	11/4/2013	45.50317	−98.4746	400.015	4,662.240
130th Street	10	11/4/2013	45.50258	−98.4644	397.452	4,662.265
130th Street	1b	11/4/2013	45.50322	−98.5497	402.178	4,669.529
130th Street	11	11/4/2013	45.50257	−98.4561	396.676	4,662.021
130th Street	12	11/4/2013	45.50248	−98.4439	396.165	4,661.789
130th Street	13	11/4/2013	45.50325	−98.4335	396.116	4,661.470
130th Street	14	11/4/2013	45.50244	−98.4277	396.231	4,661.238
130th Street	15	11/4/2013	45.50243	−98.4190	396.432	4,660.843
130th Street	16	11/4/2013	45.50256	−98.4067	395.759	4,660.853
130th Street	17	11/4/2013	45.50240	−98.4008	396.958	4,660.243
130th Street	18	11/4/2013	45.50300	−98.3922	397.042	4,659.880
130th Street	1c	11/4/2013	45.50322	−98.5497	402.189	4,669.550
WF	1a	11/5/2013	45.57513	−98.4959	406.880	4,719.457
WF	2	11/5/2013	45.57147	−98.4958	406.042	4,719.658
WF	3	11/5/2013	45.56770	−98.4958	407.192	4,719.368
WF	4	11/5/2013	45.56397	−98.4957	405.463	4,719.763
WF	5	11/5/2013	45.56078	−98.4953	405.396	4,719.825
WF	6	11/5/2013	45.56072	−98.4899	406.209	4,720.068
WF	7	11/5/2013	45.56068	−98.4846	405.970	4,720.152
WF	8	11/5/2013	45.56063	−98.4793	404.707	4,719.719
WF	9	11/5/2013	45.56086	−98.4744	404.208	4,719.286
WF	1b	11/5/2013	45.57513	−98.4959	406.886	4,719.502
WF	10	11/5/2013	45.56432	−98.4744	404.518	4,719.540
WF	11	11/5/2013	45.56807	−98.4743	404.773	4,719.864
WF	12	11/5/2013	45.57174	−98.4743	404.641	4,720.311
WF	13	11/5/2013	45.57546	−98.4743	404.689	4,720.640
WF	14	11/5/2013	45.57908	−98.4743	404.444	4,721.013
WF	15	11/5/2013	45.58308	−98.4743	407.168	4,720.629
WF	16	11/5/2013	45.58893	−98.4743	405.846	4,721.143
WF	1c	11/5/2013	45.57513	−98.4959	406.890	4,719.511
WF	0	11/5/2013	45.50322	−98.5497	402.187	4,719.796
WF	1d	11/5/2013	45.57513	−98.4959	406.879	4,719.513
WF	17	11/5/2013	45.57512	−98.4694	403.419	4,720.603
WF	18	11/5/2013	45.57514	−98.4642	402.220	4,720.545
WF	19	11/5/2013	45.57537	−98.4590	400.592	4,720.525
WF	20	11/5/2013	45.57515	−98.4538	399.733	4,720.357
WF	21	11/5/2013	45.57512	−98.4495	400.367	4,719.925

Table 1.1. Microgravity survey sites with data collected north of Aberdeen, South Dakota.—Continued

[Data generated during this study are available as a U.S. Geological Survey data release (Eldridge and others, 2018)]

Survey name	Site	Date	Latitude	Longitude	Elevation, in meters	Raw gravity reading[1], in milligals
WF	22	11/5/2013	45.57511	−98.4466	401.171	4,719.652
WF	1e	11/5/2013	45.57513	−98.4959	406.881	4,719.526
WF	1f	11/6/2013	45.57513	−98.4959	406.885	4,720.639
WF	2	11/6/2013	45.56061	−98.4691	404.310	4,719.812
WF	4	11/6/2013	45.56061	−98.4639	400.008	4,720.344
WF	5	11/6/2013	45.56061	−98.4588	400.262	4,719.975
WF	6	11/6/2013	45.56087	−98.4542	399.699	4,719.903
WF	7	11/6/2013	45.56532	−98.4542	403.404	4,719.676
WF	8	11/6/2013	45.56820	−98.4541	400.563	4,720.585
WF	9	11/6/2013	45.57181	−98.4541	400.822	4,720.888
WF	10	11/6/2013	45.57838	−98.4541	401.302	4,721.490
WF	11	11/6/2013	45.58235	−98.4541	401.417	4,721.922
WF	1g	11/6/2013	45.57513	−98.4959	406.880	4,720.655
WF	12	11/6/2013	45.56060	−98.4490	401.810	4,719.046
WF	13	11/6/2013	45.56060	−98.4437	400.603	4,718.777
WF	14	11/6/2013	45.56057	−98.4385	399.291	4,718.454
WF	15	11/6/2013	45.56071	−98.4335	398.914	4,718.090
WF	1h	11/6/2013	45.57513	−98.4959	406.882	4,720.667
WF	16	11/6/2013	45.56452	−98.4335	399.435	4,718.634
WF	17	11/6/2013	45.56816	−98.4335	400.180	4,719.185
WF	18	11/6/2013	45.57189	−98.4334	400.729	4,719.805
WF	19	11/6/2013	45.57452	−98.4302	400.686	4,720.015
WF	20	11/6/2013	45.57493	−98.4209	399.828	4,719.619
WF	21	11/6/2013	45.57554	−98.4335	400.464	4,720.342
WF	22	11/6/2013	45.57918	−98.4335	403.714	4,720.212
WF	23	11/6/2013	45.58276	−98.4335	403.394	4,720.678
WF	24	11/6/2013	45.58657	−98.4335	405.824	4,720.523
WF	25	11/6/2013	45.58945	−98.4335	404.449	4,721.161
WF	1i	11/6/2013	45.57513	−98.4959	406.875	4,720.677
AN	1a	5/19/2014	45.60429	−98.4739	406.934	4,884.376
AN	1	5/19/2014	45.60434	−98.4562	413.876	4,883.912
AN	2	5/19/2014	45.61344	−98.4562	414.763	4,884.257
AN	3	5/19/2014	45.62367	−98.4561	416.804	4,884.120
AN	4	5/19/2014	45.63438	−98.4561	417.282	4,884.904
AN	5	5/19/2014	45.64378	−98.4560	417.763	4,886.366
AN	6	5/19/2014	45.64072	−98.4768	419.575	4,885.811
AN	7	5/19/2014	45.64744	−98.4408	418.951	4,886.262
AN	8	5/19/2014	45.63997	−98.4353	413.955	4,885.936
AN	9	5/19/2014	45.62955	−98.4354	414.055	4,884.826
AN	10	5/19/2014	45.62021	−98.4354	411.974	4,885.307
AN	11	5/19/2014	45.60929	−98.4354	411.140	4,884.823
AN	12	5/19/2014	45.59915	−98.4355	409.410	4,883.964
AN	13	5/19/2014	45.58223	−98.4335	406.659	4,882.455
AN	1b	5/19/2014	45.60429	−98.4739	406.947	4,884.359
AN	1c	5/20/2014	45.60429	−98.4739	406.596	4,884.264

Table 1.1. Microgravity survey sites with data collected north of Aberdeen, South Dakota.—Continued

[Data generated during this study are available as a U.S. Geological Survey data release (Eldridge and others, 2018)]

Survey name	Site	Date	Latitude	Longitude	Elevation, in meters	Raw gravity reading[1], in milligals
AN	14	5/20/2014	45.61896	−98.4963	417.555	4,882.733
AN	15	5/20/2014	45.61873	−98.4785	417.187	4,882.601
AN	16	5/20/2014	45.61864	−98.4632	414.629	4,883.703
AN	17	5/20/2014	45.64740	−98.4240	414.496	4,886.309
AN	18	5/20/2014	45.64454	−98.4146	407.382	4,886.919
AN	19	5/20/2014	45.63288	−98.4148	407.170	4,885.820
AN	20	5/20/2014	45.62285	−98.4148	406.803	4,885.124
AN	21	5/20/2014	45.61848	−98.4221	408.525	4,885.300
AN	22	5/20/2014	45.61121	−98.4149	406.270	4,884.644
AN	23	5/20/2014	45.60407	−98.4258	408.985	4,883.988
AN	1d	5/20/2014	45.60429	−98.4739	406.597	4,884.247
AN	24	5/20/2014	45.58947	−98.4132	401.944	4,882.954
AN	25	5/20/2014	45.60387	−98.4044	402.822	4,883.798
AN	26	5/20/2014	45.61106	−98.3940	401.552	4,884.194
AN	27	5/20/2014	45.62689	−98.3938	407.744	4,884.684
AN	28	5/20/2014	45.63718	−98.3939	406.987	4,885.789
AN	29	5/20/2014	45.64732	−98.3970	407.417	4,886.939
AN	30	5/20/2014	45.64723	−98.3834	403.601	4,887.537
AN	31	5/20/2014	45.64257	−98.3731	401.317	4,886.640
AN	1e	5/20/2014	45.60429	−98.4739	406.624	4,884.235
AN	1f	5/21/2014	45.60429	−98.4739	403.697	4,893.832
AN	32	5/21/2014	45.63259	−98.3732	398.074	4,895.025
AN	33	5/21/2014	45.61925	−98.3732	397.814	4,893.116
AN	34	5/21/2014	45.60706	−98.3733	397.870	4,891.680
AN	35	5/21/2014	45.59228	−98.3734	396.692	4,889.977
AN	36	5/21/2014	45.60379	−98.3837	398.239	4,891.858
AN	37	5/21/2014	45.62046	−98.3939	401.782	4,894.266
AN	38	5/21/2014	45.59704	−98.3941	397.711	4,891.955
AN	39	5/21/2014	45.58577	−98.3922	397.350	4,890.196
AN	40	5/21/2014	45.57497	−98.3922	396.438	4,888.961
AN	41	5/21/2014	45.57490	−98.4116	399.325	4,889.934
AN	42	5/21/2014	45.58964	−98.4472	406.370	4,892.483
AN	43	5/21/2014	45.58994	−98.4874	409.311	4,892.105
AN	44	5/21/2014	45.56790	−98.4957	407.591	4,891.711
AN	46	5/21/2014	45.59621	−98.4666	402.029	4,892.977
AN	45	5/21/2014	45.57512	−98.4694	403.669	4,894.556
AN	1g	5/21/2014	45.60429	−98.4739	403.700	4,893.811
AN	1h	5/22/2014	45.60429	−98.4739	402.144	4,893.709
AN	47	5/22/2014	45.56626	−98.4335	398.334	4,890.088
AN	48	5/22/2014	45.56343	−98.4542	398.875	4,891.296
AN	49	5/22/2014	45.56159	−98.4744	402.620	4,891.664
AN	50	5/22/2014	45.56086	−98.5025	404.994	4,891.361
AN	51	5/22/2014	45.55193	−98.4955	404.098	4,892.371
AN	52	5/22/2014	45.54636	−98.5038	405.239	4,891.254

Table 1.1. Microgravity survey sites with data collected north of Aberdeen, South Dakota.—Continued

[Data generated during this study are available as a U.S. Geological Survey data release (Eldridge and others, 2018)]

Survey name	Site	Date	Latitude	Longitude	Elevation, in meters	Raw gravity reading[1], in milligals
AN	53	5/22/2014	45.54621	−98.4845	402.647	4,891.270
AN	54	5/22/2014	45.55320	−98.4744	403.258	4,890.651
AN	1i	5/22/2014	45.60429	−98.4739	402.151	4,893.697
AN	55	5/22/2014	45.53670	−98.4745	399.616	4,889.673
AN	56	5/22/2014	45.54612	−98.4614	400.596	4,888.984
AN	57	5/22/2014	45.55586	−98.4542	397.241	4,890.533
AN	58	5/22/2014	45.55345	−98.4335	398.134	4,887.784
AN	59	5/22/2014	45.54610	−98.4402	397.837	4,887.381
AN	60	5/22/2014	45.54027	−98.4542	399.456	4,887.493
AN	61	5/22/2014	45.59896	−98.4147	400.875	4,892.947
AN	62	5/22/2014	45.58951	−98.4252	400.974	4,892.461
AN	1j	5/22/2014	45.60429	−98.4739	402.159	4,893.675
AN	1k	6/3/2014	45.60429	−98.4739	401.767	4,893.535
AN	63	6/3/2014	45.56039	−98.4065	396.856	4,887.009
AN	64	6/3/2014	45.56044	−98.3890	395.139	4,886.240
AN	65	6/3/2014	45.56397	−98.3716	394.178	4,886.136
AN	66	6/3/2014	45.57473	−98.3676	393.507	4,887.065
AN	67	6/3/2014	45.58314	−98.3715	394.810	4,888.192
AN	68	6/3/2014	45.58194	−98.3510	394.019	4,887.394
AN	69	6/3/2014	45.57419	−98.3295	394.596	4,886.005
AN	70	6/3/2014	45.56186	−98.3295	395.880	4,884.303
AN	71	6/3/2014	45.54959	−98.3296	395.491	4,883.081
AN	72	6/3/2014	45.54586	−98.3511	395.924	4,883.224
AN	73	6/3/2014	45.54626	−98.3716	394.430	4,884.279
AN	74	6/3/2014	45.55699	−98.3716	395.959	4,884.938
AN	1l	6/3/2014	45.60429	−98.4739	401.755	4,893.517
AN	75	6/3/2014	45.55136	−98.4126	396.353	4,886.269
AN	76	6/3/2014	45.54598	−98.4188	395.957	4,886.057
AN	77	6/3/2014	45.54600	−98.3973	395.534	4,885.190
AN	78	6/3/2014	45.53842	−98.3296	395.339	4,882.038
AN	79	6/3/2014	45.53123	−98.3351	395.214	4,881.459
AN	80	6/3/2014	45.53275	−98.3510	395.894	4,882.127
AN	81	6/3/2014	45.53136	−98.3696	394.965	4,883.106
AN	82	6/3/2014	45.53142	−98.3926	395.016	4,884.201
AN	1m	6/3/2014	45.60429	−98.4739	401.777	4,893.501
AN	1n	6/4/2014	45.60429	−98.4739	404.878	4,902.237
AN	83	6/4/2014	45.53145	−98.4067	398.154	4,893.295
AN	84	6/4/2014	45.53153	−98.4215	399.298	4,893.589
AN	85	6/4/2014	45.53761	−98.4335	400.170	4,894.476
AN	86	6/4/2014	45.53161	−98.4443	399.832	4,894.595
AN	87	6/4/2014	45.53166	−98.4645	399.810	4,896.773
AN	88	6/4/2014	45.53176	−98.4850	408.389	4,897.455
AN	89	6/4/2014	45.53188	−98.5015	409.396	4,897.766
AN	90	6/4/2014	45.53845	−98.3924	398.322	4,893.423

Table 1.1. Microgravity survey sites with data collected north of Aberdeen, South Dakota.—Continued

[Data generated during this study are available as a U.S. Geological Survey data release (Eldridge and others, 2018)]

Survey name	Site	Date	Latitude	Longitude	Elevation, in meters	Raw gravity reading[1], in milligals
AN	91	6/4/2014	45.53946	−98.3716	399.552	4,892.113
AN	92	6/4/2014	45.58236	−98.4541	402.821	4,901.579
AN	93	6/4/2014	45.58301	−98.4743	408.597	4,901.429
AN	1o	6/4/2014	45.60429	−98.4739	404.869	4,902.222
AN	94	6/4/2014	45.51672	−98.3411	398.718	4,889.313
AN	95	6/4/2014	45.52233	−98.3510	398.690	4,890.139
AN	96	6/4/2014	45.51686	−98.3667	398.541	4,890.803
AN	97	6/4/2014	45.51690	−98.3821	400.316	4,890.867
AN	98	6/4/2014	45.52292	−98.3924	398.964	4,892.134
AN	99	6/4/2014	45.51697	−98.4060	397.958	4,892.272
AN	100	6/4/2014	45.51705	−98.4233	398.398	4,892.684
AN	101	6/4/2014	45.52512	−98.4335	399.468	4,893.415
AN	102	6/4/2014	45.51714	−98.4452	398.445	4,893.626
AN	1p	6/4/2014	45.60429	−98.4739	404.882	4,902.195
AN	1q	6/5/2014	45.60429	−98.4739	401.443	4,902.403
AN	103	6/5/2014	45.51734	−98.4947	402.629	4,895.333
AN	104	6/5/2014	45.52407	−98.4745	398.057	4,896.007
AN	105	6/5/2014	45.51718	−98.4657	397.026	4,894.639
AN	106	6/5/2014	45.52301	−98.4541	396.612	4,894.470
AN	1r	6/5/2014	45.60429	−98.4739	401.434	4,902.384
Pit	1a	11/7/2013	45.58946	−98.4335	404.467	4,722.274
Pit	2	11/7/2013	45.58957	−98.4376	404.708	4,722.332
Pit	3	11/7/2013	45.58960	−98.4419	405.682	4,722.258
Pit	4	11/7/2013	45.58964	−98.4461	405.375	4,722.481
Pit	5	11/7/2013	45.58966	−98.4502	406.886	4,722.388
Pit	6	11/7/2013	45.58969	−98.4543	403.802	4,723.222
Pit	7	11/7/2013	45.58971	−98.4584	401.428	4,723.913
Pit	8	11/7/2013	45.58972	−98.4625	401.876	4,724.069
Pit	9	11/7/2013	45.58974	−98.4668	402.301	4,724.148
Pit	10	11/7/2013	45.58971	−98.4703	402.078	4,724.269
Pit	11	11/7/2013	45.58894	−98.4743	405.841	4,723.431
Pit	12	11/7/2013	45.58967	−98.4783	405.002	4,723.457
Pit	13	11/7/2013	45.58991	−98.4826	407.429	4,722.774
Pit	14	11/7/2013	45.58994	−98.4871	408.872	4,722.054
Pit	15	11/7/2013	45.58998	−98.4914	408.993	4,721.525
Pit	16	11/7/2013	45.58972	−98.4962	408.243	4,721.155
Pit	17	11/7/2013	45.58226	−98.4960	406.977	4,721.596
Pit	18	11/7/2013	45.57518	−98.4847	409.551	4,721.701
Pit	1b	11/7/2013	45.58946	−98.4335	404.476	4,722.292
Pit	1c	11/7/2013	45.58946	−98.4335	404.469	4,722.297
Pit	19	11/7/2013	45.59267	−98.4666	402.018	4,724.384

[1]The raw gravity values are an average because three gravity readings were made at each site.

Table 1.2. Passive seismic survey sites with data collected north of Aberdeen, South Dakota.

[Data generated during this study are available as a U.S. Geological Survey data release (Eldridge and others, 2018)]

Site name	Map identifier (fig. 2)	Longitude	Latitude	Elevation, in meters above North American Verital Datum 1988	Elevation, in feet above North American Verital Datum 1988	Depth to top of Pierre Shale above North American Verital Datum 1988	Elevation of top of Pierre Shale above North American Verital Datum 1988
HVSR13a	1	−98.456580	45.575340	397.00	1,302.16	88	1,214.16
HVSR14	2	−98.453897	45.582370	398.70	1,307.74	97	1,210.74
HVSR18	3	−98.466436	45.597010	405.70	1,330.70	91	1,239.70
HVSR22	4	−98.433387	45.574840	402.50	1,320.20	92	1,228.20
HVSR29	5	−98.423083	45.545890	400.20	1,312.66	106	1,206.66
HVSR51	6	−98.474532	45.557910	410.90	1,347.75	99	1,248.75
HVSR58c	7	−98.352232	45.516750	399.60	1,310.69	131	1,179.69
HVSR60	8	−98.456251	45.604070	412.60	1,353.33	99	1,254.33
HVSR61	9	−98.435489	45.609280	407.90	1,337.91	109	1,228.91
HVSR72	10	−98.329432	45.563950	401.20	1,315.94	116	1,199.94

Table 1.3. Water-level data for generalized average potentiometric surface of Elm aquifer, Middle James aquifer, and Deep James aquifer (water years 1975–2015).

[All water-level data for these sites are available from the U.S. Geological Survey National Water Information System database (U.S. Geological Survey, 2017); --, not applicable]

Site identifier (fig. 4)	Station identification number	Local number	Earliest or single water-level date	Other identifier	Period of record for wells with multiple water-level measurements	Estimated average water-level elevation (1975–2015)[1]
			Elm aquifer			
1	454010098314402	125N64W03CAA2	08/01/1970	--	--	1,319
2	453949098321601	125N64W10BBBB	06/01/1984	--	--	1,337
3	453954098310301	125N64W02CCBB	06/05/2009	PZ6	2009	1,318
4	453921098294801	125N64W12BCCA	05/21/2009	PZ1	2009	1,317
5	453944098283801	125N64W12AAA	08/19/1981	--	--	1,358
6	453904098281901	125N63W07CCA	08/20/1981	--	--	1,317
7	453923098271601	125N63W08BCB	06/03/1983	--	--	1,338
8	453856098263901	125N63W08DCCC	08/01/1955	--	--	1,333
9	453948098260601	125N63W05DDDD	08/01/1955	--	--	1,343
10	454037098245201	125N63W04AAAA	06/07/1977	BN–77N	1977–2009	1,324
11	453853098245201	125N63W16AAAA	06/07/1977	BN–77M	1977–2015	1,332
12	453837098224001	125N64W14ADB	04/11/1983	--	--	1,286
13	453957098214101	125N63W01DCC	10/31/1983	--	--	1,290
14	453800098222002	125N63W13CCCC2	10/11/1974	MM1	1974–85	1,292
15	453734098295201	125N64W23DAA	08/01/1970	--	--	1,340
16	453911098280201	125N63W19CDDD	06/05/2009	PZ7	2009	1,310
17	453616098321201	125N64W34BBB	08/01/1970	--	--	1,356
18	453635098305701	125N64W26CBC	08/01/1970	--	--	1,339
19	453622098284201	125N64W25DDAD	06/05/2009	PZ8	2009	1,308
20	453620098275801	125N63W30CDDD	09/01/1968	--	--	1,303
21	453623098271601	125N63W29CCCC	06/07/1977	BN–77L	1977–2015	1,339
22	453639098195601	125N62W30DAA	07/01/1951	--	--	1,276
23	453520098320501	124N64W04AAAA1	05/20/1982	BN–82E	1982–2015	1,354
24	453515098280601	124N63W06BACA	07/07/2009	PZ9	2009	1,308
25	453508098273101	124N63W06ADBB	06/05/2009	PZ5	2009	1,304
26	453457098273301	124N63W06DABB	06/05/2009	PZ4	2009	1,304
27	453524098222301	125N63W35DDDD	08/01/1968	--	--	1,290
28	453438098314501	124N64W03CDC	08/01/1970	--	--	1,331
29	453437098272401	124N63W06DDBD	09/19/2005	--	--	1,300
30	453430098264501	124N63W08ABBA	05/12/2008	A–2	2008–09	1,306
31	453430098262901	124N63W08ABBA	05/12/2008	A–1	2008–09	1,308
32	453436098260101	124N63W05DDAD	07/06/2009	PZ10	2009–10	1,311
33	453424098260101	124N63W08AADA	08/01/2009	PZ11	2009–10	1,307
34	453424098271701	124N63W07AAD	09/01/1967	--	--	1,298
35	453414098265701	124N63W08BCAA	12/03/2004	--	--	1,303
36	453410098264601	124N63W08BDAC	12/02/2004	--	--	1,304
37	453359098263801	124N63W08AADD	12/02/2004	--	--	1,304
38	453351098264501	124N63W08DAC	10/30/1998	--	--	1,307
39	453351098261701	124N63W08DACC	10/30/1998	--	--	1,306
40	453439098243201	124N63W03CCAB	09/01/1967	--	--	1,299
41	453428098194202	124N62W08BBBB2	10/11/1974	BN–82K	1982–2015	1,291

Table 1.3. Water-level data for generalized average potentiometric surface of Elm aquifer, Middle James aquifer, and Deep James aquifer (water years 1975–2015).—Continued

[All water-level data for these sites are available from the U.S. Geological Survey National Water Information System database (U.S. Geological Survey, 2017); --, not applicable]

Site identifier (fig. 4)	Station identification number	Local number	Earliest or single water-level date	Other identifier	Period of record for wells with multiple water-level measurements	Estimated average water-level elevation (1975–2015)[1]
			Elm aquifer—Continued			
42	453346098343101	124N64W08CCC	08/01/1970	--	--	1,361
43	453340098311001	124N64W10DDD	08/01/2007	R0–00–41	--	1,341
44	453320098305902	124N64W15ADD2	08/01/1970	--	--	1,328
45	453341098255801	124N63W16BBCB	10/30/1998	--	--	1,306
46	453336098252401	124N63W16BAAC	10/30/1998	--	--	1,308
47	453345098243901	124N63W10CCC	02/01/1967	--	--	1,295
48	453312098244401	124N63W15CBBB	10/05/1974	MM3	1974–85	1,297
49	453402098183201	124N62W08ADDD	10/09/1974	MM2	1974–85	1,288
50	453254098340401	124N64W17CDD	07/27/1982	--	--	1,349
51	453254098304901	124N64W14CCC	08/01/1970	--	--	1,326
52	453254098301201	124N64W14DCC	08/01/1970	--	--	1,323
53	453246098294501	124N64W23AAAA	07/30/2007	R2–00–42	2007–09	1,328
54	453247098260103	124N63W17DDDD3	08/23/1999	MM5	1999–2009	1,304
55	453246098243901	124N63W22BBB	07/01/1955	--	--	1,294
56	453200098343901	124N64W20CCCB	08/01/2007	R2–00–51	2007–09	1,351
57	453155098330801	124N64W28BBA	08/01/1970	--	--	1,329
58	453203098323801	124N64W21DCCD	09/30/1987	--	--	1,329
59	453202098320301	124N64W22CCC	11/16/1982	--	--	1,322
60	453136098320302	124N64W27BCC2	08/01/1970	--	--	1,324
61	453159098282401	124N63W19CCCC	09/01/1967	--	--	1,304
62	453154098255301	124N63W28BBB	07/01/1955	--	--	1,292
63	453214098232501	124N63W23CBC	07/01/1955	--	--	1,292
64	453153098232901	124N63W23CCCD	07/31/2007	--	--	1,298
65	453147098222101	124N63W26AAD	09/01/1967	--	--	1,295
66	453103098341301	124N64W32BAB	08/01/1970	--	--	1,321
67	453109098332702	124N64W29DDD2	08/01/1970	--	--	1,324
68	453103098310801	124N64W34AAB	08/01/1970	--	--	1,320
69	453131098294203	124N64W26DAAA3	08/01/1970	--	--	1,311
70	453109098294501	124N64W26DDD	08/01/1970	--	--	1,313
71	453116098292601	124N64W25CCA	08/01/1970	--	--	1,305
72	453134098271701	124N63W30ADD	07/01/1955	--	--	1,294
73	453103098255701	124N63W28CCCC	05/20/1982	BN–82F	1982–2015	1,299
74	453128098243901	124N63W27CBB	07/01/1955	--	--	1,286
75	453054098243601	124N63W34BB	06/02/1983	--	--	1,281
76	453055098233501	124N63W34AAD	07/01/1955	--	--	1,287
77	453105098183002	124N62W28CCCC2	08/01/1967	--	--	1,274
78	452950098321502	123N64W04ADDC2	03/01/1969	--	--	1,307
79	452923098313301	123N64W03CDDD	03/01/1926	--	--	1,309
80	453016098293601	124N64W36CCDB	07/31/2007	--	--	1,309
81	452955098271401	123N63W06ADAD	06/01/1949	--	--	1,286
82	453012098255602	124N63W33CCCC2	05/01/1956	--	--	1,284

Table 1.3. Water-level data for generalized average potentiometric surface of Elm aquifer, Middle James aquifer, and Deep James aquifer (water years 1975–2015).—Continued

[All water-level data for these sites are available from the U.S. Geological Survey National Water Information System database (U.S. Geological Survey, 2017); --, not applicable]

Site identifier (fig. 4)	Station identification number	Local number	Earliest or single water-level date	Other identifier	Period of record for wells with multiple water-level measurements	Estimated average water-level elevation (1975–2015)[1]
Elm aquifer—Continued						
83	452948098233201	123N63W03ADDD	06/01/1949	--	--	1,290
84	452846098295401	123N64W11DAC	06/01/1949	--	--	1,297
85	452851098282101	123N63W07CBB	07/01/1949	--	--	1,286
86	452915098271501	123N63W08BBBB	10/10/1974	BN–77V	1977–2014	1,292
87	452917098255301	123N63W09BBB	06/01/1949	--	--	1,280
88	452924098244902	123N63W04DDD2	06/01/1949	--	--	1,287
89	452830098230101	123N63W11CDDC	07/01/1968	--	--	1,288
90	452948098194301	123N62W05BCC	06/01/1949	--	--	1,280
91	452928098194401	123N62W05CBCC	10/09/1974	MM4	1974–85	1,284
Middle James aquifer						
1	452934098231202	123N63W02C2	6/2/1976	MJ1	--	1,276
2	453110098182801	124N62W28CCC	6/20/1981	MJ2	--	1,270
3	452835098260701	123N63W08DD	8/10/1982	MJ3	--	1,275
4	453117098185101	124N62W29D	9/27/1982	MJ4	--	1,275
5	453007098244302	123N63W03BBBB2	5/17/1984	MJ7	--	1,298
6	453007098230401	123N63W02BABA	5/17/1984	MJ8	--	1,272
7	454033098210801	125N63W01AAAA	6/1/1984	MJ11	--	1,296
8	452840098282401	123N63W07CCBB	7/1/1949	s_MJ1_1	--	1,285
9	453010098183501	123N62W05AAAA	7/1/1970	s_MJ2_1	--	1,276
10	453011098210401	123N63W01AAAA	7/1/1970	s_MJ3_1	--	1,289
Deep James aquifer						
1	453705098183001	125N62W21CCCC	10/3/1974	DJ1	1974–85	1,278
2	453153098271601	124N63W30AAAA	5/17/1984	DJ3	--	1,297
3	452857098305601	123N64W10ADDD	3/1/1926	s_DJ1_1	--	1,305
4	453922098233701	125N63W10ADDD	8/1/1969	s_DJ2_1	--	1,297
5	453708098222301	125N63W25ADDD	8/1/1969	s_DJ3_1	--	1,274

[1]Datum is North American Vertical Datum of 1988.

For more information about this publication, contact:
Director, USGS Dakota Water Science Center
1608 Mountain View Road
Rapid City, SD 57702
605–394–3200

For additional information, visit: https://www.usgs.gov/centers/dakota-water

Publishing support provided by the
Rolla Publishing Service Center

USGS

Valder and others—**Revised Groundwater-Flow Model of the Glacial Aquifer System North of Aberdeen, South Dakota, Through Water Year 2015**—SIR 2018–5137

ISSN 2328-0328 (online)
https://doi.org/10.3133/sir20185137